Contract No:

This document was prepared in conjunction with work accomplished under Contract No. DE-AC09-08SR22470 with the U.S. Department of Energy (DOE) Office of Environmental Management (EM).

Disclaimer:

Geochemical Data Package for Performance Assessment Calculations Related to the Savannah River Site

D. I. Kaplan

February 2021

SRNL-STI-2021-00017, Revision 0

Key Words:
Distribution Coefficient,
Geochemistry, *Kd*
Apparent Solubility Value,
Special Analysis

Retention: Permanent

Geochemical Data Package for Performance Assessment Calculations Related to the Savannah River Site

Daniel I. Kaplan

February 2021

Prepared for the U.S. Department of Energy under contract number DE-AC09-08SR22470.

DISCLAIMER

Printed in the United States of America

Prepared for
U.S. Department of Energy

REVIEWS AND APPROVALS

AUTHOR:

Daniel I. Kaplan (Environmental, Materials, and Energy Sciences) Date

TECHNICAL REVIEW:

Dien Li (Environmental, Materials, and Energy Sciences) Date

APPROVALS:

Dennis G. Jackson, Jr. (Environmental, Materials, and Energy Sciences) Date

Gregory P. Flach (Closure & Disposal Assessment, Savannah River Remediation, LLC) Date

Table of Contents

List of Tables

List of Figures

Acronyms

BFS	Blast-furnace slag
CA	Composite analysis
CDP	Cellulose degradation products
CIG	Components-in-grout
CLSM	Controlled low strength material
CSH	Calcium-silicate-hydrate
DOC	Dissolved organic carbon
D_e	Effective diffusion coefficients
ET	Engineered Trenches
HLW	High Level Waste
IDF	Integrated Disposal Facility
ILV	Intermediate Level Vault
LAWV	Low Activity Waste Vault
LLW	Low Level Waste
Kd	Distribution coefficient
k_s	Apparent solubility value
MWCO	Molecular weight cut-off
NRCDA	Naval Reactor Component Disposal Areas
PA	Performance Assessment
RadFLEx	Radionuclide Field Lysimeter Experiment
SA	Special Analysis
SDF	Saltstone Disposal Facility
SRNL	Savannah River National Laboratory
SRNS	Savannah River Nuclear Solutions, LLC
SRR	Savannah River Remediation, LLC
SRS	Savannah River Site
ST	Slit Trenches
TRU	Transuranic
XANES	X-ray absorption near-edge structure

Elements

Ac	Actinium	Fr	Francium	Se	Selenium
Ag	Silver	Gd	Gadolinium	Sm	Samarium
Al	Aluminum	^{3}H	Tritium	Sn	Tin
Am	Americium	Hg	Mercury	Sr	Strontium
Ar	Argon	I	Iodine	Tc	Technetium
As	Arsenic	K	Potassium	Te	Tellurium
At	Astatine	Kr	Krypton	Th	Thorium
Ba	Barium	Lu	Lutetium	Tl	Thallium
Bi	Bismuth	Mn	Manganese	U	Uranium
Bk	Berkelium	Mo	Molybdenum	Y	Yttrium
C	Carbon	N	Nitrogen	Zn	Zinc
Ca	Calcium	Na	Sodium	Zr	Zirconium
Cd	Cadmium	Nb	Niobium		
Ce	Cerium	Ni	Nickel		
Cf	Californium	Np	Neptunium		
Cl	Chlorine	Pa	Protactinium		
Cm	Curium	Pb	Lead		
Co	Cobalt	Pd	Palladium		
Cr	Chromium	Po	Polonium		
Cs	Cesium	Pt	Platinum		
Cu	Copper	Pu	Plutonium		
Es	Einsteinium	Ra	Radium		
Eu	Europium	Rb	Rubidium		
F	Fluorine	Re	Rhenium		
Fe	Iron	Rn	Radon		
Fm	Fermium	Sb	Antimony		

Pd

1.0 EXECUTIVE SUMMARY

The Savannah River Site (SRS) disposes of low-level radioactive waste (LLW) and stabilizes high-level radioactive waste (HLW) tanks in the subsurface environment. Calculations used to establish the radiological limits of these facilities are referred to as Performance Assessments (PAs), Special Analyses (SAs), and Composite Analyses (CAs). The purpose of this document is to revise the existing geochemical data package used for these calculations (Kaplan, 2016). This work builds on earlier compilations of geochemical data, referred to a geochemical data packages (Kaplan, 2007; Kaplan, 2010; Kaplan, 2016; McDowell-Boyer et al., 2000). This work is being conducted as part of the on-going maintenance program of the SRS PA programs that periodically updates calculations and data packages when new information becomes available.

Because application of values without full understanding of their original purpose may lead to misuse, this document also provides the geochemical conceptual model, the approach used for selecting the values, the justification for selecting data, and the assumptions made to assure that the conceptual and numerical geochemical models are reasonably conservative (*i.e.,* bias recommended input values to reflect conditions that will predict maximum risk to the hypothetical recipient). This document provides 1,232 input parameters for geochemical parameters describing transport processes for 64 elements (>740 radioisotopes) potentially occurring within eight subsurface disposal or tank closure areas: Slit Trenches (ST), Engineered Trenches (ET), Low Activity Waste Vault (LAWV), Intermediate Level (ILV) Vaults, Naval Reactor Component Disposal Areas (NRCDA), Components-in-Grout (CIG) Trenches, Saltstone Disposal Facility, and Closed Liquid Waste Tanks. The geochemical parameters described here are the distribution coefficient, *Kd* value, apparent solubility value, k_s value, and the cementitious leachate impact factor.[1]

The primary changes included in this revision follow.

- Incorporated results from >60 new published reports or journal articles, including 19 related directly to SRS PAs. High pedigree data has been generated and used here from the Radionuclide Field Lysimeter Experiment (RadFLEx), a 9-year old field experiment quantifying radionuclide migration under SRS vadose zone conditions. Research related to the Hanford's Integrated Disposal Facility (IDF) PA and the European Joint Program on Radioactive Waste Management (EURAD) have provided a wealth of new data and insight into geochemical behavior of radionuclides in cementitious environments. Both programs have generated high quality experimental data related to reducing cementitious waste forms, providing insight to geochemical processes application to SRS conditions. Additionally, the European Union's program assembled an expert panel that completed a 5-year exhaustive literature review and identified conservative *Kd* values and their ranges for cementitious materials (Ochs et al., 2016).

[1] As will be described in more detail in Sections 4.4.5 and 4.4.6, the cementitious leachate impact factors are element-specific values used to modify *Kd* values to account for the influence of leachate from cement structures on groundwater chemistry that may alter radionuclide partitioning to subsurface sediment.

- New equations were introduced to estimate the log-normal distributions of *Kd* and k_s values based on "best estimates." Previous distributions were normally distributed around the "best estimates." The log-normal distributions reflect better recent experimental data. An important outcome of this change is that the lower 95% confidence limits is greater than previous estimates based on normal distributions.
- Additional sediment and cementitious material *Kd* values were paired to solubility concentrations, such that models can use "if-then" statements to use *Kd* values when the constituent of concern concentrations are below the apparent solubility value, and the solubility value, when the constituent of concern concentrations exceed this limit.
- Solute binding to cementitious materials changes as the material ages. Previously there were three Stages of cement degradation plus a duration when "cementitious leachate impacted *Kd*" were used. This latter duration was renamed here as Stage IV, to be consistent with other data bases. No new values were introduced for Stage IV.

For the vast majority of the dataset, the new information supported use of the original recommended input values, thereby reaffirming the pedigree of these values. Among recommended input values that were changed, those that may have the greatest impact on PA calculations are shown below.

Element	Data Package Version[a]	Sediment		Oxidizing Cement			Reducing Cement		
		Sandy *Kd* (mL/g)	Clayey *Kd* (mL/g)	Stage I *Kd* (mL/g)	Stage II *Kd* (mL/g)	Stage III *Kd* (mL/g)	Stage I *Kd* (mL/g)	Stage II *Kd* (mL/g)	Stage III *Kd* (mL/g)
As	Previous	[b]					200	200	
	New						300	300	
Ba	Previous	20	100						
	New	8	30						
Cs, Fr, Rb	Previous	10	50						
	New	20	300						
Np	Previous	3	9						
	New	4	20						
Pu	Previous	650							
	New	1000							
Sb	Previous			200	200		200	200	
	New			300	300		300	300	

[a] Previous = Kaplan (2016)
[b] Empty cells indicate no change in values recommended in this document.

As part of the PA maintenance plan, future geochemical data-needs were identified, including: (1) develop cementitious leachate impact factors (used to factor the influence of cementitious leachate on constituent of concern sorption to sediments), (2) develop a reactive transport code for certain aspects of the PA, (3) conduct studies to understand ^{14}C and radioiodine geochemistry in cementitious environments, and (4) develop solubility limits and paired *Kd* values (for lower constituent of concern concentration conditions) for Ba, Cr, Np, Pa, Pb, Pu, Sr, and U under reducing and/or oxidized cementitious conditions.

2.0 OBJECTIVE AND SCOPE

The objectives of this document are to explain the following as they relate to the PA, CA, and SA (henceforth, collectively referred to simply as PA) calculations conducted at the Savannah River Site (SRS):

1. the geochemical conceptual model,
2. the approach used to select values for the numerical parameters of these conceptual models,
3. the assumptions made to assure that the conceptual and numerical models are reasonable, and
4. the recommended geochemical input values for the PA and justification for their selection.

The scope of this document includes providing geochemical direction and input values appropriate for eight SRS facilities and 64 constituents of concern.

1. **SRS Facilities:** To provide geochemical input values for PA modeling of the:

    - Slit Trenches (ST),
    - Engineered Trenches (ET),
    - Low Activity Waste Vault (LAWV),
    - Intermediate Level Vault (ILV),
    - Naval Reactor Component Disposal Areas (NRCDA),
    - Components-in-Grout (CIG) Trenches,
    - Saltstone Disposal Facility (SDF), and
    - Closed Liquid Waste Tanks.

2. **Constituents of Concern:** To provide geochemical input values for PA modeling of isotopes of the following 64 elements: Ac, Ag, Al, Am, Ar, As, At, Ba, Bi, Bk, C, Ca, Cd, Ce, Cf, Cl, Cm, Co, Cr, Cs, Cu, Es, Eu, F, Fe, Fm, Fr, Gd, H (as ^{3}H), Hg, I, K, Kr, Lu, Mn, Mo, N (as NO_3^- and NO_2^-) Na, Nb, Ni, Np, Pa, Pb, Pd, Po, Pt, Pu, Ra, Rb, Re, Rn, Sb, Se, Sm, Sn, Sr, Tc, Te, Th, Tl, U, Y, Zn, and Zr.

3. **Duration:** The duration of interest varies between the various types of calculations, but is commonly 1,000 years, 10,000 years, or the duration required for the maximum dose to be manifested. Thus, if geochemical conditions are expected to change during these periods of interest, then appropriate adjustments to the geochemical conceptual and numerical models were also made.

4. **Geochemical Conditions:** The tendency of constituents of concern to migrate can be greatly influenced by the geochemical conditions of the subsurface system. The primary environmental systems include here are:

- sandy sediment,
- clayey sediment,
- young (Stage I) cement,
- middle aged (Stage II) cement,
- aged (Stage III) cement,
- young (Stage I) reduced cement,
- middle aged (Stage II) reduced cement,
- aged (Stage III) reduced cement,
- cementitious leachate impacted sandy sediment, and
- cementitious leachate impacted clayey sediment.

3.0 PHILOSOPHY AND ASSUMPTIONS

The basic philosophy used to develop and to parameterize the geochemical models originated from a broad range of basic and applied research. Basic mechanistic studies and first principles of chemistry and geochemistry were used to provide guidance for the conceptual geochemical models. Empirical studies, preferably with site-specific materials and conditions, were used to provide input estimates to help quantify the conceptual models. Solute partitioning between the aqueous and solid phases was described using the distribution coefficient, *Kd* value and the apparent solubility value, k_s (defined in Section 3.1). A series of look-up tables were prepared containing these parameters that vary with the type of porous media (*e.g.*, sandy sediment, clayey sediment, cementitious material, reducing cementitious material), and in the case of cementitious materials, the age of the solid and the presence or absence of slag (a strong reducing agent).

Section 3.1 contains a description of the differences between the theoretical and empirical *Kd* values and their relation to the retardation factor, a parameter used in reactive transport models that describes solute interactions with the solid phase. Section 3.1 is followed by a description of the apparent solubility values and how they differ from *Kd* values (Section 3.2). Importantly, it was decided not to employ throughout the PAs more mechanistic surface complexation models, which are discussed in Section 3.3. While the PA models routinely use such models under limited conditions to inform the larger PA (Denham, 2006; Denham, 2007, 2009; Denham and Millings, 2012; Miller et al., 2010; Serkiz and Kaplan, 2006), their widespread application have not yet been developed, primarily because an extraordinarily large number of model input values would need to be generated to support the large number of constituents of concern (64 elements) and wide range of environmental conditions (12 geochemical environments) existing in the various PA scenarios.

3.1 Distribution Coefficients

Coupled reactive-transport modeling, as the name implies, combines chemical equations to describe solute interaction with the sediment or waste form with equations to describe the flow of water through porous or fractured media. The outcome is a prediction of the temporal and spatial distribution of the solute. The solute-sediment interactions are complex, and include adsorption, absorption, partitioning into organic matter, complexation, precipitation, and co-

precipitation. The magnitude of these interactions for a given solute may vary greatly depending on solid phase composition or porewater chemical composition. Each type of interaction between the solute and solid phase has a unique numerical representation. However, the most common approach used in coupled reactive-transport modeling is to incorporate the effect of all reactions into one *Kd* value. The *Kd* value is the simplest construct describing solute sorption to sediments. Sorption is used here in a manner consistent with the definition provided by Sposito (1989), that is, all processes that remove solutes from the aqueous phase. The *Kd* value (mL/g) is the ratio of the solute concentration sorbed to the solid phase (C_{solid} (mol/g)) divided by the solute concentration in the liquid surrounding the solid phase (C_{liquid} (mol/mL) (Equation 1):

$$Kd = \frac{C_{solid}}{C_{liquid}}, \quad (1)$$

Sorption as expressed by *Kd* values is normalized by mass and not volume (as transport modelers use) or surface area (as surface chemist use). First and foremost, it is assumed that steady state is achieved and that kinetics, the rate that sorption occurs, is not important under the assumed modeling conditions. Sorption kinetics is typically not an issue for groundwater flow rates that generally do not exceed a few centimeters per day, thereby providing long aqueous/solid phase contact times. *Kd* also assumes that sorption is linear, *i.e.,* changes in aqueous concentrations do not impact the extent of sorption (Figure 1–Top). As the concentration of a solute on the solid phase increases, the sorption isotherm becomes non-linear, *i.e*., it takes on a Freundlich sorption profile. The non-linearity has been attributed to the number of available sorption sites diminishing to a point that it becomes less likely for the solute to find an available sorption site. The aqueous phase concentration where this transition from linear to non-linear sorption occurs varies with solute. For example, in a carbonate sandy soil, this transition was noted at 10^{-5} M Sr, whereas it occurred at 10^{-6} M Cs (Krupka et al., 1999b). Similarly, the apparent solubility of Pu(IV) in a goethite suspension approaches 10^{-8} M (Zhao et al., 2016). Upon adding more solute to the solubility-controlled system, as may occur near a source term, precipitation occurs (Figure 1–Top).

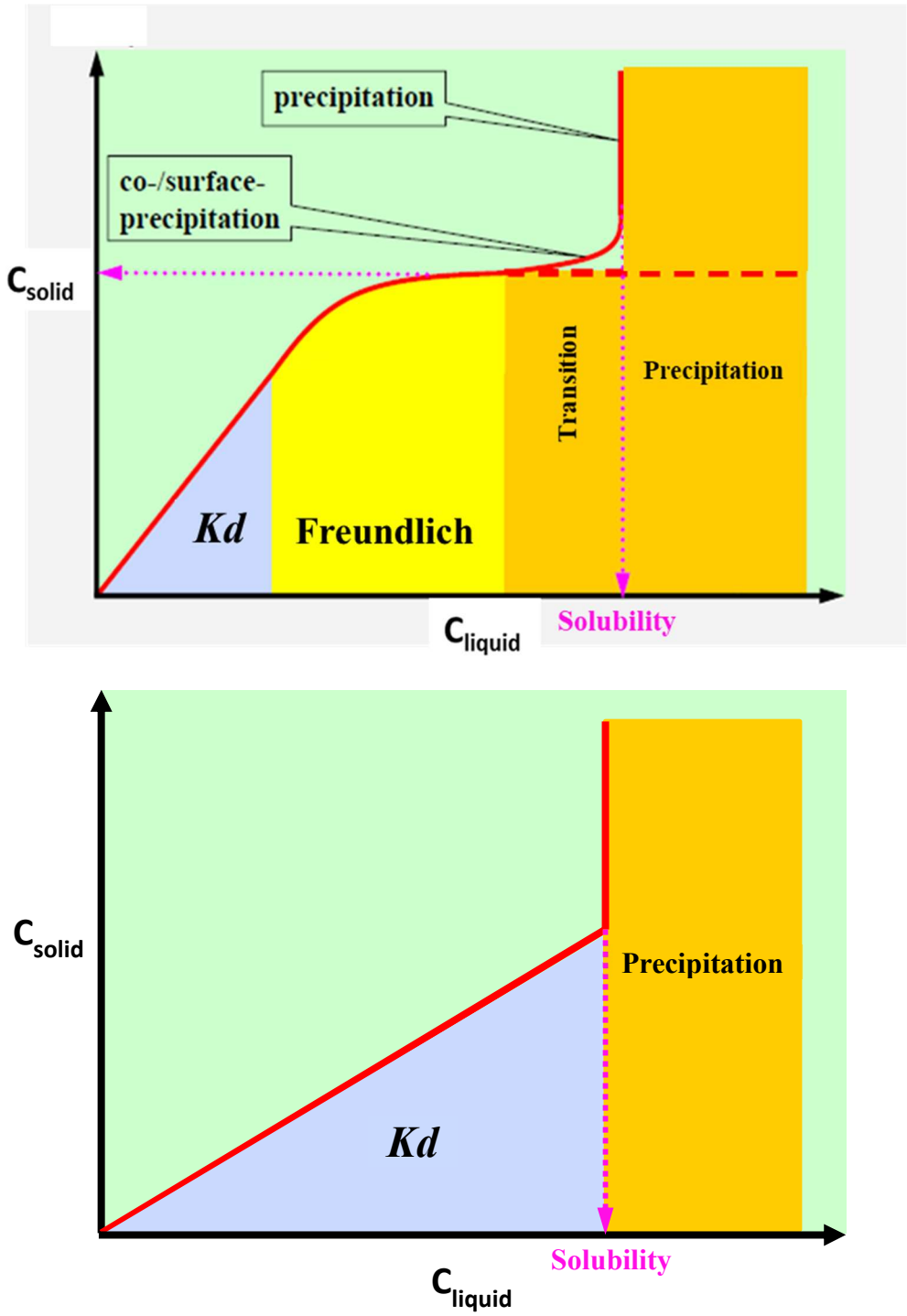

Figure 1. (Top) Idealized sorption isotherm, showing constituent of concern aqueous concentration, C_{liquid}, versus surface-bound, C_{solid} concentration, identifying the linear sorption range (*Kd* sorption), non-linear range (Freundlich sorption), and the apparent solubility concentration (k_s). (Bottom) Simplified sorption isotherm, as assumed in the proposed model, consists of only the linear sorption (*Kd*) and precipitation (k_s) ranges.

3.1.1 Theoretical Distribution Coefficient

The theoretical distribution coefficient is a thermodynamic construct (Kd_{thermo}) (Sposito, 1989). It is the ratio of the concentration of a species reversibly adsorbed/exchanged to surface sites divided by the concentration of the species in the surrounding solution. For example, the species-specific *Kd* value for uranyl is written as follows:

$$Kd_{thermo} = \frac{X{\equiv}UO_2^{2+}}{UO_2^{2+}} \quad (2)$$

where $X{\equiv}UO_2^{2+}$ is the activity of the uranyl species reversibly adsorbed to a specific surface site X, and UO_2^{2+} is the activity of dissolved "free" uranyl species at equilibrium with the surface site X. There are typically several different types of surface sites on a single mineral. For example, goethite (FeOOH) consists of three types of surface sites. Among the many assumptions underpinning Kd_{thermo} is that adsorption is instantaneous, fully reversible (*i.e.,* the rate of adsorption is equal to the rate of desorption), linear (*i.e.,* the proportional adsorption of a solute is not influenced by the aqueous solute concentration; Figure 1) and the presence of adsorbed species does not influence subsequent adsorption of other dissolved species. Thus, a single distribution coefficient is used to represent both sorption and desorption of each solute species in association with each adsorbent site.

Clearly, the Kd_{thermo} construct is overly restrictive for application in the real world where we are interested in describing solute interactions with sediments consisting of dozens of different types of surfaces sites, and where there is a multitude of aqueous species for a single constituent of concern. Therefore, in order to apply the *Kd* construct to solute transport and PA calculations, the definition of the construct needs to be relaxed. For this reason, this text differentiates between Kd_{thermo} and *Kd*, whereby the latter is the more common usage.

Another practical reason for using *Kd* instead of Kd_{thermo} is that it is very difficult to measure the activity of individual chemical species on the adsorbents' surfaces. There are no analytical methods available that permit measuring the thermodynamic activity,[2] as opposed to concentration of a single species bound to a surface. The parameters that can be readily measured are the total solute concentration and not the concentration of the individual species of a solute. Thus, the Kd_{thermo} construct requires differentiating and quantifying each type of surface site and each solution species. Additionally, spatial variability of the surface sites and groundwater chemistry in natural systems cannot practicably be characterized to the degree necessary for the full implementation of species' specific sorption models, such as the triple layer surface complexation model (Jenne, 1998; Kent et al., 1988).

[2] The term "activity" is used here to indicate the concentration of the contaminant at the thermodynamic reference state, a reference state that accounts for, amongst other things, electrostatics. The term is not used here as the activity resulting from radiological decay.

3.1.2 Empirical Distribution Coefficient

The empirical definition of the *Kd* construct is the ratio of the concentration of the complete suite of species bound to the surface divided by the suite of species in solution. Again, using uranyl as an example, the definition of the thermodynamic *Kd* would be for a system containing three U(VI) species [UO_2^{2+}, $UO_2(OH)^+$, and $UO_2(OH)_2^0$]:

$$Kd_{thermo} = \frac{\sum Adsorbed\ U\ Species}{\sum Dissolved\ U\ Species} = \frac{X{\equiv}UO_2^{2+} + X{\equiv}UO_2(OH)^+ + X{\equiv}UO_2(OH)_2^0}{UO_2^{2+} + UO_2(OH)^+ + UO_2(OH)_2^0} \quad (3)$$

where X≡ is the concentration of an average sorbent site (more than one sorbent site-type is expected in nature). Rewriting equation 3, the *Kd* value can be defined as the sum of the sorbed species, the denominator, divided by the sum of the aqueous species, the numerator:

$$Kd = \frac{total\ U(VI) on\ solid}{total\ U(VI) in\ solution}. \quad (4)$$

An important limitation of this empirical *Kd* is that, in theory and in practice, it is not a robust parameter, *i.e.,* it describes solute sorption under a limited set of aqueous and solid phase environmental conditions. Changes in either may be expected to alter the *Kd* value.

Reasons for selecting the *Kd* construct for the PA (and under limited conditions, the apparent solubility values, k_s) include:

1) Most existing sorption literature on radionuclide sorption, especially at SRS can be classified as empirical *Kd* values.
2) Under the expected low concentrations of the solutes in the far field, sorption is expected to be linear, *i.e.*, can be considered to be independent of solute concentration.
3) *Kd* can be used directly in all PA transport codes.
4) Presently, there are not any thermodynamically based conceptual models that are robust enough to predict accurately the degree of constituent of concern adsorption by multiple natural sediments/environments, as needed for the PA (see below).

By using site-specific materials, namely sediments or cementitious materials and groundwater from disposal areas, it is possible to gather relevant data and not rely on extrapolation from other sediment and aqueous systems reported in the literature. The problem with the rigorous thermodynamic species approach is that there is presently no numerical or conceptual model developed that is sufficiently robust to predict accurately the degree of adsorption by natural sediment (Davis et al., 1998; Sposito, 1984; Wang et al., 1997; Westall, 1986, 1994). However, mechanistic models provide the necessary conceptualizations upon which technically defensible empirical *Kd* values must be based. For many of the *Kd* data used in the PA geochemical data package, sorption experiments have been conducted with site-specific sediment, cementitious materials, and groundwater. This approach provides additional

assurance that the correct solid phase and aqueous phase speciation is included in the measurements, without knowing exactly which species comprise these phases.

Another aspect of the *Kd* construct that is typically relaxed when used in solute transport calculations is the strict adherence to the assumption of reversibility. As pointed out earlier, Equation 2 implies an adsorption or exchange reaction that is reversible. The laboratory *Kd* measured with natural sediments and groundwater, often reflect not only adsorption and exchange reactions, but also absorption, specific or somewhat irreversible adsorption, surface complexation, and varying degrees of (co)precipitation reactions. In fact, desorption experiments (described below) have shown that true reversibility is the exception and not the rule (Krupka et al., 1999a). The desorption process occurs either at the same rate or slower than the (ad)sorption process. The reason for this is that during desorption, the solute must first break the bond with the surface, whereas in adsorption, the solute does not need to break a bonding energy.

The importance of first identifying the dominant geochemical process affecting solute concentrations in the mobile aqueous phase can be illustrated through an experiment conducted by Powell et al. (2014). In this experiment, as the pH of SRS sediment-groundwater slurries were increased 1 pH unit, from pH 5.5 to 6.5, Pu(V)-*Kd* values after one day of contact systematically increased from 9 to 1100 mL/g. This trend was explained by corresponding changes in mineral surface charge, and to a smaller extent by changes in the Pu speciation. After 33 days of contact, all the *Kd* values greatly increased; the pH 5.5 *Kd* increased from 9 to 4900 mL/g. Speciation measurements of the bound and aqueous Pu indicated that the added Pu(V) had undergone reduction to Pu(IV), a species that sorbs very strongly to mineral surfaces. Furthermore, the sorption process had also changed from being primarily controlled by Pu(V) surface complexation at 1 day to Pu(IV) surface precipitation after 33 days. This study exemplifies two points. First that *Kd* values can vary greatly with slight changes in the chemistry or mineralogy of the system. A pH change of 1 unit within a plume is not uncommon. Secondly, this example underscores the importance of understanding the sorption process. Once the sorption process is understood, it is appreciably easier to select the experimental conditions needed to measure a *Kd* or select a *Kd* from the literature. On a practical level, this knowledge also often permits greatly reduces the range of potential *Kd* values.

3.1.3 Relation Between Distribution Coefficient and Retardation Factor

In solute transport models, the *Kd* value is used to define the retardation factor, (R_f, unitless) which is the ratio of the average linear velocity of water (υ_w, m/s) divided by the average linear velocity of the solute (υ_c, m/s). For water saturated systems, such as aquifer systems, the *Kd* value is related to the R_f by the bulk density (ρ_b, g/cm^3) and the porosity (η, cm^3/cm^3) as shown in Equation 5 (Bower, 1991; Valocchi, 1984):

$$R_f = \frac{\upsilon_w}{\upsilon_c} = \left(1 + \frac{Kd\rho_b}{\eta}\right). \quad (5)$$

The bulk density and porosity terms in Equation 5 convert the mass-normalized *Kd* value into a volume-normalized value. Note that for partially saturated sediments, such as in the vadose

zone, the porosity term, η, is replaced by the volumetric water content of the vadose zone sediments.

3.2 Apparent Solubility Values

In addition to the *Kd* construct, the apparent solubility values, k_s, (mol/L or M,) were used to describe constituent of concern geochemical behavior, especially within disposal sites and within waste forms (Figure 1). Values of k_s were proposed for conditions where the concentrations of the constituents of concern may exceed the solubility of an assumed solubility-controlling mineral phase. Identification of controlling solid phases for SRS PA activities was based on laboratory experiments, calculations, and the literature. Once the solubility-controlling solid phase was identified, the upper limit (the conservative value for the groundwater pathway) concentration was calculated with the appropriate background electrolyte composition (groundwater composition). When constituents of concern concentrations exceed the solubility concentration for a given mineral, precipitation occurs, and subsequent the constituent of concern aqueous concentrations cannot exceed the k_s. At concentrations below the solubility limit the constituent of concern concentration is assumed to be controlled by the *Kd* construct (Figure 1 – Bottom).

3.3 Brief Overview of Mechanistic Complexation Models

Mechanistic models explicitly accommodate the dependency of *Kd* values on: solute concentration, competing ion concentrations, pH-dependent surface charge, and/or solute species distribution. Incorporating mechanistic, or semi-mechanistic, concepts into models is advantageous because the models become more robust and technically more defensible. There are several mechanistic models that can describe solute adsorption; some are accurate only under limited environmental conditions (Sposito, 1984). For instance, the Stern model is a better model for describing adsorption of inner-sphere complexes, whereas the Gouy-Chapman model is a better model for describing outer-sphere or diffuse-swarm adsorption (Sposito, 1984; Westall, 1986). To fully employ complexation models in the PA requires an increase in data collection to accommodate the wide range of elements and experimental conditions of interest. A brief description of the state of this science is presented below. References to excellent review articles have been included in the discussion to provide the interested reader with additional information.

Experimental data on interactions at the mineral-electrolyte interface can be represented mathematically through two different approaches: 1) empirical models and 2) mechanistic models. An empirical model can be defined as a mathematical description of the experimental data without ascribing any particular sorption mechanism. For example, the *Kd*, Freundlich isotherm, Langmuir isotherm, Langmuir Two-Surface Isotherm, and Competitive Langmuir are considered empirical models by this definition (Sposito, 1984). Mechanistic models refer to models based on thermodynamic concepts such as reactions described by mass action laws and material balance equations. Four of the most commonly used mechanistic models include the Helmholtz, Gouy-Chapman, Stern, and Triple Layer models (Sposito, 1984). The empirical models are often mathematically simpler than mechanistic models and are suitable for characterizing sets of experimental data with a few adjustable parameters or for interpolating between data points. Conversely, mechanistic models contribute to an understanding of the chemistry at the interface and

are often used for describing data from complex multi-component systems for which the mathematical formulation (*i.e*., functional relations) for an empirical model might not be obvious. Mechanistic models can also be used for interpolation and characterization of data sets using adjustable parameters. Adjustable parameters are required for both mechanistic and empirical models, but not for the *Kd* model.

Several mechanistic models have been proposed; however, their application to complex natural sediments is not resolved (Davis and Kent, 1990; Schindler and Sposito, 1991; Sposito, 1984; Westall and Hohl, 1980; Westall, 1986). Any complete mechanistic description of chemical reactions at the mineral-electrolyte interface must include a description of the electrical double layer. While this fact has been recognized for years, a satisfactory description of the double layer at the mineral-electrolyte interface still does not exist.

Part of the difficulty of characterizing this interface stems from the fact that natural mineral surfaces are very irregular and non-homogeneous. They consist of many different micro-crystalline structures that exhibit quite different chemical properties when exposed to solutions. Thus, examination of the surface by virtually any experimental method yields only averaged characteristics of the surface and the interface. Parson (1982) discussed the surface chemistry of single crystals of pure metals and showed that the potential of zero charge (the electrical potential where the surface charge is zero mV) of different crystal faces of the same pure metal can differ by over 400 mV. For an oxide surface, this difference was calculated by Westall (1986) to be energetically equivalent to a variation in the zero-point-of-charge of more than six pH units. This example indicated that a measurable macroscopic property, such as pH, might be the result of a combination of widely different microscopic properties. Another fundamental problem encountered in characterizing reactions at the mineral-electrolyte interface is the coupling between electrostatic and chemical interactions, which makes it difficult to distinguish between their effects. Westall and Hohl (1980) showed that many models for reactions at the mineral-electrolyte interface are indeterminate in this regard.

Mechanistic or surface-complexation models are designed to describe well-defined systems with little or no heterogeneity, unlike natural sediments. One method of addressing heterogeneous systems is an empirical approach that Davis et al. (1998) and Davis et al. (2004) refer to as the generalized composite approach. In this approach, data from experimental soil sorption studies are fitted to various stoichiometric sorption reactions and model formulations based on reaction scheme simplicity and goodness-of-fit (Herbelin and Westall, 1999). This avoids the necessity of detailed mineralogical characterization required in the more general approach that Davis et al. (1998) and Davis et al. (2004) called the “component additivity” approach. It is also important to note that the authors of this approach do not assign specific binding sites (*e.g.,* Fe-oxide “B” sites or planar kaolinite sites) to the solid phases, instead they state that the solid phase has a series of “types of binding sites” that have a similar tendency to bind the constituent of concern. A given soil or mineral, may have two or three such “types of binding sites,” the number is dictated by fitting algorithms, and not by *a priori* assumptions.

Data collection to support the generalized composite approach requires experimental determination of surface complexation under all mineralogical and chemical conditions expected within a plume. The resulting data permits calculating semi-empirical geochemical sorption

parameters that can then be used to describe solute sorption for a wide range of environmental conditions at the study site. Less site-specific data is required to support the component additivity approach and this approach can simulate changing conditions more realistically than the generalized composite approach. For example, if a phase is predicted to precipitate (or disappear) in the future it cannot be accounted for in the generalized composite approach, whereas this can be incorporated into the component additivity approach. The inclusion of these geochemical models into the PA is an eventual goal. One recent successful application of this modeling approach has been with Eu (an analogue for trivalent radionuclides), natural organic matter, and SRS sediment (Kaplan et al., 2010b). The attribute of this approach, albeit still quite limited in application, is that the sorption behavior of a solute can be described in a wide range of environmental conditions, a far more robust description of the system than would be available using a single *Kd* value.

3.4 Colloid-Facilitated Transport of Contaminants

Introduction: Contaminant transport is traditionally modeled in a two-phase system: a mobile aqueous phase and an immobile solid phase. There has been an increasing awareness of a third phase, a mobile solid phase, or colloidal phase. Mobile colloids consist of organic and/or inorganic submicron-particles that move with groundwater flow. When constituents of concern are associated with the mobile colloids, the net effect is that the constituents of concern can move faster through the subsurface system than would be predicted by transport models that do not include mobile colloids. The earliest review of colloid-facilitated transport of contaminants was presented by McDowell-Boyer et al. (1986), and many of their conclusions and most of their references were repeated in a second review by McCarthy and Degueldre (1993). A recent review including the role of nanoparticles was provided by Kretzschmar and Schafer (2006). There have been four locations where subsurface colloid facilitated transport has been observed: 1) Pu at the Nevada Test Site (Kersting et al., 1999), 2) Pu and Am at the Los Alamos National Laboratory (Penrose, 1990), 3) Pu at the Mayak Production Association in Russia (Novikov et al., 2006), and 4) Pu and Am in F-Area, SRS (Buesseler et al., 2009; Dai et al., 2002; Kaplan et al., 1994).

Mobile colloid formation is commonly described as a three-step process: genesis, stabilization, and transport. Colloid genesis describes how the submicron particles are formed in groundwater. Stabilization describes how the colloids are brought into suspension, which is a function of the colloid and groundwater composition and water flow forces. Transport describes how the suspended colloids move through the porous media or are retained by physical forces (such as diffusion, straining, or gravitational settling) or physicochemical attraction to the matrix.

Regarding the first step, colloid genesis, there is little doubt that radionuclide-bearing colloids will be generated at the SRS disposal facilities. Ramsay (1988) presented strong evidence for the existence of colloid particles in glass and cement leachate and provided an in-depth review of the various types of colloids that can/may exist (*e.g.,* glass fragments, precipitation products, geological materials, secondary phases formed from glass leachate). However, it is not clear whether environmental conditions at the SRS are conducive for colloid stabilization and subsequent transport.

Kaplan (2006) conducted a series of colloid dispersion experiments using a series of SRS sediments as a function of ionic strength (the amount of salts in solution), pH, and soil type. pH values had a significant effect on the dispersion of five SRS sediments. At background sediment pH values (pH 4.2 to 5.9), there was minimal or no tendency for clays to disperse. As the pH was increased, there was generally a critical pH value, above which significant dispersion occurred. These critical pH values (between 5.7 and 6.2) were only about half a pH unit higher than corresponding background pH levels. These findings have implications to the PA systems where cementitious materials are present. Cementitious materials will likely elevate pH conditions above ambient levels. However, cementitious materials also create leachates that have chemical properties that promote colloid flocculation, namely they have higher ionic strengths and greater divalent cation concentrations than typical SRS groundwater. (Divalent cations tend to flocculate or agglomerate colloidal particles in suspensions than monovalent cations, because divalent cations reduce more the thickness of the double electric layers and thus the surface potential of the colloidal particles than monovalent cations.)

In a study designed to evaluate the effect of a high-pH cementitious leachate on colloid mobilization, columns studies were conducted with SRS subsurface sediments (Li et al., 2012). The extreme alkaline pH environments of the cementitious leachate resulted in a sharp spike in leachate turbidity, demonstrating that the leachate temporarily promoted the formation of mobile colloids. The mobile colloids consisted primarily of goethite, but they were formed only in the alkaline front as it penetrated through the sediment column. Turbidity sharply decreased, even though the groundwater chemistry did not change. Experiments to evaluate the conditions away from the cementitious source indicated that there were essentially no mobile colloids present.

In a second set of column studies, Li et al. (2013) tested whether the presence of organic matter could promote the formation of mobile colloids. They reported that increases in natural organic matter concentrations resulted in a systematic increase in colloid charge. However, even when chemical conditions favored colloid dispersion (e.g., elevated pH values or organic matter concentrations) subsequent colloid transport was almost completely eliminated due to the SRS sediments' innate capacity to filter out dispersed colloids from moving freely through the pore spaces.

Field studies of colloid facilitated transport of Pu have been studied on the SRS by two groups, the University of Georgia/SRNL (Kaplan et al., 1994; Seaman et al., 1995; Seaman et al., 1997)[3] and Woods Hole Oceanographic Institution (Buesseler et al., 2009; Dai et al., 2002). Together their results detected the presence of Pu on mobile colloids about 700 m from the source (F-Area Seepage Basin). Kaplan et al. (1994) measured Pu associated with a filterable fraction in groundwater recovered in F-Area, which is near the E-Area burial grounds and the Saltstone disposal facility. Very little Pu was found in association with colloids, 0.003 pCi/L $^{239/240}$Pu. To put this concentration in perspective, the Maximum Contaminant Level (MCL) for $^{239/240}$Pu is 15 pCi/L (Federal Register, Vol. 65, No. 236, December 2, 2000); thus, the amount found associated with colloids was 5000 time less than the MCL. However, it does demonstrate that Pu-bound to colloids can move considerable distances, much faster than if described by the conventional two-phase model.

[3] Kaplan et al. (1994) also detected Th, U, Am, Cm and Ra on colloids, and the fraction of radionuclides associated with colloids increased as: Pu > Th > U > Am = Cm > Ra.

The percentage of Pu retained by filters, increased as the pH of the plume increased, which was also concomitant with distance from the point source. Inversely, the percentage of Pu that passed through the smallest membrane, 500 molecular weight cut off (MWCO; ~0.5 nm) decreased with distance from the point source. The ratio between the Pu concentration of colloids in well water and liquid in the source zone did not change in a systematic manner with distance from the source (or pH) (Kaplan et al. 1994).

Dai et al. (2002) also conducted a colloid study in F-Area and concluded that colloids were not involved in Pu transport. The difference between these two results, Kaplan et al. (1994) reporting 28 to 100% colloidal Pu and Dai et al. (2002) reporting no colloidal Pu, may be attributed to significant differences in sampling and analytical techniques. Dai et al. (2002) used more sensitive analytical methods but larger molecular weight cut-off membranes (permitted larger particles to pass through (1000 MWCO (~1 nm)) to separate colloidal from the dissolved fractions than those used by Kaplan et al. (1994; 500 MWCO, (~0.7nm)).

Woods Hole Oceanographic Institution and SRNL returned to F-Area in 2004 to characterize changes in Pu oxidation states and Pu association with colloids in groundwater samples collected six years earlier (Buesseler et al., 2009). They reported small concentrations of Pu associated with colloids. The percentage of Pu associated with colloids, 1 to 23%, was less than that reported by Kaplan et al. (1994), 28 to 100%, but was more than that reported by Dai et al. (2002), 0 to 10%. They concluded that Pu moved primarily in the dissolved state (and in the higher Pu oxidation states). They reported that colloidal Pu increased systematically with decreases in redox conditions. They observed greater dynamic shifts in Pu speciation, colloid association, and transport in groundwater on both seasonal and decadal time scales and over short field spatial scales than commonly believed.

Colloid Models: Accurate colloid-facilitated contaminant transport models are important to estimate the role this mode of transport may contribute. Models have always been more advanced than the ability of scientists to measure accurate input values for these models. They serve an important role as a tool for helping to understand what cannot be measured accurately. But because the input to these models is still lacking, the results from modeling studies are not quantitative. As discussed above, most models described colloid facilitated contaminant transport as an equilibrium partitioning of contaminants between the solution phase, colloid surfaces, and media surfaces (Grindrod, 1993; Hwang et al., 1989; Smith, 1993). The equilibrium assumptions can be simplified considerably, permitting analytical or semi-analytical solutions to be implemented (Grindrod, 1993; Hwang et al., 1989). Corapcioglu and Jiang (1993) included numerical models with first-order reversible rate expressions to describe contaminant sorption onto both colloid and media surfaces, as well as first-order expressions describing colloid attachment and detachment to media surfaces. Noell et al. (1998) used the model of Corapcioglu and Jiang (1993) to describe a ^{137}Cs silica colloid transport model through a glass bead column. Ibaraki and Sudicky (1995b) and Ibaraki and Sudicky (1995a) and Oswald and Ibaraki (2001) incorporated kinetic expressions to explicitly describe colloid-facilitated contaminant transport in fractures and matrix diffusion.

Thermodynamic databases are employed to estimate the formation of facilitated transport species, whether they are complexed species, precipitated colloidal species, or strongly sorbed species on minerals. Thermodynamic properties or stability constants for 246 lanthanide complexes with chloride, fluoride, hydroxide, carbonate, sulfate, bicarbonate, nitrate, and orthophosphate were calculated at pressures of 1 to 5,000 bars and 0 to 1,000 °C (Haas et al., 1995). This database of stability constants can be used to predict colloid formation under different environmental conditions. An especially useful review of how to treat natural and anthropogenic organics in numerical and conceptual models and a large number of constants is provided by Schwarzenbach et al. (2005). EQ3/EQ6 is a reaction path code, which describes the evolution of a water/rock system as reaction progress over (Wolery, 1992). This is especially important in waste packages as the solid phase changes properties, such as glass and its binding properties to radionuclide changes. EQ3/EQ6 also has a large radionuclide database and Pitzer input. MINTEQA2 (http://www.epa.gov/ceampubl/mmedia/minteq/) is an EPA equilibrium speciation model that can be used to calculate the equilibrium composition of dilute aqueous solutions in the laboratory or in natural aqueous systems. Its database, PRODEFA2, includes numerous radionuclides, but few of the actinides of concern for facilitated transport are included. Also, radiological decay is not included as a subroutine. Geochemist's Workbench (http://www.rockware.com) (Bethke and Yeakel, 2009) is commonly used software because of its ease of use, graphics capability, large existing thermodynamic database, and ability to import new thermodynamic data. Like EQ3/EQ6, Geochemist's Workbench is a reaction path code. An important caveat with the use of each of these thermodynamic codes is that it is incumbent upon the user to make sure that the appropriate constants are present within the database for the conditions being modeled. For example, if EDTA is present in a reducing plutonium contaminated system, it is necessary to ensure that, at a minimum, there are constants for EDTA with Pu(IV) in the database.

Modeling colloid facilitated transport of radionuclides in the SRS subsurface environment is greatly hindered by the paucity of data on the subject. Measurements presented by Kaplan et al. (1994), Dai et al. (2002), and Buesseler et al. (2009) were conducted in the F-Area Seepage Basin plume, which is very acidic, pH 3 to 5.5 (background). As such, it does not reflect conditions expected in any of the PA scenarios. In fact, if anything, plumes of interest to SRS PAs will likely have a background pH of ~5.5 or an alkaline pH due to the common use of cementitious engineered barriers (Section 5.0). Given this important caveat, the Pu concentration carried by colloids, based on F-Area results, were thousands of times below the MCL (15 pCi/L), even though an estimated 7,000,000,000 pCi of $^{239/240}$Pu was disposed in the seepage basins. At higher pH systems than that of F-Area, it is likely that colloids would play a greater role in transporting contaminants. It is difficult to determine to what extent more mobile colloids would exist in the various plumes of interest to the PA. If the number of colloids increases by a couple orders of magnitude above that detected in F-Area, it is likely that the groundwater concentration of strongly sorbing contaminants, such as Pu, Ac, Am, Cm, Eu, or Th, would increase due to the rise of their association with colloids. It is not clear that this increase would necessarily produce conditions that would lead to these radionuclides exceeding the MCL limits.

4.0 CONCEPTUAL GEOCHEMICAL MODEL

As discussed in Section 3.0, a simplified geochemical model with respect to the state-of-the-science is required for SRS PA calculations because of the large number of constants and supporting characterization necessary for 64 constituents of interest and because of the wide range of SRS geochemical conditions expected in the near and far fields over the thousands of years of interest. The simplified conceptual model includes two types of parameters, the empirical *Kd* and apparent solubility value, k_s (Figure 1 – Bottom). In the conceptual model, we assume that aqueous solute concentrations are controlled primarily by the *Kd* construct, but in limited geochemical conditions, both the *Kd* and the k_s terms will be used, the former for conditions below the critical solubility concentration, and the latter for conditions above the critical solubility concentration. Furthermore, we assume that the *Kd* and k_s of the 64 constituents of interest may vary between 12 Conceptual Environments, which are generalized geochemical conditions (discussed immediately below in Section 4.1). For each constituent of concern and Conceptual Environment a "best," "minimum," and "maximum" estimate of the *Kd* values and k_s, are provided. The "best" estimates are provided as guidance for the most likely *Kd* values and apparent solubility values for a given Conceptual Environment (the approach to selecting these "best" estimates is provided in Section 4.2). These values are based primarily on the literature, SRS site-specific experimental data, or on expert judgment. Assignment of *Kd* value and apparent solubility value ranges are presented below in Section 4.8.

4.1 Conceptual Environments

To facilitate modeling the wide range of chemical conditions needed for PAs and CAs on the SRS, 12 Conceptual Environments were established. These Conceptual Environments account for important geochemical parameters influencing constituent of concern sorption within a setting. As such, the Conceptual Environments are operationally defined by their aqueous and mineralogical environmental properties. Following is a list of each Conceptual Environment and the section in which they are described:

1. Clayey Sediment (described in more detail in Section 4.3.1),
2. Sandy Sediment (Section 4.3.2),
3. Young Cementitious Materials (Section 4.4.1),
4. Moderately Aged Cementitious Materials (Section 4.4.2),
5. Aged Cementitious Materials (Section 4.4.3),
6. Cementitious-Leachate Impacted Sandy Sediment (Section 4.4.5),
7. Cementitious-Leachate Impacted Clayey Sediment (Section 4.4.6),
8. Young Reducing Cementitious Materials (Section 4.5.3),
9. Moderately Aged Reducing Cementitious Materials (Section 4.5.4),
10. Aged Reducing Cementitious Materials (Section 4.5.5),
11. General Waste Forms (Section 4.6), and
12. Special Waste Forms (Section 4.7).

4.2 Approach to Selecting Geochemical Values

Ideally, all input data would be derived from experiments conducted using site-specific materials and under the appropriate Conceptual Environmental conditions. For example, much of the Clayey Sediment and Sandy Sediment *Kd* data were, in fact, derived from sorption experiments conducted with site-specific sediments and site-specific groundwater. A major recent effort has been directed at understanding and quantifying constituents of concern transport through SRS vadose zone sediments at longer durations (years), and larger scales (kg) than is typically provided through laboratory experiments. These experiments are housed in the Radionuclide Field Lysimeter Experiment, or RadFLEx. This facility was initiated in July 2012 and will continue through July 2032. A summary of recent technical RadFLEx accomplishments were presented by Kaplan et al. (2018).

Where site-specific data was not available, literature *Kd* values using non-SRS solid and aqueous phases were used. Careful selection of these literature values was required to ensure that the experimental conditions used to generate the *Kd* values were appropriate for SRS conditions. For example, literature *Kd* values were used for the selection of K, Mn, and Fe recommended "best" clayey and "best" sandy sediment Conceptual Environments. Finally, when site-specific and literature values were not available, expert judgement was used to estimate values based on chemical analogue information. For example, no site-specific sorption data is available for Fr (francium) and Rb (rubidium), however, a great deal of SRS sediment sorption data is available for Cs. Cesium has many chemical characteristics that are similar to Fr and Rb; all three elements: are in Group 1A in the periodic chart, have a +1 valence, form weak complexes to anions, and exist in groundwater primarily as an uncomplexed monovalent free ion (Greenwood and Earnshaw, 1998). For these reasons, Fr and Rb *Kd* values were assumed to be approximated by measured Cs *Kd* values on SRS sediments.

In summary, a ranking of the priority for selecting *Kd* and apparent solubility values (k_s) is:

1. site-specific measured data,
2. literature experimental data, and
3. technical judgment based on analogue.

Uncertainty in the selected "best" values was bounded by "minimum" and "maximum" estimates based on experimental work (Grogan, 2008; Grogan et al., 2010; Kaplan et al., 2008c), and are included to provide ranges of potential values needed for stochastic modeling. The experimental data provided the distributions of the sample mean *Kd* and the 95% confidence levels from hundreds of *Kd* value measurements made from 27 E-Area subsurface sediments using monovalent, divalent, trivalent and tetravalent radionuclides. These "minimum" and the "maximum" estimates were based on the 95% confidence limits of the mean *Kd* (discussed in Section 4.8).

4.3 Sediment Conceptual Environments

The subsurface environments beneath the waste units in the SRS are assumed to consist of two primary geological strata. This simplification of the subsurface is taken from Phifer et al. (2006) and was based on particle-size distribution data and observations of several borehole specimens made in the E-Area subsurface environment. Phifer et al. (2006) described the upper strata as extending about 7 m below the surface and having a finer texture than the underlying strata, which may extend some 27 m below ground surface, depending on the specifics of the site lithology. The upper layer was referred to as the Upper Vadose Zone, whereas the lower zone included both the Lower Vadose Zone and the Aquifer Zone. The water table in E- and Z-Area is approximately 15 to 25 m below the ground surface. An example of the sediment texture and the delineation of the Upper and Lower Vadose Zone and the Aquifer Zone is presented in Figure 2.

There were unique sorption values for Clayey Sediment and Sandy Sediment Conceptual Environments, meant to represent the Upper Vadose Zone and Lower Vadose/Aquifer Zones, respectively. Also important to note is that the data provided in the data look-up table in Section 5.0 are assigned to each of the 12 Conceptual Environments. The extent that environmental conditions deviate from their "ideal" descriptions in this section, compromise the applicability of the selected data values. For example, the *Kd* values provided for a Sandy Sediment Environment or a Clay Sediment Environment would not be especially applicable for a wetland because the "ideal" description is for a subsurface sediment with a much lower organic matter content than for a typical wetland.

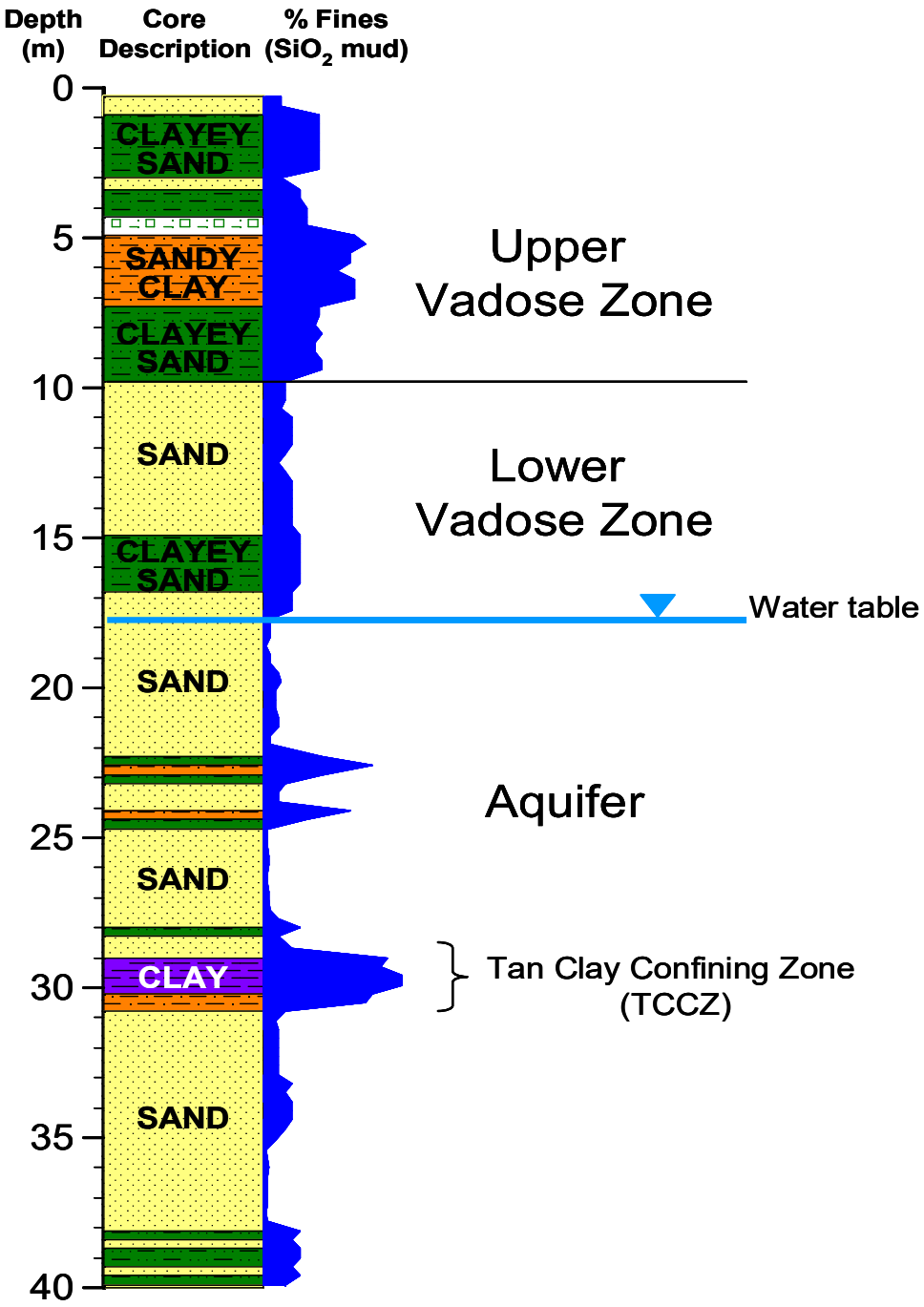

Figure 2. Example of a borehole profile in E-Area demonstrating the tendency for sediments with a more clayey texture to exist in the Upper Vadose Zone, whereas sediments with a sandier texture to exist in the Lower Vadose and Aquifer Zones (Well BGO-3A) (Grogan et al., 2010; Grogan et al., 2008).

4.3.1 Clayey Sediment Conceptual Environment

The Clayey Sediment Conceptual Environment represents a subsurface sediment environment that contains:

- a clay and silt content greater than about 25 wt-%,
- a mineralogy composed primarily of kaolinite, hydroxyl-interlayered vermiculite, quartz, gibbsite, goethite, and hematite (most notable about its mineralogy is that it contains very low concentrations of 2:1 clays, such as smectites and vermiculites),
- a low organic matter concentration (<0.01 wt-%),
- a pH of about 5.5, and
- iron-oxide surface coatings, giving it a reddish color.

4.3.2 Sandy Sediment Conceptual Environment

The Sandy Sediment Conceptual Environment represents a subsurface environment that is similar to that of the Clayey Sediment Conceptual Environment except the clay and silt content was <25 wt-%. Most of the sorption experiments considered for the look-up tables came from sandy sediments with clay and silt concentrations appreciably <25 wt-%, closer to 2 to 8 wt-%. This Conceptual Environment has a pH of 5.5, very low organic matter concentrations, and the sediment tends to have a yellowish color derived from Fe-oxide coatings (most noticeably, goethite).

4.4 Cementitious Materials Conceptual Environments

The conceptual model used to describe constituent of concern geochemistry in cementitious environments was taken largely from Bradbury and Sarott (1995) and has since been used in PA modeling in several countries in Europe, Yucca Mountain, Idaho National Laboratory, Hanford Site, and SRS. They described three Conceptual Environments, or stages, that all cementitious materials progress through as they age (Figure 3). The duration of each stage is controlled by how much water passes through them, measured in units of pore volumes or exchange cycles (X-axis of Figure 3). The advantage of using Figure 3 and the concept of exchange cycles is that it is generic to a wide range of cementitious material configurations. Once flow models have been established for a specific facility, the exchange cycles for that facility can be quantified. Facilities with more concrete will have longer exchange cycles (larger pore volumes) than those with less concrete.

Development of this conceptual model was based on laboratory studies as well as on natural analogue and ancient cement/concrete characterization studies. One of the key aqueous parameters used to identify when one stage ends and the next one begins is pH (Figure 3). The pH changes are the result of mineralogical transformations that occur as the cement ages. The cement solids present in each stage are assumed to have unique sorption properties and for this reason, unique *Kd* values and apparent solubility values were assigned to the cement solids in each stage. A brief description of each of the three stages is provided in Sections 4.4.1 through

4.4.3, while a more detailed discussion is presented in Ochs et al. (2016). Unique *Kd* values and apparent solubility values for oxidizing and reducing cementitious materials are provided in Section 5.0.

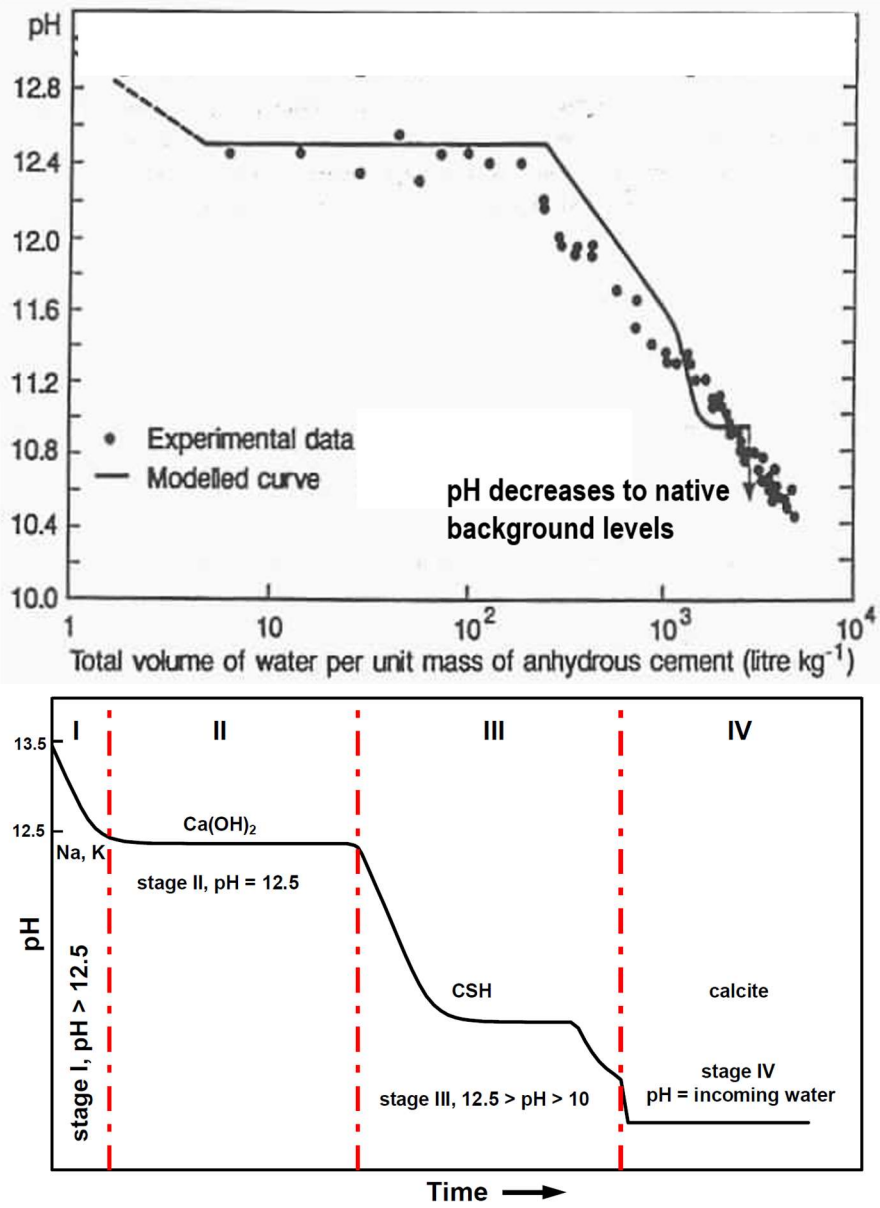

Figure 3. (Top) Experimental data describing the influence of exchange cycles (X-axis) on pH and the designated Stages (Atkinson et al., 1988), and (Bottom) Four Stages identified by (Ochs et al., 2016; Wang et al., 2009). Exchange cycles and time, X-axes, can be converted to each other with knowledge of flow rate (L/yr).

A fourth stage has recently been suggested for the European Union PA (Ochs et al., 2016; Wang et al., 2009). This added stage is in equilibrium with calcite and is experimentally equivalent to our cementitious-leachate impacted sediment environment (Sections 4.4.5 and

4.4.6). This fourth stage was slightly modified for use in the SRS system. Unlike most European sediments, the background sediment at SRS (pH 5.5) is not in equilibrium with calcite (pH ~8.2). While Stage IV in Ochs et al. (2016) system is continuously in equilibrium with calcite (note the flat line in Figure 3 for Stage IV), the Stage IV is defined here as that region that progresses from one being in equilibrium with calcite and once the calcite is dissolved approach the background pH of 5.5, as experimentally captured by Atkinson et al. (1988).

4.4.1 Young Cementitious Materials Conceptual Environment (Stage I)

The Young Cementitious Solids Environment, referred to as Stage I, occurs immediately after the cementitious material hardens and water infiltrates it. The cementitious material porewater is characterized as having a high pH (>12.5), high ionic strength, and high concentrations of potassium and sodium. The high concentrations of these monovalent cations result from the dissolution of alkali impurities in the various constituents comprising the solids (*e.g.,* Portland cement, fly ash, aggregate and sometimes slag). Hydration continues during Stage I with the formation of calcium-silicate-hydrate gels (a common shorthand for this gel is CSH, which is a $CaO\text{-}SiO_2\text{-}H_2O$ amorphous material that hardens and constitutes "cement") and portlandite [$Ca(OH)_2$]. The composition of the cement pore fluid is at equilibrium with portlandite during this time.

Based on the modeling estimates provided by Berner (1992), Stage I may last between 1 and 100 exchange cycles. An exchange cycle, or cycle, is a unitless parameter that represents the length of time it takes for a pore volume to pass through a cementitious structure. This parameter in turn can be quickly converted into units of time once the water travel rate through a specific cementitious facility is established. Unfortunately, assuming a low exchange cycle value for this stage may be conservative for some constituents of concern, such as Pb, but not conservative for other constituents of concern that tend to form precipitates at high pH values (*i.e.,* constituents of concern that have low solubility values). Therefore, it was assumed that the Stage I lasts 50 exchange cycles for SRS relevant scenarios.[4]

4.4.2 Moderately Aged Cementitious Materials Conceptual Environment (Stage II)

During this stage, the soluble salts of the alkali metals are all dissolved and washed out of the cement solids. The pH value of the cement pore water stabilizes at about pH ~12.5, controlled by the solubility of portlandite. The calcium-silicate-hydrate gel and portlandite are the major solid phases present. Stage II may last for a long time, and its duration depends on how much water percolates through the system and the mass of cement present in the concrete structure. The total dissolved calcium is 20 mM, the pH is strongly buffered at pH ~12.5, and the silica

[4] This value of 50 exchange cycles or pore volumes is a recommended value if a project-specific value is not calculated using a reactive transport model. For example, for calculations associated with the SRS Liquid Waste Tanks Closure PA, a reactive transport model was used based a site-specific data to estimate transitions between Stages 1, 2 and 3 (Denham 2007; Denham 2008). Based on pH and Eh transformations estimated by Geochemist's Workbench calculations, the first stage ended after about 30 pore volumes through the tank grout.

concentration is very low, <0.03 mM/L. The flux of water must dissolve all the slightly soluble portlandite before the leachate chemistry changes.

Berner (1992) determined that Stage II lasts between 100 and 1000 cycles. According to Ochs et al. (2016) and adopted here, most constituents of concern have higher *Kd* values and solubility concentration limits in Stage II than in Stage III. Therefore, a shorter Stage II lifespan is generally a conservative estimate because it yields greater estimated risk. The Stage II *Kd* values and apparent solubility values are generally higher than those in the Stage I. Notable exceptions include when cation (Sr) or anion (I, Tc, Se) adsorption are expected to be the dominant mode of solid phase uptake, in which case the *Kd* in Stage I will be lower than in Stage II due to high salt concentrations in the porewater. Taking into consideration the dissolving attributes of the low-carbonate SRS groundwater when in contact with cementitious solids, an exchange cycle of 500 cycles was assumed.

4.4.3 Aged Cementitious Materials Conceptual Environment (Stage III)

In Stage III, the portlandite has been fully dissolved/reacted and the solubility or reactions of calcium-silicate-hydrate (CSH) gel with the infiltrating water control the pH of the cement porewater/leachate (Figure 3). The CSH gel starts to dissolve incongruently[5] with a continual decrease in pH until it reaches the pH controlled by calcite, the only Ca-bearing mineral remaining, which is pH ~8.2. The CSH at the start of Stage III has a calcium-silicate ratio of about 1.7; by the end of this stage, only silicate (SiO_2) is left as the solubility control for the pore water pH. The ionic strength of the cement leachate during this period is relatively low. Solution calcium concentrations decrease to 1 to 5 mM and silica concentrations increases to 2- to 6-mM. At very high cycle numbers, other sparingly soluble solids, such as brucite [$Mg(OH)_2$], may buffer the solution pH and dissolved cation concentrations.

Berner (1992) suggested that the duration of the 3rd Stage is between 1000 and 10,000 cycles. Because SRS groundwater is low in carbonate concentrations, a shorter duration for this stage would be appropriate; a "lifetime" of 4000 cycles was selected for the SRS PA calculations. A discussion of estimating the longevity of concrete in the subsurface is presented in Kaplan (2010).

4.4.4 Near-Completely Degraded Cementitious Materials Conceptual Environment (Stage IV)

This stage is defined as progressing from a system in equilibrium calcite (pH ~8.2) to one in which the calcite is totally dissolved and the pH of the system returns to background levels (pH 5.5). This system is experimentally equivalent to our cementitious-leachate impacted sediment environment (Sections 4.4.5 and 4.4.6). This fourth stage was slightly modified from that posed by Ochs et al. (2016) to represent better the SRS system. Unlike most European sediments, the background sediments at SRS are not naturally in equilibrium with calcite.

[5] Incongruent dissolution is the non-stoichiometric dissolution to a solid, resulting in the release of dissolved materials into the aqueous that have different proportionalities than the existed in the solid phase.

Berner (1992) suggested that the duration of the 3rd Stage is between 1000 and 10,000 cycles. Berner's 3rd Stage includes Stage III and IV in this model, which is based on the model proposed by Och et al. (2016). Because SRS groundwater is low in carbonate concentrations, a shorter duration for Stage III was selected, 4000 cycles. Based on these considerations, it was recommended that 6000 cycles be used in the 4th Stage of the SRS PA calculations (10,000 – 4000 = 6000 cycles).

4.4.5 Cementitious Leachate Impacted Clayey Sediment Environment

Cementitious porewater contains moderate levels of ionic strength (a measure of the total salt content), perhaps 150 times greater than ionic strength concentrations of unimpacted groundwater (Table 1). When it enters the underlying sediment, it alters the porewater chemistry, which in turn may alter the tendency of mobile aqueous constituents of concern to sorb onto the sediment. Demonstrating this point under SRS conditions, thermodynamic simulations were conducted of the porewater chemistry during each of the three idealized stages of cement aging (Denham 2007). During Stage I, Stage II, Stage III, and Stage IV, alkali impurities, portlandite, CSH gel, and calcite were assumed to be the dominant phase controlling aqueous composition, respectively (Table 1). The most important point to take away from this table is that the pH and ionic strength during the two early stages of cement aging, Stages I and II, are very different from the background SRS groundwater. The leachates have a much higher pH and ionic strength. Such solutions can increase sorption by promoting precipitation, *e.g.,* UO_2^{2+} (Kaplan et al. 1998), and in other cases decrease sorption by promoting competition for sorption sites (Kaplan et al. 1998; Cantrell et al. 2007). For example, using Hanford sediments, Kaplan et al. (1998) showed that Se had *Kd* values of 6 mL/g under natural groundwater conditions (pH 8.1). When the ionic strength was increased, the *Kd* values decreased (*Kd* = 4.11 mL/g at 1 M $NaClO_4$) and when the pH was increased the Se *Kd* values decreased (*Kd* = 0.04 mL/g at pH 11.9), suggesting that anionic competition, likely hydroxide or carbonate, and/or anion exchange capacity was involved in the desorption process. Neither I^- nor TcO_4^- sorption was measurable (i.e., *Kd* = 0 mL/g) in the Hanford sediment under natural conditions or when the pH was increased to pH 12.

Table 1. Calculated leachate chemical compositions during the three stages of cement degradation. For comparison, the chemical composition of an SRS groundwater (Denham, 2007).

	Cementitious Leachate – Stage II[(a)]	Cementitious Leachate – Stage III[(b)]	Cementitious Leachate – Stage IV[(c)]	SRS Groundwater[(d)]
pH	12.37	11.14	9.56	5.79
Eh (V)	0.49	0.56	0.66	0.33
Ionic Strength	4.6E-2	8.2E-3	7.0E-4	3.0E-4
Al^{3+} (mol/L)	2.19E-5	1.05E-7	1.32E-5	3.33E-5
Ca^{2+} (mol/L)	1.83E -2	2.92E-3	1.43E-4	1.01E-5
Cl^{-} (mol/L)	2.64E-4	2.65E-4	2.65E-4	7.65E-5
Fe^{3} (mol/L)	6.87E-10	3.63E-11	1.70E-12	9.93E-7
HCO_3^{-} (mol/L)	4.59E-6	6.90E-6	1.81E-4	~0
Mg^{2+} (mol/L)	1.04E-8	2.16E-5	4.99E-5	2.92E-5
Na^{+} (mol/L)	1.33E-4	1.33E-4	1.33E-4	1.20E-4
SO_4^{2+} (mol/L)	5.16E-5	2.08E-6	2.08E-6	6.41E-5
SiO_2^{-} (mol/L)	1.29E-3	2.95E-3	~0	1.69E-4

[(a)] Stage II solid phase (portlandite dominant) was modeled consisting of 50-g hematite, 176-g ettringite, 669-g Ca-silica-hydride phase, 13-g hydrotalcite, 171-g C_4AH_{13} phase, 138-g portlandite, and 1-g calcite; 110 pore volumes.
[(b)] Stage III solid phase (CSH dominant) was modeled consisting of 51-g hematite, 366-g CSH, 17-g hydrotalcite, and 6-g calcite; 1143 pore volumes.
[(c)] Stage IV solid phase (Calcite dominant) was modeled consisting of 52-g hematite, 19-g hydrotalcite and 7-g calcite; 2380 pore volumes.
[(d)] Uncontaminated groundwater on the SRS, Well No P19D.

The influence of cementitious-leachates on uranyl sorption to Hanford sediment was found to gradually increase from 1.07 to 2.22 mL/g as the pH increased from 8.3 to 9.3 (Kaplan et al., 1998). At pH ≥10.3, precipitation occurred and the apparent *Kd* value increased sharply to >400 mL/g; the precipitation did not occur unless the sediment was present, suggesting the mechanism was heterogeneous precipitation.[6] Thus, at the Hanford Site they use much higher *Kd* values to describe U sorption to sediments in a cementitious leachate impacted environment, 100 mL/g, than they use to describe U sorption under ambient conditions, *Kd* = 0.2 mL/g (Cantrell et al., 2007) (Cementitious Leachate Sediment Value came from "Waste Chemistry/Source Category 6: IDF Cementitious Waste High Impact, Table 3.2, Page 3.10;" and Ambient value came from "Waste Chemistry/Source Category 4: Low Organic/Low Salt/Near Neutral, Table 3.2, page 3.9").

[6] Heterogeneous precipitation requires a mineral surface present for precipitation to occur. Homogenous precipitation can occur in the absence of a surface.

Kaplan (2010) presented calculations that demonstrated that the hydroxides emanating from the cementitious leachate during Stages I and II of concrete degradation (pH 11 and ionic strength of 20 mM) will likely overwhelm the buffering capacity of SRS subsurface vadose zone sediments. The hypothetical high ionic strength plume was dominated by hydroxides and Ca^{2+} (Table 1). In this calculation, a 1-m thick cementitious slab overwhelmed the sediment buffering capacity in a 30-m thick vadose zone. Once this high pH front reached the aquifer it would be rapidly diluted and likely have negligible influence on subsequent solute sorption.

Cementitious Leachate-Impacted Clayey Sediment Environment is defined as a Clayey Sediment Conceptual Environment between a cementitious waste form and the aquifer. This Conceptual Environment has a nominal pH of 10.5 and an elevated ionic strength >20 mM dominated by hydroxide and Ca^{2+} ions. Early guidance will rely on measured differences between cementitious-leachate impacted and non-impacted *Kd* values for the Hanford PAs (Cantrell et al. 2007). Cementitious Leachate Impact Factors, $f_{CementLeach}$, are used to convert traditional *Kd* values into $Kd_{CementLeach}$ values that are more representative of a cementitious impacted sediment:

$$f_{CementLeach} = \frac{Kd_{CementLeach}}{Kd} \quad (6)$$

where $Kd_{CementLeach}$ and *Kd* are the *Kd* values measured under cementitious-leachate and natural groundwater conditions, respectively. To calculate SRS $Kd_{CementLeach}$ values to use in SRS PAs, Eq. 6 is reorganized:

$$Kd_{CementLeach} = f_{CementLeach} \times Kd \quad (7)$$

Equations 6 and 7 are practical but lack geochemical rigor. They are intended to provide provisional guidance until a more robust sorption model can be created that incorporates the changing chemistry (especially pH and ionic strength) of cementitious leachate as it evolves through the various cement aging stages. It is important to note that the $f_{CementLeach}$ is a simplified construct of a dynamic PA environment; one that can readily be made more robust with additional measurements. The complexity of estimating geochemical parameters in a cementitious leachate sediment environment stems from: 1) there being several different types of cementitious materials of interest to PAs (reducing grout, Saltstone, CLSM, traditional concrete, high strength concrete, etc.), 2) the leachate chemistry is expected to change over time, and 3) the impact cementitious leachate on traditional *Kd* values will vary with sediment properties. As measurements continue to be made, it is expected that this simplified conceptual model will be replaced with a more robust model, one that explicitly accounts for changes in pH, ionic strength, and sediment type.

A discussion of the basis for selecting Cementitious Leachate Impact Factors is presented in an earlier versions of this data package (Kaplan, 2016). As noted above, most of these factors are based on data compiled by Cantrell et al. (2007) for the Hanford Site's PA. There was some confirmation of these estimates based on testing conducted by Seaman and Chang (2013) using site specific sediments and groundwater (Table 2). Additional work is needed to quantify *Kd*

values appropriate for these environmental conditions (a list of recommended research needs is provided in Section 7.0).

Table 2. Literature-based Cementitious Leachate Impact Factors (Eq. 6).

Radio-nuclide	Hanford Ground water[a] Best *Kd*	Hanford IDF Cementitious Waste[b] Intermediate Impact Sand – Best *Kd*	Cementitious Leachate Impact Factor, $f_{CementLeach}$[c] (Unitless)	Suggested $f_{CementLeach}$ (Unitless)	Comments[d]
H	0	0	NA	1	
Tc	0	0	NA	0.1	High pH will greatly reduce anion exchange capacity. Furthermore, high ionic strength will promote desorption of ion that are weakly sorbed. Unlike Hanford sediment, SRS sediments tend to sorb small quantities of TcO_4^-, but only under low pH environments (Kaplan, 2002; Kaplan et al., 2008c)
Cl	0	0	NA	0.1	Similar chemistry as Tc.
I	0.2	0.2	1	0.1	Using Hanford sediment, Kaplan et al. (1998) showed that I *Kd* decreased from 0.22 mL/g at pH 8.1 to 0.01 mL/g at pH 9.9.
U	0.8	1	1.25	5	The Hanford recommended value (3rd column) suggests the authors Cantrell et al. (2007) believe that sorption and not precipitation occurs under these conditions. Kaplan et al. (1998) reported uranyl precipitation under mildly cementitious environments, at pH ≥10.3. pH will be ≥10.3 in this plume and therefore much larger *Kd* values are recommended here.
Se	5	7	1.4	1.4	
Np	10	15	1.5	1.5	
C	0	5	NA	5	
Sr	2.2	14	6.4	3	Cantrell et al. (2007) did not comment on why the Sr *Kd* increased. Co-precipitation as Sr, Ca-carbonate is not expected, but perhaps some have occurred in microenvironments. *A prior* it was anticipated that Sr exchange would occur resulting in lower *Kd* values.
Cs	2000	2000	1	1	
Pu	600	150	0.25	2	In cementitious environments, pH 7 solubility of Pu is 10^{-5}. Above the pH of 9, the solubility of Pu drops to 10^{-10} M (Ewart et al., 1992).
Eu	200	300	1.5	1.5	

[a] Taken from page 3.9, Table 3.2 in Cantrell et al. (2007).
[b] Taken from Table 3.10, Table 3.2 Cantrell et al. (2007) . Selected "Intermediate Impact" and not "High Impact" because the former is more conservative with respect to the groundwater scenario (lower *Kd* values, and over the course of multiple ages (Stage I, Stage II, and Stage III). It was thought that "intermediate impact" would be more representative than "high impact" over the entire age of the facility. IDF = Intergraded Disposal Facility
[c] Equation 6.
[d] Additional discussion of the assumptions and limitations of the Cementitious Leachate Impact Factor is presented in previous version of this geochemical data package (Kaplan, 2010; Kaplan, 2016).

4.4.6 Cementitious Leachate Impacted Sandy Sediment Environment

The Cementitious Leachate Impacted Sandy Sediment Environment is similar to the Cementitious Leachate Impacted Clayey Sediment Environment discussed in Section 4.4.5 except it is for the lower Sandy Sediment Environment that exists between cementitious waste forms and the aquifer. $Kd_{CementLeachate}$ values for this Environment are created in the same manner as above, namely, using Equation 6, Equation 7, and Table 2.

4.5 Reducing Cementitious Materials

4.5.1 Chemistry Associated with Reducing Cementitious Wasteforms

Some cementitious materials have blast-furnace slag (BFS) included in their formulations to promote stabilizing radionuclides by reductive precipitation, thus decreasing the tendency of some redox-sensitive radionuclides (e.g., Np, Pu, and Tc) to leach from the solid waste form. There have been several recent reviews evaluating the effect of reducing cementitious materials on Tc immobilization, the key risk drivers in several DOE PAs (Cantrell et al., 2016; Chung et al., 2012; Icenhower et al., 2010; Kaplan et al., 2011; Pearce et al., 2018; Pierce et al., 2010; Serne et al., 2015; Um et al., 2013; Um et al., 2011; Westsik Jr et al., 2014).

4.5.2 Porewater Pathway of Redox-sensitive Radionuclides from Reduced-Cementitious Materials – Shrinking Core Model

The reductive capacity of the BFS-cementitious material is expected to decrease over time. As the waste form ages and becomes increasingly oxidized, it is expected that the capacity of the waste form to immobilize redox-sensitive radionuclides will decrease. One geochemical approach to model the advancement of the oxidation front within reducing cementitious materials is the Shrinking Core Model (Smith and Walton, 1993). This model describes the advancement of the oxidized front as resulting from oxidized water diffusing into cement and then chemically consuming (oxidizing) the unspecified reductant in the cementitious material. Application of this model in cementitious waste forms has been described previously (Kaplan and Hang, 2003; SRR, 2013).

Electron milli-equivalents (meq/L) are the units used to describe the concentration (more precisely, the activity) of free electrons that can participate in an oxidation-reduction, or redox, reaction. The generalized redox equation is

$$O + e^{-} = R \tag{8}$$

where:

O	oxidizing agent, meq/L,
R	reducing agent, meq/L, and
e^-	electron.

The greatest concentration of reductant existed in the waste form when it is initially placed in the ground. Over time, the concentration of reductant will slowly decrease as more dissolved oxygen in the groundwater, $O_{2(aq)}$, migrates into the grout and reacts (consumes) the grout reductant. Once the reduction capacity is exhausted, the reducing cementitious waste form will no longer sequester the targeted constituent of concern, such as ^{99}Tc.

The total oxidizing capacity should be set equal to the amount of dissolved oxygen introduced into the system by infiltrating water. The concentration of reductant present in the slag will decrease over time as more dissolved oxygen in groundwater consumes the grout's reduction capacity. The consumption of the reduction capacity is presented in the following reaction.

$$O_{2(aq)} + R_{(grout)} \rightarrow RO_{2(grout)} \quad (9)$$

where:

$O_{2(aq)}$	O_2 dissolved in water (meq/cm^3 of the fluid),
$R_{(grout)}$	reduction capacity of the grout (meq/gram of solid), and
$RO_{2(grout)}$	oxygenated grout (meq/gram of solid; shown in traditional stoichiometric chemistry as a product of the two reactants, rather than as an oxidized species).

The expression used to calculate the rate of oxidation (R_O; (meq/gram of solid)/yr) for the above reaction is:

$$R_o = kC_{O2}C_R \quad (10)$$

where k is the oxidation rate coefficient in units of 1/(yr·meq/cm^3), C_{O2} is the concentration of $O_{2(aq)}$ (meq/cm^3) and C_R is the concentration of reductant in the grout (meq/g).

Previous data indicates that oxidation of slag is a fast reaction once the O_2 comes in contact with the reductant in the grout (Cantrell and Williams, 2012; Estes et al., 2012; Lukens et al., 2005; Shuh et al., 2000). Kaplan and Hang (2003) showed that the k value of 1.0 x 10^6 (1/(yr · meq/cm^3)) adequately represents a fast reaction.

Perhaps one of the key attributes of this model is that it can be parameterized and as such, it has immediate appeal from a practical point of view. While models based on thermodynamic and reactive transport used to describe this process in SRS disposal systems (Denham, 2007; Denham and Millings, 2012) are theoretically more acceptable, they require more assumptions and many more input values that are often not available for cementitious waste form conditions. As an

example of the type of information needed in these more theoretically acceptable calculations, it is not only necessary to know what the reduction capacity is, you must also know what phases (*i.e.,* the composition of the reductant) are responsible for redox status and the kinetic information about how they change to other phases as a result of oxidation. These more theoretical models have an important role in understanding the geochemistry in the system and can, if needed, provide necessary ancillary information to the broader PA type calculations.

There are several simplifying assumptions about the geochemistry that are associated with the shrinking core model (Table 3). As with any model, it is important to identify them so that we can direct efforts to substantiate, dismiss, or improve upon them. They also provide direction towards future research needs. Some of the assumptions exist because experimental data is not presently available to offer alternative guidance. For instance, there are conflicting results about the merits of the Ce(IV) method for measuring reduction capacity, yet an alternative method has not been identified (Assumption 2 in Table 3). Similarly, the potential role of waste form oxidation directly by air intrusion has not been validated or quantified (Assumption 1 in (Table 3).

Table 3. Key geochemical assumptions associated with the use of the porewater pathway to describe the oxidation of a reducing cementitious waste form.

1	The only oxidant in the porewater pathway is $O_2(aq)$ that enters the reducing cementitious waste form with recharge water. Because it is assumed that the cementitious waste form pore space is saturated with moisture, there is no air pathway by which $O_2(g)$ would enter the system. Based on X-ray Absorption Spectroscopy (XAS) measurements, Shuh et al. (2000) concluded that nitrate and nitrite do not oxidize Tc(IV) at any appreciable rate in reducing cementitious materials. After 9 months, saltstone samples amended with nitrate and nitrite had a greater proportion of Tc in the +4 state than saltstone samples amended with Cl^- (a non-redox active anion) without nitrate or nitrite. They note that while NO_3^- and NO_2^- are capable of oxidizing reduced Tc species at low pH environments, the oxidizing species, NO_2^+ and HNO_2, respectively, were not formed in high pH systems. The authors concluded, "The results clearly implicate oxygen as the species responsible for the oxidation of Tc(IV) to TcO_4^-. In addition, these results strongly suggest that nitrate and nitrite do not appreciably oxidize Tc(IV) in the cement."
2	The Ce(IV) method of measuring reduction capacity is representative of the available reduction capacity. It is believed that this method measures essentially all the reduction capacity in the system. The assumption is that over time, all of the reductant is eventually consumed and that grain rimes do not stop the electrons from coming into contact with the dissolved solute (*e.g.,* Tc and Cr). By way of analogy to another reducing system, it has been shown that when Fe(0) forms oxidized coatings when placed in oxygenated water, the rusted-Fe(0) particle continues to be effective at promoting solute reduction (Henderson and Demond, 2007). This was attributed to semi-conductor properties of the iron system and/or cracks in the coatings that permitted underlying electrons from the Fe(0) to enter the aqueous phase. No research supports the idea that a similar process occurs with reducing cementitious waste forms.
3	The source of the reduction capacity does not change with time (i.e., there is no loss of sulfides or ferrous iron as water moves through the waste form. Cantrell and Williams (2012) in a flow through test with saltstone measured loss of S in the leachate, contrary to this assumption. However, many potential forms and sources of sulfur exist in reducing cementitious waste forms (*e.g.*, Harbour et al. (2006) reported that OPC and BFS can each contain a few percent of S while fly ash has an order of magnitude less). It is not clear whether all of these sources of S contribute to the reduction capacity. Furthermore, it is not clear whether just the oxidized S species were selectively washed out during the early part of the study, and as such would not necessarily adversely affect the reduction capacity.
4	The potential oxidizing agents in simulant liquid waste do not lower the reduction capacity to a measurable extent. This assumption was supported by recent measurements by Um et al. (2015) and calculations by Kaplan and Hang (2003).
5	Porewater is fully saturated with $O_2(aq)$. This assumption is based on measurements made at the SRS and calculations based on Henry's Law (Kaplan and Hang, 2003). It is expected that the Hanford recharge water $O_2(aq)$ concentration will be much lower. $O_2(aq)$ concentrations are expected to decrease upon contact with soil due to microbial activity and abiotic reduction by the relatively high concentrations of Fe(II) in Hanford clay fractions (Fredrickson et al., 2004). For example, the SRS subsurface sediment has a reduction capacity of 5.1 meq/kg (Kaplan and Hang, 2003). A SRS simulation of saltstone disposal revealed that the overlying horizontal moisture barrier accounts for 14% of the reduction capacity of the disposal system (Kaplan and Hang 2003; page v, Table 2). The Hanford subsurface sediment is expected to have a greater reduction capacity than SRS sediment. SRS vadose zone sediment clay-fraction has <1% Fe(II), Hanford vadose zone sediment clay-fraction can be >10% Fe(II) (Dong et al., 2003; Fredrickson et al., 2004).
6	There is a 100% efficiency in the reaction of $O_2(aq)$ oxidizing the reduction capacity of the reducing cementitious waste form (*i.e.,* for each equivalent of O_2 there are 4 equivalents of reduction potential consumed (*i.e.,* 4 e^- per $O_2(aq)$ molecule). 100% efficiency of $O_2(aq)$ oxidizing the BFS will not happen.

Lukens et al. (2005) presented experimental data that was largely in agreement with calculations based on the shrinking core model (Kaplan and Hang, 2003). Lukens et al. (2005) provided an estimate of the rate that the oxidation front moved through saltstone based on spectroscopy considerations. Using a simulant saltstone sample that was cured under reducing

conditions for about two years, followed by 120 days of exposure to air, they measured Tc(VII) concentrations using XANES measurements and estimated that the oxidized front had moved 0.28-mm during the 120 days (or 0.85 mm/yr). They went on to evaluate this estimate by comparing it to estimates based on reduction capacity consumption as a result of O_2 diffusion during the 120-day exposure period. They concluded that their spectroscopy-based estimate was reasonable (specifically, assuming that the molecular diffusion, $D_{m(O2)} = 2 \times 10^{-5}$ cm^2/s, sample density of 1.7 g/cm^3, $O_2(aq)$ concentration of 2.7×10^{-7} mol/cm^3, and reduction capacity of 0.82 meq/g; and knowledge of Tc total concentration in their sample). It is important to note, that the spectroscopic measurement and the diffusion-based calculation they used to compare the results have categorically different assumptions, providing additional credence to the estimate.

The oxidation-front rate value generated by Lukens et al. (2005) was compared with calculations made regarding the Saltstone Disposal Facility (Kaplan and Hang 2003) (Figure 4). A comparison was made by using the facility geometry, time of exposure, and the 0.85 mm/yr oxidation front value generated by Lukens et al. (2005). Both the shrinking core model calculations based on Kaplan and Hang (2003) and Lukens et al. (2005) data indicate about ~16% of the saltstone reduction capacity would be consumed after 213,000 years. (Importantly, this value of ~16% is very dependent on the dimensions of the facility, and therefore is not applicable to other disposal systems).

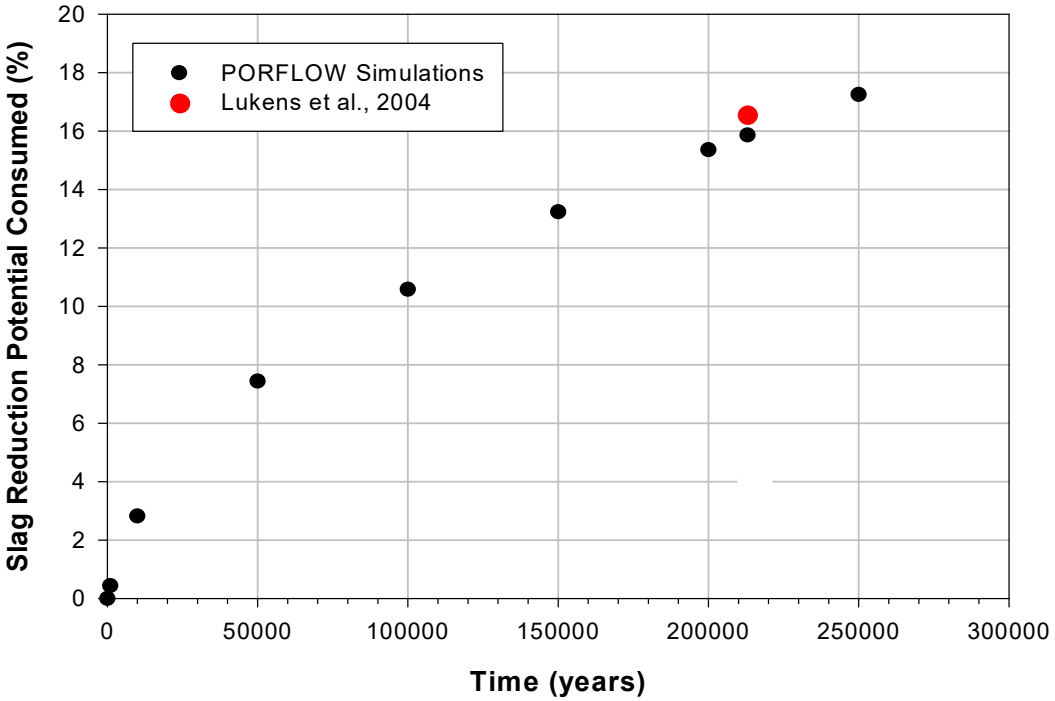

Figure 4. Estimate consumption of slag reduction potential by permitting dissolved oxygen to diffuse into the Saltstone Disposal Facility, and at the same time oxidizing/consuming the slag reduction potential (Kaplan and Hang, 2003). The single point based on spectroscopic measurements by Lukens et al. (2005) is also presented.

There are also laboratory results that contradict aspects of the shrinking core model (Langton et al., 2014). Langton et al. (2014) noted that the oxidation front of saltstone cores left exposed to air for 118 days moved faster than expected based on $O_2(aq)$ diffusion calculations (additional details related to the saltstone experiments are provided by Almond et al. (2012a)). While the authors did not explain the observed contradiction, it may in part be because they used partially desiccated saltstone samples in their experiment. The shrinking core model assumes that oxidation of the reducing cementitious material occurs only by $O_2(aq)$ entering through the porewater pathway. In desiccated samples, the air pathway would also be expected to promote oxidation. O_2 diffusion through air is 10^4 times faster (not accounting for tortuosity) than through water and would explain the unpredicted rapid oxidation reported by Langton et al. (2014). The saltstone samples used in Langton et al. (2014) were collected from a container left outside with neither temperature nor humidity controls (they reported that temperatures ranged from 14 to 41°C and relative humidity ranged from 26 to 100% during two spring months). Almond et al. (2012a) noted color changes between the exterior and interior of the sample that they attributed to oxidation and/or sample desiccation. Cracks were also noted in the sample. These studies support the need to develop an alternative pathway, such as the air pathway, to describe the oxidation of partially saturated reducing cementitious materials, such as exists at the Hanford's IDF (Flach et al., 2016). Furthermore, it demonstrates the need for more moisture-controlled and redox-controlled studies, permitting the distinction and the quantification of the two pathways.

Unsaturated cementitious waste form conditions are less of a concern at SRS because of its semi-tropical climate.

4.5.3 Young Reducing Cementitious Solids Conceptual Environment (Stage I)

This Environment is conceptually identical to that of the Young Cementitious Solids (Stage I) Environment (Section 4.4.1) except that it contains reducing slag. The reducing slag, as discussed above creates a reducing environment that promotes the reduction of several radionuclides, including Pu and Tc. It has its own set of *Kd* and solubility concentration values in look up tables (discussed in 6.0).

4.5.4 Moderately aged Reducing Cementitious Solids Conceptual Environment (Stage II)

This Environment is conceptually identical to that of the Moderately Aged Cementitious Solids (Stage I) Environment (Section 4.4.2) except it contains reducing slag. It has its own set of *Kd* and solubility concentration values in look up tables (discussed in 6.0).

4.5.5 Aged Reducing Cementitious Solids Conceptual Environment (Stage III)

This Environment is conceptually identical to that of the Moderately Aged Cementitious Solids (Stage III) Environment (Section 4.4.3) except it contains reducing slag. It has its own set of *Kd* and solubility concentration values in look up tables (discussed in 6.0).

4.5.6 Example Application of Conceptual Model to a Reducing Cementitious System

To model the release of redox sensitive radionuclides from a reducing cementitious system, it is sometimes necessary to first conduct a flow model to assign durations to the three cement stages. Based on these assigned cement stages, appropriate geochemical parameters are selected. Also, calculations are conducted to determine when to consider the wasteform in the reducing or oxidized state (described in Section 4.5.2). One recent example of this is presented in the Saltstone Disposal Facility (SDF) PA (SRR, 2013: SRR-CWDA-2013-00062, Rev. 2) as described in the following paragraphs and summarized in Table 4. The Saltstone Disposal Facility is described in Section 5.6.

There are six possible cementitious environments: Oxidized Stage I, Reduced Stage I, Oxidized Stage II, Reduced Stage II, Oxidized Stage III, and Reduced Stage III (again, the stage number increases as the cement ages). The total volume of pore water within a modeled stage of cementitious material is referred to as the stage's pore volume, and the amount of fluid moving through that region is measured by the count of its pore volumes (Denham, 2009). The number of pore volumes for each stage was based on thermodynamic calculations of pH and Eh of successive pore volumes coming to equilibrium with "aging grout". The hypothetical infiltrating water used in these calculations was groundwater equilibrated with calcium-silicate-hydrate (CSH) gel associated with Oxidized Stage 2 cementitious materials. The saltstone was assumed

to have a reduction capacity based on measured values, 0.6 meq/g (Roberts and Kaplan, 2009). Initial calculations of the SDF, using the Geochemist's Workbench® thermodynamic model, indicated that the Stage I (young cement) was not important because it was extremely short lived, on the order of 30 pore volumes (Denham, 2009). All the reductant in the Saltstone Disposal Facility was estimated to be consumed after 1220 pore volumes. These results also indicate that Stage I plays a negligible role in saltstone aging. The point of 1220 pore volumes in the simulation also identified when the Reduced Stage II system transitioned to the Oxidized Stage II. Additional modeling indicated that the next transition, between Oxidized Stage II to Oxidized Stage III occurred by estimating when all the CSH had dissolved. This transition occurred after 11,213 pore volumes (SRR, 2013). Therefore, there were three different Conceptual Environments in this SDF PA: Reduced Stage II, Oxidized Stage II, and Oxidized Stage III.

In addition to assigned transitions times (pore volumes) from one stage to the next, it was also necessary to assign geochemical parameters to represent Tc interactions in the three Conceptual Environments. Technetium release in saltstone was modeled as a shrinking core. The release of Tc from the saltstone during the Reduced Stage II was assumed to be solubility controlled ($k_s = 10^{-8}$ M; Li and Kaplan (2012)). In addition to evaluating likely solid phases, this study also evaluated different thermodynamic databases. Once the system became oxidized, generally anticipated to occur during the 2nd stage of cement aging, then solubility no longer controlled aqueous Tc concentrations. Under oxidizing conditions, Tc adsorption to solid phases becomes the predominant mechanisms controlling the concentration of Tc in pore water, and thus the *Kd* construct was used to predict aqueous Tc concentrations. Similarly, once sufficient pore water had leached through the saltstone to advance the modeling into the 3rd and final stage of aged cement, a Tc *Kd* for an oxidized system was use. Finally, beneath the Saltstone Disposal Facility, cementitious-leachate impacted *Kd* values were used to describe the interaction of Tc with the vadose zone sediments. Different facilities will have different points of transition between the Conceptual Environments in the reducing cement, mainly because of differences in the size and duration for a pore volume to pass through a specific facility and the amount of total reduction capacity in the facility.

Table 4. Tc geochemical input values used in an example demonstrating modeling spatial and temporal transitions of plume moving through a Saltstone Disposal Facility into the underlying aquifer (SRR 2013; Table 4.1-1).

System	Conceptual Environment	Geochemical Parameter
Saltstone	Cementitious Reduced Stage II[(a)]	$k_s = 10^{-8}$ M
Saltstone	Cementitious Oxidized Stage II[(a)]	Kd =0.5 mL/g
Saltstone	Cementitious Oxidized Stage III	Kd =0.5 mL/g
Upper Vadose Zone	Cementitious Impact Clayey Sediment	$Kd_{CementLeach}$ = 0.2 mL/g[(b)]
Lower Vadose Zone	Cementitious Impact Sandy Sediment	$Kd_{CementLeach}$ = 0.1 mL/g[(b)]
Aquifer Zone	Cementitious Impact Sandy Sediment	$Kd_{CementLeach}$ = 0.1 mL/g[(b)]

[(a)] The transition between the Reduced Stage II to the Oxidized Stage II was estimated based on thermodynamic calculations to occur after 1220 pore volumes of oxygenated, CSH-equilibrated groundwater passed through the facility. Similarly, transition from Oxidized Stage 2 to Oxidized Stage III occurred after 11,213, pore volumes.
[(b)] Calculated using Equation 6; $f_{CementLeach}$ = 0.1 (Table 2); Clayey Tc Kd = 1.8 mL/g (Table 16; Sandy Tc Kd = 0.6 mL/g (Table 16)

4.6 Constituents of Concern Leaching from Waste Materials

Radioactive waste is disposed on the SRS in several different forms. How radionuclides sorb and desorb from these materials, once disposed in the subsurface, is important because they are source terms for radionuclides entering the environment. A great deal of research has been directed at understanding how radionuclides interact with various cementitious materials (Section 6.0), but much less is known about how radionuclides interact with the large number of other buried solid phases. Therefore, the following simplified assumptions were made. Unless waste-form specific data are available (Section 4.7), the extent that a radionuclide sorbs to the waste material is assumed to be similar to the extent that the radionuclide sorbs to the sediment immediately in contact with the waste. For example, the leaching rate of Th associated with lumber disposed in the Slit Trench Facility will be calculated using the Th *Kd* value reported in the Clayey Sediment look-up table (discussed in more detail below in relation to Table 16). The Clayey Sediment (Section 4.3.1) is the solid phase in contact with the waste.

4.7 Constituent of Concern Leaching from Special Waste Forms

There are some, not many, waste-specific *Kd* values and apparent solubility values, especially for anions sorbing to anionic resins (Kaplan and Serkiz, 2000a; Kaplan et al., 1999). The extent that constituents of concern desorb from waste can be estimated using *Kd* values and solubility concentration values. The use of these parameters to estimate desorption is simply the reverse of adsorption. One of the assumptions of the *Kd* construct is that it is fully reversible, meaning that adsorption occurs at the same rate as desorption. The list of special waste form *Kd*

values (Table 15) is not complete, but rather provides desorption *Kd* values that have been measured previously.

4.8 Geochemical Parameters' Ranges and Distributions

Associated with the "best" *Kd* and apparent solubility values are parameters that address the expected variability associated with these parameters. The distribution and range of geochemical parameters are especially important for stochastic modeling. Additionally, the lower 95% value also provides a likely minimum or conservative estimate for the groundwater pathway. The range and distribution of Am, Cd, Cs, Ce, Co, Hg, Sr, Sn, Tc, and Y *Kd* values were measured in 27 sediment (triplicate measurements resulting in 81 *Kd* measurements per element; 810 *Kd* measurements in total) collected from the subsurface vadose and aquifer zones of E-Area (Grogan, 2008; Grogan et al., 2010; Kaplan et al., 2008c). Similar tests with grout were conducted (Almond et al., 2012b).

Based on these studies, the 95-percentile range and type of distributions assigned to constituent of concern *Kd* values should be assigned as follows:

- Distributions of *Kd* values were most closely log-normally distributed in sediments and grout.
- The width of 95% confidence interval for the estimated mean *Kd* was twice the mean in the Aquifer Zone (Sandy Sediment Environment), equal to the mean for the Upper Vadose Zone (Clayey Sediment Environment), and half the mean for the Lower Vadose Zone (Sandy Sediment Environment).
- The distribution of *Kd* values in grout was log normal and the 95% confidence interval for the estimated mean *Kd* was twice the mean.

Based on these findings, the *Kd* distributions and ranges were estimated for each of the various Environments.

4.8.1 Distribution and Ranges for Mean *Kd* values in Sandy Sediment Environments

For the Sandy Sediment Environments (and the Cementitious Leachate Impacted), which is the dominant type of Environment in the Aquifer and Lower Vadose Zones, it was assumed that the range between the 95% confidence levels above and below the mean *Kd* value was 1.5 times the mean, which is a combination of the recommended multiplying factors for the Aquifer Zone and the Lower Vadose Zone. This would result in a calculation for the minimum ("Min") and maximum ("Max") *Kd* values defining the limits of the range with a log-normal distribution as follows:

$$\text{Sandy Sediment } Kd_{Min} = Kd \div 2 \quad \text{(Eq. 11)}$$

$$\text{Sandy Sediment } Kd_{Max} = Kd \times 2 \quad \text{(Eq. 12)}$$

4.8.1 Distribution and Ranges for Mean *Kd* Values in Clayey Sediment Environments

For the Clayey Sediment Environments (and the Cementitious Leachate Impacted), which is the dominant type of Environment in the Upper Vadose Zone, it was assumed that the range between the 95% confidence levels above and below the mean *Kd* value was 1.0 times the mean, which corresponds to the value recommended by Grogan et al. (2008) for the Upper Vadose Zone. This would result in a calculation for the minimum ("Min") and maximum ("Max") *Kd* values defining the limits of the range with a log-normal distribution as follows:

$$\text{Clayey Sediment } Kd_{Min} = Kd \times 0.618 \quad \text{(Eq. 13)}$$

$$\text{Clayey Sediment } Kd_{Max} = Kd \div 0.618 \quad \text{(Eq. 14)}$$

4.8.2 Distribution and Ranges for Mean *Kd* Values in Cementitious Environments

For cementitious Conceptual Environments, the range was assumed to be the same as for Sandy Sediment Environments (Equations 11 and 12). The distributions were assumed to be log-normal (Almond et al., 2012b).

4.8.3 Distribution and Ranges for Apparent Solubility Values in Cementitious Environments

Apparent solubility values were assumed to have a range of 2 orders of magnitude and to be log-normally distributed. For example, a constituent of interest with a k_s value of 10^{-9} M would have a $k_s(min)$ of 10^{-10} M and a $k_s(max)$ of 10^{-8} M.

[7] The multiplier reported in Equations 11 - 14, are different from those reported in Grogan et al. (2009); they yield the same *Kd* range but better represent the log-normal distributions observed in the data. The original multipliers placed the 95% confidence levels eqi-distanced from the mean *Kd* value, contrary to log-normal distributions that have a smaller range below the mean than above the mean.

5.0 WASTE FACILITIES DESCRIPTIONS: ASSIGNMENT OF GEOCHEMICAL ENVIRONMENTS AND TYPES OF CONSTANTS TO USE IN SIMULATIONS

The purpose of this section is to describe the key features of the waste units and facilities and to assign geochemical Conceptual Environments. More specifically, this section describes the geochemical conceptual model of each waste facility in terms of the various solid phases and aqueous chemistry comprising each facility and recommends assignment of geochemical parameters to these material zones

For each facility, there are a schematic and photograph(s), followed by a table containing the conceptual geochemical materials (*e.g.,* concrete, reducing concrete, sandy sediment) of the facility and the associated geochemical parameters needed to describe the geochemistry of the constituent of concern interaction with these features. The schematic is a nominal representation of the disposal unit cross-section with dimensionality and facility-specific details being applied in the numerical model. Section 6.0 has the various look-up tables containing the *Kd* and solubility concentration values associated with the assigned Conceptual Environments. The disposal facilities described in this section are:

- Slit and Engineered Trenches (Figure 5, Figure 6, Figure 7, and Table 5),
- Low Activity Waste (LAW) Vault (Figure 8, Figure 9, and Table 6),
- Components-in-Grout Trenches (Figure 10, Figure 11, and Table 7),
- Intermediate Level (ILV)Vault (Figure 12, Figure 13, and Table 8),
- Naval Reactor Component Disposal Areas (Figure 14, Figure 15, and Table 9),
- Saltstone Disposal Facility (Figure 16, Figure 17, and Table 10), and
- High Level Waste Tank (Figure 18, Figure 19, and Table 11).

5.1 Slit Trenches (STs) and Engineered Trenches (ETs)

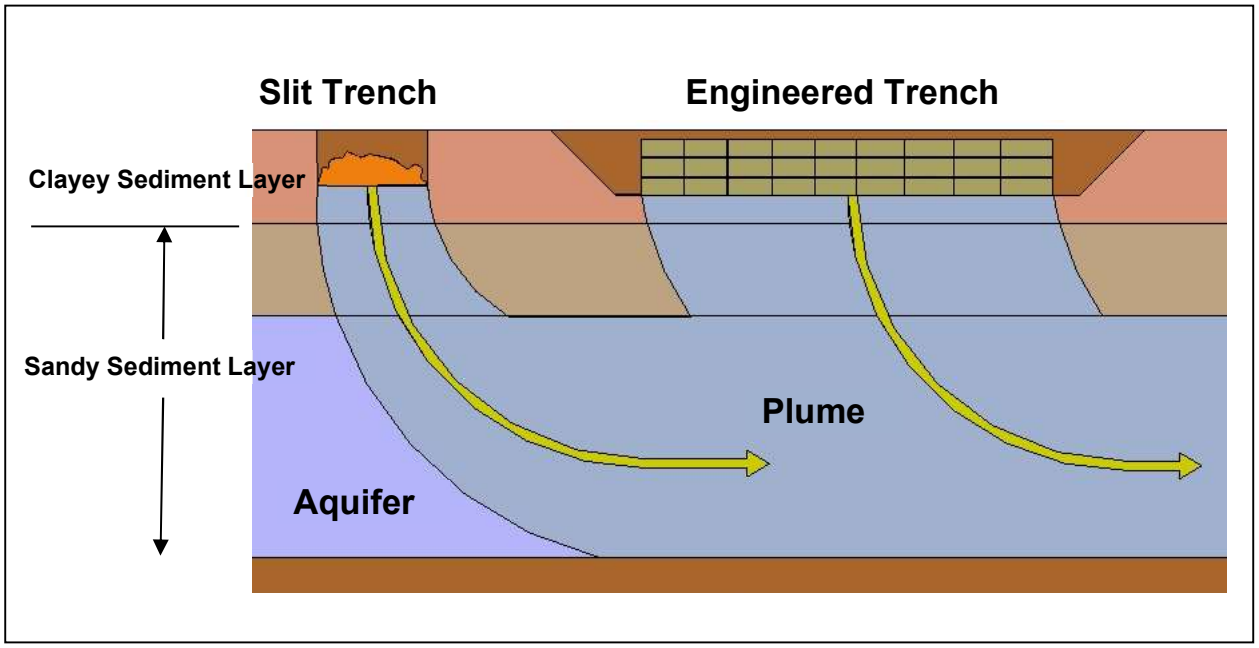

Figure 5. Schematic representation of the geochemical conceptual model of a Slit and Engineered Trench Unit. Not shown is a multilayered-closure cap that will be added above these units at the end of Institutional Control.

Figure 6. E-Area Slit Trench Facility showing a range of waste materials. Also note the red clayey sediment, characteristic of the upper sediment strata.

Figure 7. Engineered Trench: (top) aerial view and (bottom) close up of metal containers holding low level waste (WSRC 2008).

Table 5. Slit Trenches (STs) and Engineered Trenches (ETs): conceptual geochemical model of features and parameters (see Figure 5).

Solid Phases	Aqueous Phase	Geochemical Parameter
Waste Zone: Active components are iron metal and corrosion products. Metal containers will rust to form Fe-oxides. Cellulosic materials are also present but do not degrade to form CDP's in sufficient quantity to affect sorption. [a],[b]	Same as SRS ground water: pH 5.5, ionic strength 0.01, except for trace levels of radionuclides	Use Clayey Sediment *Kd*. Fe-oxide content will control the sorption chemistry of this zone. It is assumed that the geochemistry of the Clayey Sediment will approximate that of the rusted metal waste form. The rusted waste form will contain much greater Fe-oxide content than the typical clayey SRS sediment. Thus, the use of clayey sediment *Kd* is a conservative assumption. No cementitious materials are included as engineered barriers.
Clayey Sediment: Upper Vadose Zone	As above.	Use Clayey Sediment *Kd*.
Sandy Sediment: Lower Vadose Zone	As above.	Use Sandy Sediment *Kd*.
Sandy Sediment: Aquifer Zone	As above	As above.

[a] A Slit Trench disposal unit nominally consists of a series of five narrow (7-m wide) parallel trench segments not accessible by personnel or vehicles. Waste is typically dumped at the top on one end and pushed by dozer into the trench or crane lifted into place. Slit Trenches receive a wide variety of materials containing very low concentrations of radioactivity including soil, rubble, wood debris, large components, tanks and job control waste. The Engineered Trench disposal unit is a vehicle-accessible, open trench design that allows stacking of containerized waste by forklift. The Engineered Trenches typically receive job control waste and small equipment packaged in B-25 boxes, B-12 boxes and Sealand containers. Filled Slit Trenches and completed section of the Engineered Trenches are filled with stacked boxes to grade with a minimum of 1.3 m of clean sediment.

[b] In Kaplan (2012), it was determined that cellulose degradation products (CDP) were not present in sufficient concentrations in the groundwater beneath the ORWBG (a closed solid-waste burial ground) to warrant application of a CDP correction factor to any *Kd* values for E-Area. The 2016 update of the geochemistry data package reflected the elimination of CDP effects on all categories of *Kd* values.

5.2 Low-Activity Waste (LAW) Vaults

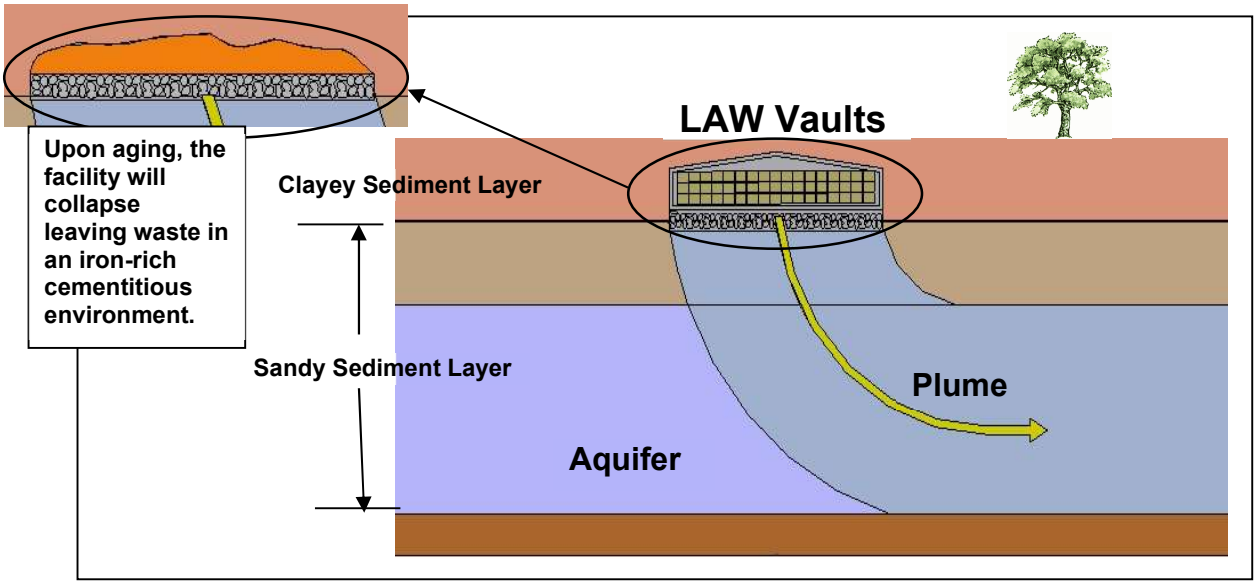

Figure 8. Schematic representation of the geochemical conceptual model of the Low-Activity Waste Vault. Not shown is a multi-layered closure cap that will be added above the vault at the end of Institutional Control.

Exterior View

Interior View

Figure 9. Low Activity Waste (LAW) Vaults: (top) exterior view and (bottom) interior of a disposal cell (WSRC, 2008).

Table 6. Low Activity Waste Vaults (LAWV): conceptual geochemical model of features and parameters (See Figure 8).

Solid Phases	Aqueous Phase	Geochemical Parameter
Waste Zone: Active components are iron metal, corrosion products and surrounding concrete barrier. Metal containers will rust to form Fe-oxides. Eventually the concrete vault structure and B-25 boxes collapse leaving waste in an iron-rich cementitious environment. Celluosic materials are also present but do not degrade to form cellulose degradation products in sufficient quantity to affect sorption. [a, b]	Cementitious leachate comes in contact with metal boxes or collapsed rusted iron rubble, entering through joints, cracks and ultimate collapse of the concrete vault. This is a cementitious leachate impacted aqueous phase (elevated pH and ionic strength).	Use cementitious leachate impacted Clayey Sediment *Kd*; $Kd_{CementLeach}$[c]. Fe-oxide content will control the sorption chemistry of this zone. It is assumed that the geochemistry of the Clayey Sediment will approximate that of the rusted metal waste form. In reality the rusted waste form will contain much greater Fe-oxide content than the typical clayey SRS sediment. Also, applying Clayey Sediment *Kd* values (which have an assumed pH of 5.5) to a system with a higher pH (concrete pH is typically >10) will be conservative because metal sorption (*Kd* values) will be greater in high pH than in low pH systems.
Reducing Concrete Vault: Active components are cement and slag added to concrete in roof, walls and floor. [d]	Cementitious Impacted Leachate: Three general types of reducing concrete leachate chemistries are controlled by different aged cement phases characterized by elevated pH and ionic strength relative to SRS groundwater. Leachate will contain sulfides released from slag.	Use Reducing Cement *Kd* or apparent solubility values for the three cement ages.
Crushed Stone: Layer beneath LAWV facility.[e]	Fe-oxide impacted cementitious leachate: Cement leachate chemistry altered by passing through Fe-oxide controlled environment. Still characterized by elevated pH and ionic strength relative to SRS groundwater.	Use cementitious leachate impacted Clayey Sediment *Kd* .[c] See footnote (e).
Clayey Sediment: Upper Vadose Zone	As above.	Use cementitious leachate impacted Clayey Sediment *Kd*; $Kd_{CementLeach}$.[c]
Sandy Sediment: Lower Vadose Zone	As above.	Use cementitious leachate impacted Sandy Sediment *Kd*; $Kd_{CementLeach}$.[c]
Sandy Sediment: Aquifer Zone	Cementitious leachate pore water gets diluted with typical SRS groundwater and the aqueous phase takes on the properties of the latter: pH 5.8 and ionic strength 0.01, except for trace levels of radionuclides.	Use Sandy Sediment *Kd*.

[a] Waste designated for the LAW Vault contains greater radioactivity than the waste disposed in the Slit & Engineered Trenches. Waste is packaged in standard metal boxes (B-25 and B-12 boxes) which are stacked

within twelve individual disposal cells in the vault. Some cellulosic materials will be disposed in the LAW Vault.

(b) In Kaplan (2012), it was determined that cellulose degradation products (CDP) were not present in sufficient concentrations in the groundwater beneath the ORWBG (a closed solid-waste burial ground) to warrant application of a CDP correction factor to any *Kd* values for E-Area. The 2016 update of the geochemistry data package reflected the elimination of CDP effects on all categories of *Kd* values; this data package continues elimination of CDP effects.

(c) The 2010 geochemical data package (Kaplan 2010) introduced the concept of a cementitious leachate impacted zone beneath concrete/grout disposal units. This change specifically affected the Components in Grout Trenches, Low Activity Waste Vaults, and Intermediate Level Vault models, but has never been formally evaluated through the Unreviewed Disposal Question Evaluation (UDQE) process for inclusion in the PA baseline. This update of the geochemistry data package maintains this concept which will be evaluated in the next Solid Waste PA revision.

(d) Reducing cementitious materials are those that contain slag and change the pore water chemistry sufficiently to require unique geochemical parameters (Section 4.5). The LAWV is constructed with a 40-cm thick concrete roof, 60-cm thick interior and exterior concrete walls, and 30-cm thick concrete floor.

(e) A 114-cm thick layer of crushed stone exists immediately beneath the concrete floor of the LAWV. It has not been included in previous PA modeling efforts, because it was believed that this layer would become “silted in” within a relatively short period of time. For this same reason, it is not included in the conceptual geochemical model of this disposal unit and will be modeled as behaving like the cementitious leachate impacted Clayey Sediment: Upper Vadose Zone.

5.3 Components-in-Grout (CIG) Trenches

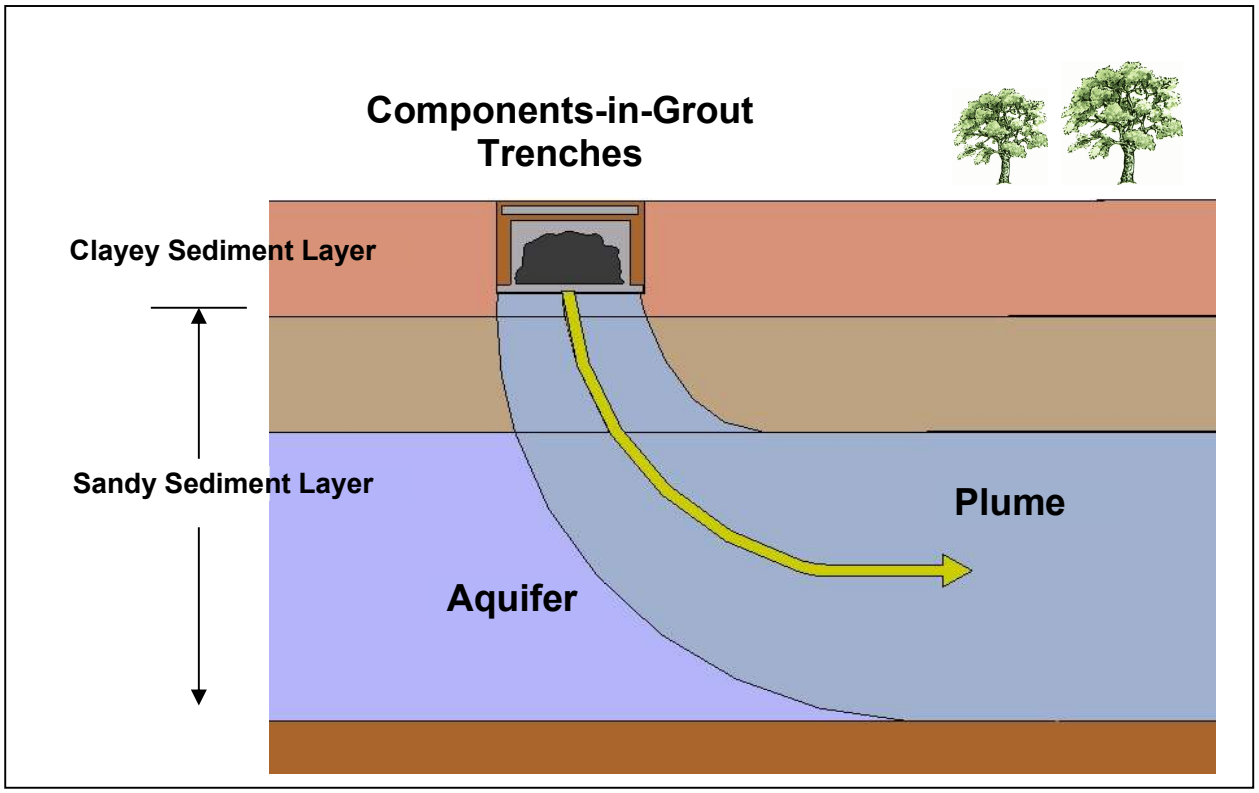

Figure 10. Schematic representation of the geochemical conceptual model of a Components-in-Grout Trench. Not shown is a multi-layered closure cap that will be added above the vault at the end of Institutional Control.

Figure 11. Sequence of steps in the disposing of waste as Components in Grout (WSRC 2008).

Table 7. Components-in-Grout (CIG) Trenches: conceptual geochemical model of features and parameters (Figure 10).

Solid Phases	Aqueous Phase	Geochemical Parameter
Waste Zone: Active components are grout, iron metal and corrosion products. Because of intimate contact between encapsulating grout and waste form, cement phases are considered to be controlling sorption chemistry. The impact of Fe-oxides is ignored. Celluosic materials are also present but do not degrade to form CDP's in sufficient quantity to affect sorption. [(a),(b)]	Cementitious Impacted Leachate: Three general types of oxidizing grout leachate chemistries controlled by different aged cement phases characterized by elevated pH and ionic strength relative to SRS groundwater.	Use Oxidizing Cement *Kd* or apparent solubility values for the three cement ages.
Grout / Concrete: Active components are cement phases. [(a)]	As above.	Use Oxidizing Cement *Kd* or apparent solubility values for the three cement ages.
Clayey Sediment: Upper Vadose Zone	Fe-oxide impacted cementitious leachate: Cement leachate chemistry altered by passing through Fe-oxide controlled environment. Still characterized by elevated pH and ionic strength relative to SRS groundwater.	Use cementitious leachate impacted Clayey Sediment *Kd*; $Kd_{CementLeach}$.[(c)]
Sandy Sediment: Lower Vadose Zone	As above.	Use cementitious leachate impacted Sandy Sediment *Kd*; $Kd_{CementLeach}$.[(c)]
Sandy Sediment: Aquifer Zone	Cementitious leachate pore water gets diluted with typical SRS groundwater and the aqueous phase takes on the properties of the latter: pH 5.8, ionic strength 0.01, trace levels of radionuclides.	Use Sandy Sediment *Kd*.

[(a)] CIG Trench waste typically consists of equipment (components) too bulky and too large to place in the Low-Activity Waste Vault or the Intermediate Level Vault but containing more radioactivity than allowed for Slit and Engineered Trenches. A section of trench is excavated to act as a form and a 30-cm thick grout floor is poured and cured. The waste component is placed on the floor and grout is pumped into the trench to encapsulate the component with a minimum one foot of grout. If needed, a 45-cm thick reinforced concrete slab is installed directly on top of the grout layer above the newly installed waste component for long term (300-year) structural support of the final closure cap. Soil backfill is added to bring the trench to grade and to promote positive drainage. It is expected that some cellulosic material is included in this waste.

[(b)] In Kaplan (2012), it was determined that cellulose degradation products (CDP) were not present in sufficient concentrations in the groundwater beneath the ORWBG (a closed solid-waste burial ground) to warrant application of a CDP correction factor to any *Kd* values for E-Area. The 2016 update of the geochemistry data package reflected the elimination of CDP effects on all categories of *Kd* values; this data package continues elimination of CDP effects.

[(c)] The 2010 geochemical data package (Kaplan 2010) introduced the concept of a cementitious leachate impacted zone beneath concrete/grout disposal units. This change specifically affected the Components in Grout Trenches, Low Activity Waste Vaults, and Intermediate Level Vault models, but was never formally evaluated through the Unreviewed Disposal Question Evaluation (UDQE) process for inclusion in the PA baseline. This update of the geochemistry data package maintains this concept which will be evaluated in the next Solid Waste PA revision.

5.4 Intermediate-Level Vault (ILV)

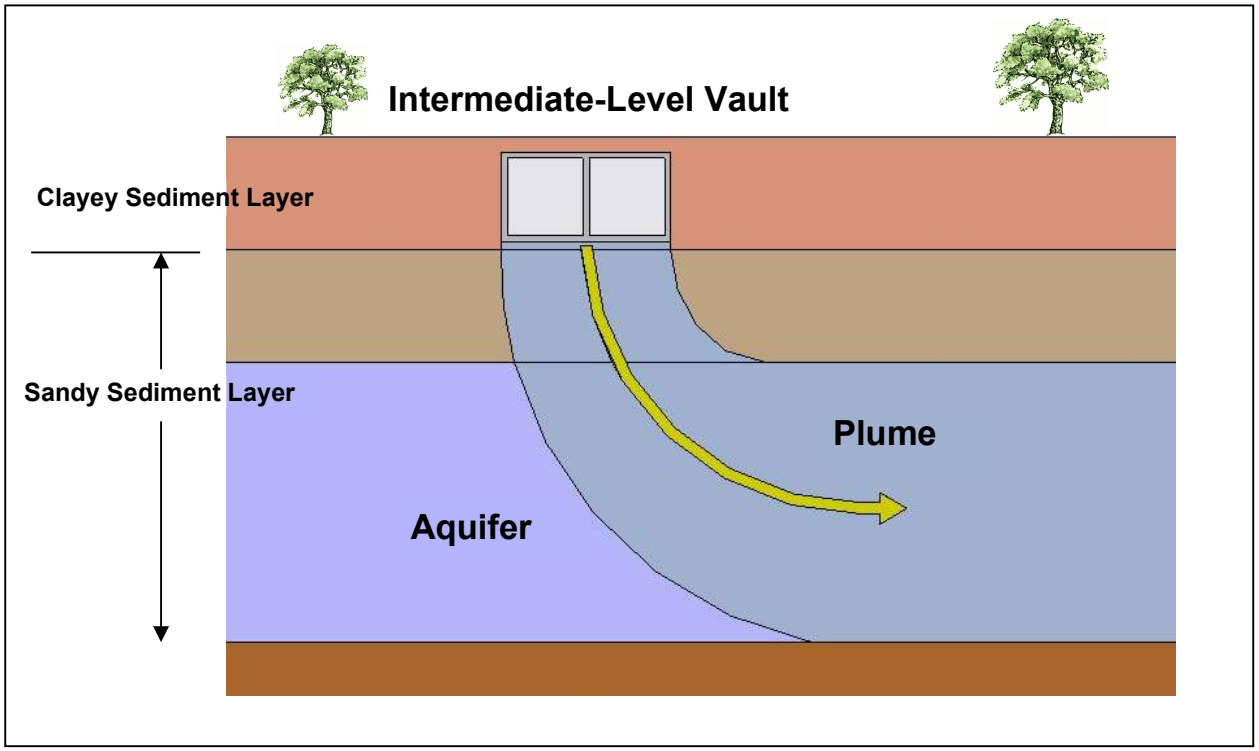

Figure 12. Schematic representation of the geochemical conceptual model of the Intermediate-Level Vault. Not shown is a multi-layered closure cap that will be added above the vault at the end of Institutional Control.

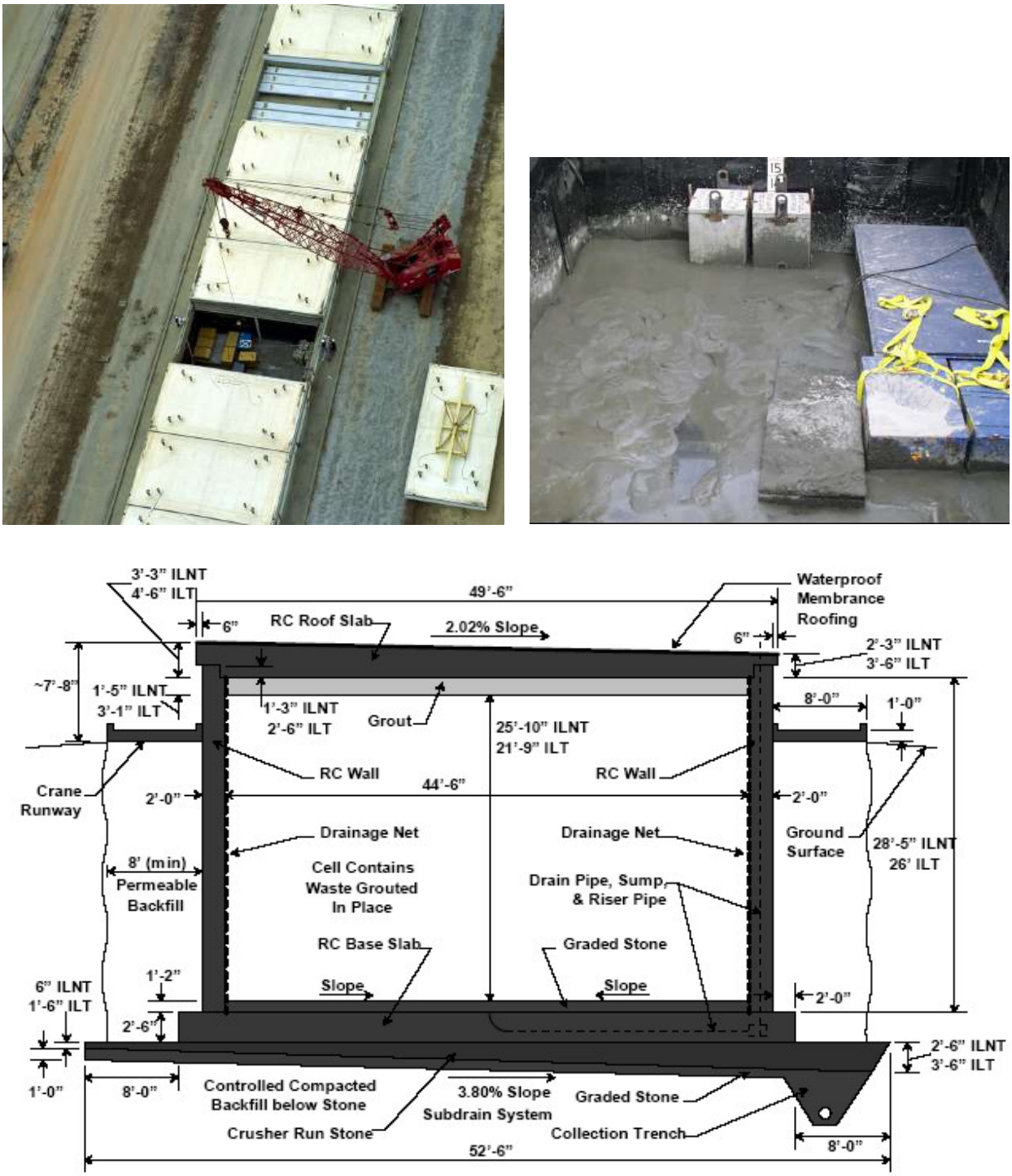

Figure 13. Intermediate-Level Vault: (top left) aerial photograph with roof removed from one cell; (top right) waste components cemented within a partially filled cell; (bottom) cross-sectional diagram of unit (WSRC 2008).

Table 8. Intermediate-Level Vault: conceptual geochemical model of features and parameters (Figure 12).[a]

Solid Phases	Aqueous Phase	Geochemical Parameter
Waste Zone: Active components are grout, iron metal and corrosion products. Because of intimate contact between encapsulating grout and waste form, cement phases are considered to be controlling sorption chemistry. The impact of Fe-oxides is ignored. [a]	Cementitious Impacted Leachate: Three general types of oxidizing grout leachate chemistries controlled by different aged cement phases characterized by elevated pH and ionic strength relative to SRS groundwater.	Use Oxidizing Cement *Kd* or apparent solubility values for the three cement ages. [b]
Reducing Concrete Vault: Active components are cement and slag added to concrete in roof, walls and floor. [c]	Cementitious Impacted Leachate: Three general types of reducing concrete leachate chemistries controlled by different aged cement phases characterized by elevated pH and ionic strength relative to SRS groundwater. Leachate will contain sulfides released from slag.	Use Reducing Cement *Kd* or apparent solubility values for the three cement ages. [c]
Clayey Sediment: Upper Vadose Zone	Fe-oxide impacted cementitious leachate: Cement leachate chemistry altered by passing through Fe-oxide controlled environment. Still characterized by elevated pH and ionic strength relative to SRS groundwater.	Use cementitious leachate impacted Clayey Sediment *Kd* values; $Kd_{CementLeach}$.[d]
Sandy Sediment: Lower Vadose Zone	As above.	Use cementitious leachate impacted Sandy Sediment *Kd* values; $Kd_{CementLeach}$.[d]
Sandy Sediment: Aquifer Zone	Cementitious leachate pore water gets diluted with typical SRS groundwater and the aqueous phase takes on the properties of the latter: pH 5.8, ionic strength 0.01, trace levels of radionuclides.	Use Sandy Sediment *Kd*.

[a] Waste designated for the Intermediate Level Vaults (ILV) contains greater radioactivity than the waste disposed in the Low Activity Waste Vaults. The ILV consists of two modules containing eight bulk waste cells and one cell constructed with 144 silos. Waste is packaged in a variety of metal or concrete containers. Within each bulk waste cell, the first layer of waste is placed directly on top of the graded stone drainage layer. The first layer of waste is encapsulated in grout which forms the surface for the placement of the next layer. Subsequent layers of waste are placed directly on top of the previously encapsulated waste. Subsequent layers may be encapsulated with CLSM rather than grout. The cell with silos is used for disposal and storage of tritium-bearing waste packed in 38-L drums, spent tritium extraction crucibles, and tritium job control waste.

[b] Oxidizing grout or Controlled low strength material (CLSM) used to encapsulate waste containers is assumed to control the chemistry of the waste layer rather than the surrounding reducing concrete vault.

[c] Reducing cementitious materials are those that contain slag and change the pore water chemistry sufficiently to require unique geochemical parameters. The ILV is constructed with a 70 – 140 cm thick concrete roof, 45 to 76 -cm thick interior and exterior concrete walls, and 76-cm thick base slab. Reducing concrete roof will be added at time of operational closure.

[d] The 2010 geochemical data package (Kaplan 2010) introduced the concept of a cementitious leachate impacted zone beneath concrete/grout disposal units. This change specifically affected the Components in Grout Trenches, Low Activity Waste Vaults, and Intermediate Level Vault models, but has never been formally evaluated through the Unreviewed Disposal Question Evaluation (UDQE) process for inclusion in the PA baseline. This update of the geochemistry data package maintains this concept which will be evaluated in the next PA revision.

5.5 Naval Reactor Component Disposal Areas (NRCDAs)

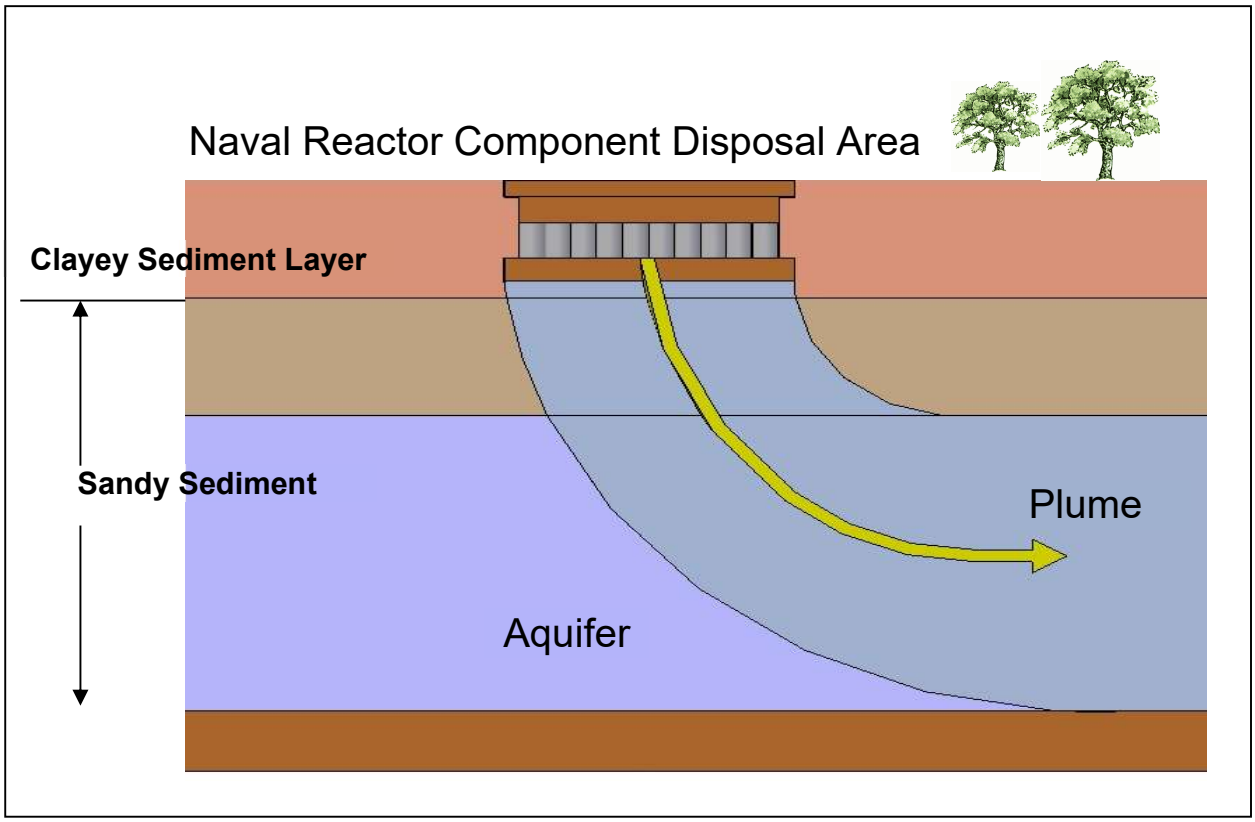

Figure 14. Schematic representation of the geochemical conceptual model of the Naval Reactor Component Disposal Areas. Not shown is a multi-layered closure cap that will be added above the pads at the end of Institutional Control. See Table 9 for facility description and Figure 15 for photographs of the facility.

Figure 15. (Top) Photo showing partially covered naval reactor components of various sizes. Earth and a clay cap will be mounded over naval reactor waste prior to final closure. There are two such facilities, the "old" (two top photos) and "new" (bottom photo) facilities. (Bottom) Naval reactor component before it is placed in the disposal area (WSRC, 2008).

Table 9. Naval Reactor Component Disposal Areas (NRCDAs): conceptual geochemical model of features and parameters (see Figure 14).

Solid Phases	Aqueous Phase	Geochemical Parameter
Waste Zone: Active components are activated metal and corrosion products. It is assumed that the activated metal waste will rust to form Fe-oxides (crud) and that radionuclides will sorb to these Fe-oxides. [(a)]	Same as SRS ground water: pH 5.5, ionic strength 0.01, except for trace levels of radionuclides.	Use Clayey Sediment *Kd*. Fe-oxide content will control the sorption chemistry of this zone. It is assumed that the geochemistry of the Clayey Sediment will approximate that of the rusted metal waste form. In reality the rusted waste form will contain much greater Fe-oxide content than the typical clayey SRS sediment. Thus, the use of clayey sediment *Kd* is a conservative assumption. [(b),(c)]
Clayey Sediment: Upper Vadose Zone	As above.	Use Clayey Sediment *Kd*. [(b),(c)]
Sandy Sediment: Lower Vadose Zone	As above.	Use Sandy Sediment *Kd*. [(b),(c)]
Sandy Sediment: Aquifer Zone	As above	Use Sandy Sediment *Kd*.

[(a)] Naval Reactor wastes are highly radioactive components consisting of activated corrosion-resistant metal alloy (Inconel and Zircaloy) contained within thick steel welded casks, and auxiliary equipment primarily contaminated with activated corrosion products (crud) at low levels and contained within thinner-walled bolted casks. The crud component is assumed to be instantaneously released when the container is breached (750 years after placement on the pad). The activation product component is released based on the corrosion rate of the steel and radioactive decay of the radionuclides. The waste zone consists of these welded casks and bolted containers placed on an above-grade gravel pad. The casks are assumed to be structurally stable well past the 1,000-year period of performance. Two separate areas within the E-Area Low Level Waste Facility (ELLWF) have been used for NRCDA's.

[(b)] As part of final closure, the casks will be surrounded with a structurally suitable material. This backfill may be emplaced sooner if radiation shielding is required for personnel protection during the operational or institutional-control period. The solid could be sand, aggregate, onsite soil, or a flowable cementitious material (ELLWF PA Closure Plan, (Phifer et al., 2009)). It is assumed that Fe-oxide content from the rusted waste form will control radionuclide sorption in the Waste Zone irrespective of whether clay, sand or aggregate is used as the backfill. If a flowable cementitious fill is used, then cementitious-leachate impacted *Kd* values should be used in the Waste Zone and Upper and Lower Vadose Zone. In the Aquifer Zone, cementitious leachate pore water gets diluted with typical SRS groundwater and the aqueous phase takes on the properties of SRS groundwater, i.e., pH 5.8 and ionic strength 0.01 M, except for trace levels of radionuclides.

[(c)] Note that a simple GoldSim model was used to represent the NRCDA in the 2008 PA (WSRC, 2008). As a conservative measure, this model placed the NRCDA source term in the saturated zone and instantaneously released the entire inventory into the aquifer, thus ignoring the Waste Zone and Vadose Zone geochemical properties.

5.6 Saltstone Disposal Facility

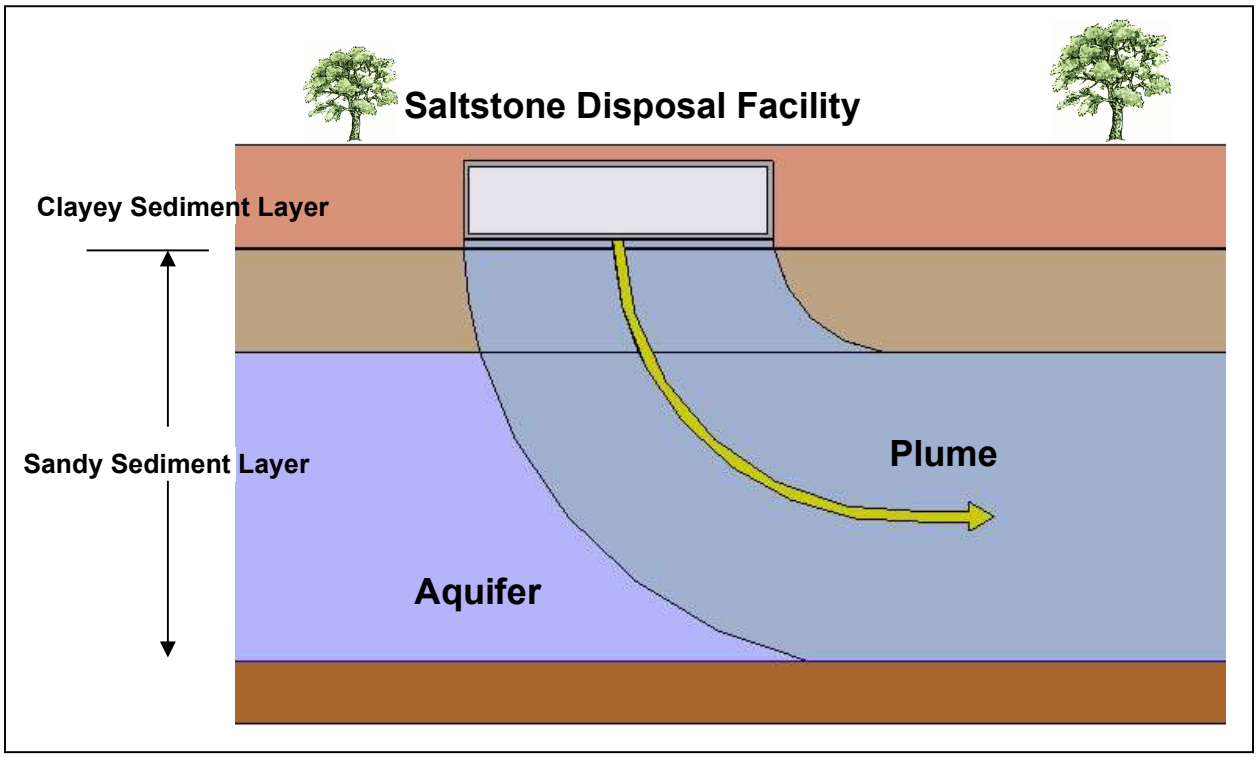

Figure 16. Schematic representation of the geochemical conceptual model of the Saltstone Disposal Facility. Not shown is a multi-layered closure cap that will be added above the Saltstone Disposal Facility at the start of Institutional Control.

Figure 17. Aerial photographs of the Z-Area Saltstone Production and Disposal Facilities. The Saltstone Disposal Units (SDUs) reflect multiple design changes and improvements since the original rectangular SDU 1 and SDU 4 that were constructed in the 1980s. Since 2010, SDUs 2, 3, 5, 6, 7, 8, and 9 have been built or are under construction and circular and are based on a commercial water tank design that has been adapted for waste grout disposal.

Table 10. Saltstone Disposal Facility: conceptual geochemical model of features and parameters (see Figures 16 and 17).

Solid Phases	Aqueous Phase	Geochemical Parameter
Waste Zone [a]	Reducing Cementitious[c]: Three types of concrete leachate chemistries controlled by different aged solid phases: young concrete leachate pH ~12, then pH 10.5, final pH 5.5 (Figure 3); generally higher in ionic strength than SRS groundwater. Leachate will contain sulfides released from slag (Angus and Glasser 1985).	Reducing Concrete *Kd* or Reducing Concrete solubility values
Reducing Concrete[b]: walls, roof, and floors are made of reducing concrete	Reducing Concrete (as immediately above)	Reducing Concrete *Kd* or Reducing Concrete solubility concentration limits[b]
Clayey Sediment: Upper Vadose Zone	Cementitious (as above).	Use cementitious leachate impacted clayey *Kd* values; $Kd_{CementLeach}$.
Sandy Sediment: Lower Vadose Zone	Cementitious (as above).	Use cementitious leachate impacted sandy *Kd* values; $Kd_{CementLeach}$. for sandy sediment.
Sandy Sediment: Aquifer Zone	Cementitious leachate pore water gets diluted with typical SRS groundwater and the aqueous phase takes on the properties of the latter: pH 5.8, ionic strength 10^{-4} M, trace levels of radionuclide concentrations and CDPs.	Initially use Sandy Sediment Kd_{CDP} until all the CDP[d] has leached from the Waste Zone. Then use Sandy Sediment *Kd*.

[a] The Saltstone contains blast-furnace slag (a strong reducing agent). The dimensions of the Saltstone Disposal Units vary; some are rectangular, while others are cylindrical.
[b] Reducing cementitious materials are those that contain slag and change the pore water chemistry sufficiently to require unique geochemical parameters (see Section 4.5).

5.7 Closed Liquid Waste Tanks

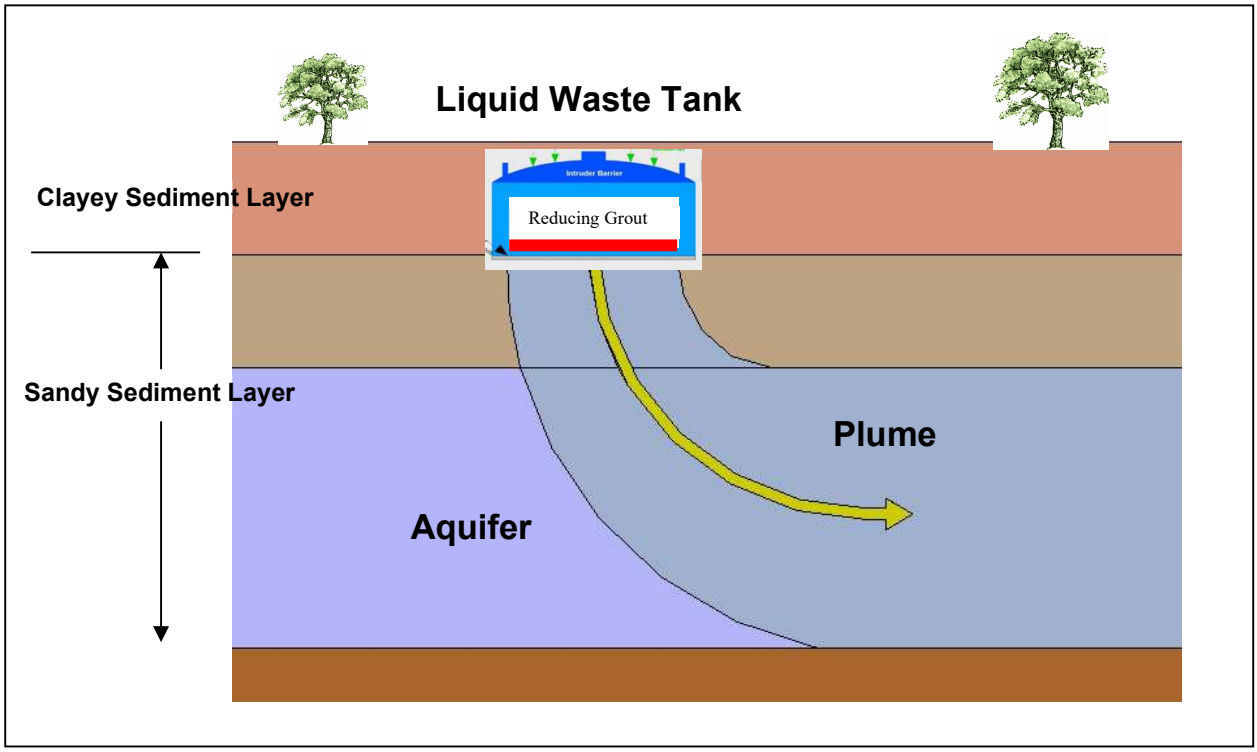

Figure 18. Schematic representation of the geochemical conceptual model of the Closed Liquid Waste Tanks Closure Concept. In some instances the Liquid Waste Tank rests within the aquifer layer. See Table 11 for facility description.

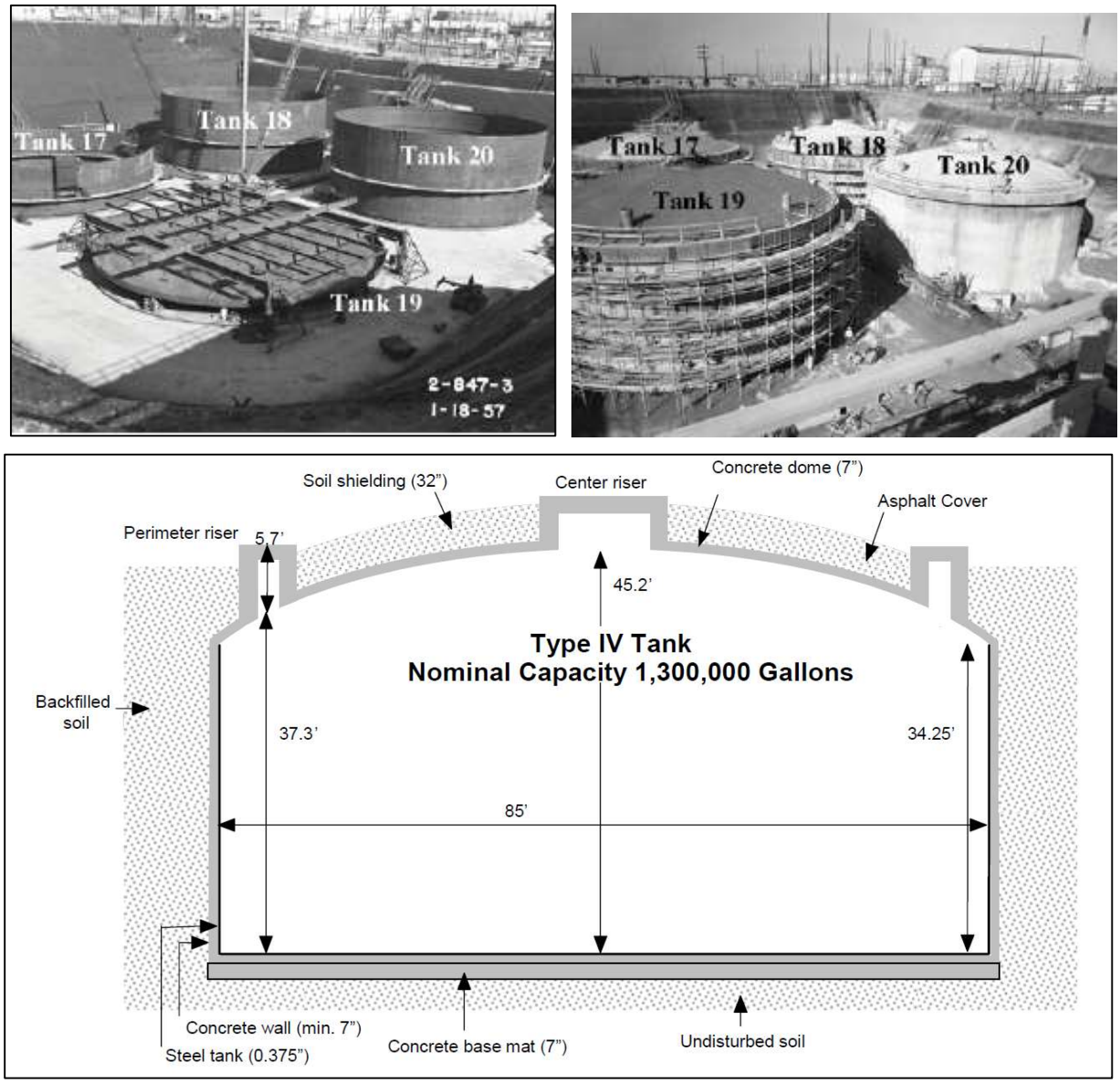

Figure 19. (Top) Photographs taken while waste tanks were under construction. (Bottom) dimensions of the Type IV tanks.

Table 11. Closed Liquid Waste Tanks: conceptual geochemical model of typical features and parameters (see Figure 18 and Figure 19).

Solid Phases	Aqueous Phase	Geochemical Parameter
Waste Zone [a]	Reducing Cementitious Leachate[b]: The rad waste consists typically of a thin layer (averaging 1.2 to 2 cm thick) existing on bottom of tank, ranging from ~0.3 cm for most of the bottom to ~4.5 cm along the edges. It is covered with reducing grout. Three types of concrete leachate chemistries controlled by different aged solid phases: young concrete leachate pH ~12, then pH 10.5, final pH 5.5; generally higher in ionic strength than SRS groundwater. Leachate will contain sulfides released from slag (Angus and Glasser, 1985).	Reducing Concrete *Kd* or Reducing Concrete solubility concentration limits[b] [c]
Basemat Concrete: Reducing concrete basemat	Reducing Cementitious Leachate: we model as if the aqueous phase is a reducing leachate because essentially all the water will originate from the closed tank above	Reducing Concrete *Kd* or Reducing Concrete solubility concentration limits[b]
Clayey Sediment: Upper Vadose Zone	Oxidized Cementitious Leachate: Oxidized cementitious leachate with three types of water chemistries, as described above.	Use cementitious leachate impacted clayey *Kd* values; $Kd_{CementLeach}$.
Sandy Sediment: Lower Vadose Zone	Oxidized Cementitious Leachate:	Use cementitious leachate impacted sandy *Kd* values; $Kd_{CementLeach}$. for sandy sediment.
Sandy Sediment: Aquifer Zone	Cementitious leachate pore water gets diluted with typical SRS groundwater and the aqueous phase takes on the properties of the latter: pH 5.8, ionic strength 10^{-4}, trace levels of radionuclide concentrations.	Use Sandy Sediment *Kd*.

[a] Release of radionuclides from the Contamination Zone is described by Denham (2009). In this model, radionuclides are solubility controlled.
[b] Reducing cementitious materials are those that contain slag and change the pore water chemistry sufficiently to require unique geochemical parameters (see Section 4.5).
[c] This table is not applicable for all tanks. The intruder barrier would not have to be treated differently than the grout.

6.0 DATA TABLES

Data tables are presented in this section based on the conceptual models presented in Section 4.0. Table 12 provides a list of the assumed oxidation states or speciation under the various Conceptual Environments. Table 13 is a look-up table of *Kd* values for Sandy Sediment, Clayey Sediment, and Cementitious Leachate Impacted Sediment Environments. Table 14 is a look-up table of *Kd* values for oxidizing and reducing cementitious Environments. The remaining tables in this section provide references and justification for the selection of the recommended values (Table 15 - Table 21).

- Table 15. Special waste form distribution coefficients (*Kd* values) under ambient and cementitious leachate environments.
- Table 16. Distribution coefficients (*Kd* values, mL/g): Sandy Sediment Environment and Clay Sediment Environment.
- Table 17. Distribution coefficients (*Kd* values, mL/g): Oxidizing Cementitious Environment.
- Table 18. Distribution coefficients (*Kd* values, mL/g): Reducing Cementitious Environment.
- Table 19. Distribution coefficients (*Kd* values, mL/g): Reoxidizing cementitious materials (*i.e.,* oxidized BFS-cementitious materials).
- Table 20. Apparent solubility values (k_s, mol/L) for the Oxidizing Cementitious Environment.**Error! Reference source not found.**
- Table 21. Apparent solubility values (*ks*; mol/L) for the Reducing Cementitious Environment.

6.1 Paired Apparent Solubility (k_s) and Distribution Coefficients (*Kd*)

By definition, when constituents of concern concentrations exceed the solubility concentration for a given mineral, precipitation occurs, and subsequently the constituent of concern aqueous concentrations cannot exceed the k_s. At concentrations below the solubility limit the constituent of concern concentration is assumed to be controlled by the *Kd* construct (Figure 1 – Bottom). Aqueous concentrations generally only exceed solubility limits in cementitious waste forms, such as in saltstone and tank closure (these facilities are discussed below in sections 5.6 and 5.7, respectively). The pairing of *Kd* and k_s values adhere to the following rules.

- k_s values assigned to reducing cementitious environments Table 21 are paired with *Kd* values for reducing cementitious environments Table 18.
- k_s values assigned to oxidizing cementitious environments **Error! Reference source not found.**are paired with *Kd* values for oxidizing cementitious environments (Table 17),
    - Except for Ba, Sr, and Ra in cementitious environments that have undergone reoxidation, in which case the *ks* values are paired with *Kd* values for reducing cementitious environments. This exception is in place to address the specific conditions of an aged reducing cementitious system that has undergone re-oxidation, as may occur with saltstone or for tank closure.

Table 12. Constituents of concern and their assumed oxidation states or speciation under varying environments.

	Chemical Grouping[(a)]	Sandy Sediment, Clayey Sediment, Cementitious Leachate Impacted Sandy/Clayey Sediment	Oxidizing Cement	Reducing Cement
Tritium (T)		HTO	HTO, OH^-	HTO, OH^-
Inorganic C		CO_3^{2-}, HCO_3^-	CO_3^{2-}, HCO_3^-	CO_3^{2-}, HCO_3^-
Ag, Tl	Monovalent soft metal	+1	+1	+1
Al	Trivalent metal	+3	+3	+3
As, Sb	Divalent Oxyanion	XO_4^{2-}	+5	+3
Co, Cd, Ni, Pt	Divalent Transition	+2	+2	+2
Cr		CrO_4^{2-}	+6	+3
Cu			+2	+1
Fe		Fe^{+3}	+3	+2
Mn			+4	+2
Mo			+6	+4
N		NO_3^-/NO_2^-	+5/+3	-3
Se, Te	VIB Elements	XO_4^{2-}, XO_3^{2-} [(c)]	XO_4^{2-}, XO_3^{2-}	XO_3^{2-}
Kr, Rn, Ar	Noble Gas	0	0	0
Sr, Ra, Ba, Ca	Alkali-earth metals	+2	+2	+2
Zr, Th	Group VI Elements	+4	+4	+4
Nb		$Nb(OH)_6$	$Nb(OH)_6^-$/ $Nb(OH)_7^{2-}$	$Nb(OH)_4^-$ [(b)]
Tc, Re	XO_4^-[(c)]	XO_4^-	XO_4^-	X^{4+}
Sn		+4	+4	+4
Cl, F, I, At	VIIB, Halides	-1	-1	-1
Cs, Fr, K, Na, Rb	Alkali metal	+1	+1	+1
Ac, Am, Bk, Bi, Ce,Cf Cm, Es, Eu, Fm, Gd, Lu, Sm, Y	Trivalent Actinides & Rare Earth Elements	+3	+3	+3
Hg, Pb, Po,	Soft, divalent cation	+2	+2	+2
U		UO_2^{2+}	UO_2^{2+}	U^{4+}
Np, Pa		XO_3^- [(c)]	XO_3^-	X^{4+}
Pu		$Pu^{VI}O_2^{2+}$, $Pu^{V}O_2^{+}$, colloid	$Pu^{VI}O_2^{2+}$, $Pu^{V}O_2^{+}$, colloid	Pu^{4+}, colloid

[(a)] These groupings of radionuclides will be used in the following *Kd* and solubility limit value tables in the absence of experimental data. These groupings are based on basic chemical considerations including periodicity and basic aqueous chemical properties.
[(b)] Nb likely exists as Nb(III) under reducing conditions, but little sorption data is available for this species (Baes and Mesmer, 1976). Nb speciation for sediment and oxidizing cement taken from Soderlund et al. (2015).
[(c)] *X* = generic metal

Table 13. Look-up table of various sediment distribution coefficients (*Kd* values) and cement leachate impact factors (Equations 6 and 7).

Constituent of Concern	Best Sand *Kd*	Best Clay *Kd*	Cement Leachate Impact Factor, f(CemLech)
	(mL/g)	(mL/g)	(unitless)
Ac	1E+03	9E+03	1.5
Ag	1E+01	3E+01	3.2
Al	1E+03	1E+03	1.5
Am	1E+03	9E+03	1.5
Ar	0E+00	0E+00	1
As	1E+02	2E+02	1.4
At	1E+00	3E+00	0.1
Ba	8E+00	3E+01	3
Bi	1E+03	9E+03	1.5
Bk	1E+03	9E+03	1.5
C	1E+01	4E+02	5
Ca	5E+00	2E+01	3
Cd	2E+01	3E+01	3
Ce	1E+03	9E+03	1.5
Cf	1E+03	9E+03	1.5
Cl	1E+00	8E+00	0.1
Cm	1E+03	9E+03	1.5
Co	4E+01	1E+02	3.2
Cr	4E+02	1E+03	1.4
Cs	2E+01	3E+02	1
Cu	5E+01	7E+01	3.2
Es	1E+03	9E+03	1.5
Eu	1E+03	9E+03	1.5
F	1E+00	8E+00	0.1
Fe	2E+02	4E+02	1.5
Fm	1E+03	9E+03	1.5
Fr	2E+01	3E+02	1
Gd	1E+03	9E+03	1.5
H	0E+00	0E+00	1
Hg	8E+02	1E+03	3.2
I	1E+00	3E+00	0.1
K	5E+00	3E+01	1
Kr	0E+00	0E+00	1
Lu	1E+03	9E+03	1.5
Mn	2E+01	2E+02	1.4
Mo	1E+03	1E+03	1.4
N	1E+00	8E+00	0.1
Na	5E+00	3E+01	1
Nb	1E+03	1E+03	1.4
Ni	7E+00	3E+01	3.2
Np	4E+00	2E+01	1.5
Pa	4E+00	2E+01	1.5
Pb	2E+03	5E+03	3.2
Pd	7E+00	3E+01	3.2
Po	2E+03	5E+03	2
Pt	7E+00	3E+01	3.2
Pu	1E+03	6.0E+03	2
Ra	3E+01	2E+02	3
Rb	2E+01	3E+02	1

Constituent of Concern	Best Sand *Kd*	Best Clay *Kd*	Cement Leachate Impact Factor, f(CemLech)
	(mL/g)	(mL/g)	(unitless)
Re	6E-01	2E+00	0.1
Rn	0E+00	0E+00	1
Sb	3E+03	3E+03	1.4
Se	1E+03	1E+03	1.4
Sm	1E+03	9E+03	1.5
Sn	2E+03	5E+03	3
Sr	5E+00	2E+01	3
Tc	6.0E-01	1.8E+00	0.1
Te	1E+03	1E+03	1.4
Th	9E+02	2E+03	2
Tl	3E+01	7E+01	1
U	3E+02	4E+02	3
Y	1E+03	9E+03	1.5
Zn	2E+01	3E+01	3
Zr	9E+02	2E+03	2

Table 14. Look-up table of cementitious material distribution coefficients (*Kd* values) and apparent solubility values (k_s) under oxidizing and reducing conditions.

Rad	Best Oxidizing Cement *Kd* Stage I	Best Oxidizing Cement *Kd* Stage II	Best Oxidizing Cement Kd Stage III	Best Reducing Cement *Kd* Stage I	Best Reducing Cement *Kd* Stage II	Best Reducing Cement Kd Stage III	Oxidizing Apparent Solubility Stage I	Oxidizing Apparent Solubility Stage II	Oxidizing Apparent Solubility Stage III	Reducing Apparent Solubility Stage I	Reducing Apparent Solubility Stage II	Reducing Apparent Solubility Stage III
	(mL/g)	(mL/g)	(mL/g)	(mL/g)	(mL/g)	(mL/g)	Mole/L (10^x)	Mole/L (10^x)	Mole/L (10^x)	Mole/L (10^x)	Mole/L (10^x)	Mole/L (10^x)
Ac	6E+03	6E+03	6E+02	7E+03	7E+03	1E+03	-11	-8	-7	-11	-8	-7
Ag	4E+03	4E+03	4E+02	5E+03	5E+03	1E+03	-7	-7	-6	-7	-7	-6
Al	6E+03	6E+03	6E+02	7E+03	7E+03	1E+03	-11	-8	-7	-11	-8	-7
Am	6E+03	6E+03	6E+02	7E+03	7E+03	1E+03	-11	-8	-7	-11	-8	-7
Ar	0E+00	0E+00	0E+00	0E+00	0E+00	0E+00	NA	NA	NA	NA	NA	NA
As	3E+02	3E+02	1E+02	3E+02	3E+02	1E+02	NA	NA	NA	NA	NA	NA
At	8E+00	1E+01	4E+00	0E+00	2E+00	0E+00	NA	NA	NA	NA	NA	NA
Ba	2E+02[(a)]	1E+02[(a)]	2E+02[(a)]	6E+03	6E+03	6E+02	-5	-5	NA	-7	-7	-7
Bi	6E+03	6E+03	6E+02	7E+03	7E+03	1E+03	-11	-8	-7	-11	-8	-7
Bk	6E+03	6E+03	6E+02	7E+03	7E+03	1E+03	-11	-8	-7	-11	-8	-7
C	2E+03	5E+03	5E+01	2E+03	5E+03	5E+01	-5	-6	-5	-5	-6	-5
Ca	9E+01	2E+01	9E+01	9E+01	2E+01	9E+01	-5	-5	NA	-5	-5	NA
Cd	4E+03	4E+03	4E+02	5E+03	5E+03	1E+03	-7	-7	-6	-7	-7	-6
Ce	6E+03	6E+03	6E+02	7E+03	7E+03	1E+03	-11	-8	-7	-11	-8	-7
Cf	6E+03	6E+03	6E+02	7E+03	7E+03	1E+03	-11	-8	-7	-11	-8	-7
Cl	0E+00	1E+01	1E+00	0E+00	1E+01	1E+00	NA	NA	NA	NA	NA	NA
Cm	6E+03	6E+03	6E+02	7E+03	7E+03	1E+03	-11	-8	-7	-11	-8	-7
Co	4E+03	4E+03	4E+02	5E+03	5E+03	1E+03	-7	-7	-6	-7	-7	-6
Cr	1E+01	1E+01	1E+00	1E+03	1E+03	1E+03	NA	NA	NA	-7	-7	-6
Cs	2E+00	2E+01	1E+01	2E+00	2E+01	1E+01	NA	NA	NA	NA	NA	NA
Cu	4E+03	4E+03	4E+02	5E+03	5E+03	1E+03	-7	-7	-6	-7	-7	-6
Es	6E+03	6E+03	6E+02	7E+03	7E+03	1E+03	-11	-8	-7	-11	-8	-7
Eu	6E+03	6E+03	6E+02	7E+03	7E+03	1E+03	-11	-8	-7	-11	-8	-7
F	0E+00	1E+01	1E+00	0E+00	1E+01	1E+00	NA	NA	NA	NA	NA	NA
Fe	6E+03	6E+03	6E+02	7E+03	7E+03	1E+03	-11	-8	-7	-11	-8	-7
Fm	6E+03	6E+03	6E+02	7E+03	7E+03	1E+03	-11	-8	-7	-11	-8	-7
Fr	2E+00	2E+01	1E+01	2E+00	2E+01	1E+01	NA	NA	NA	NA	NA	NA
Gd	6E+03	6E+03	6E+02	7E+03	7E+03	1E+03	-11	-8	-7	-11	-8	-7
H	0E+00	0E+00	0E+00	0E+00	0E+00	0E+00	NA	NA	NA	NA	NA	NA
Hg	3E+02	3E+02	1E+02	5E+02	5E+02	1E+02	-7	-7	-6	-7	-7	-6

Rad	Best Oxidizing Cement *Kd* Stage I	Best Oxidizing Cement *Kd* Stage II	Best Oxidizing Cement Kd Stage III	Best Reducing Cement *Kd* Stage I	Best Reducing Cement *Kd* Stage II	Best Reducing Cement Kd Stage III	Oxidizing Apparent Solubility Stage I	Oxidizing Apparent Solubility Stage II	Oxidizing Apparent Solubility Stage III	Reducing Apparent Solubility Stage I	Reducing Apparent Solubility Stage II	Reducing Apparent Solubility Stage III
	(mL/g)	(mL/g)	(mL/g)	(mL/g)	(mL/g)	(mL/g)	Mole/L (10^x)	Mole/L (10^x)	Mole/L (10^x)	Mole/L (10^x)	Mole/L (10^x)	Mole/L (10^x)
I	8E+00	1E+01	4E+00	0E+00	2E+00	0E+00	NA	NA	NA	NA	NA	NA
K	2E+00	2E+01	1E+01	2E+00	2E+01	1E+01	NA	NA	NA	NA	NA	NA
Kr	0E+00	0E+00	0E+00	0E+00	0E+00	0E+00	NA	NA	NA	NA	NA	NA
Lu	6E+03	6E+03	6E+02	7E+03	7E+03	1E+03	-11	-8	-7	-11	-8	-7
Mn	1E+02	1E+02	1E+01	1E+02	1E+02	1E+01	NA	NA	NA	NA	NA	NA
Mo	3E+00	3E+00	3E+00	3E+02	3E+02	2E+02	NA	NA	NA	NA	NA	NA
N	0E+00	0E+00	0E+00	0E+00	0E+00	0E+00	NA	NA	NA	NA	NA	NA
Na	0E+00	0E+00	0E+00	0E+00	0E+00	0E+00	NA	NA	NA	NA	NA	NA
Nb	1E+03	1E+03	5E+02	1E+03	1E+03	5E+02	NA	NA	NA	NA	NA	NA
Ni	7E+01	4E+02	4E+02	7E+01	4E+02	4E+02	-7	-7	-6	-7	-7	-6
Np	1E+04	1E+04	5E+03	1E+04	1E+04	5E+03	-13	-13	-7	-13	-13	-5
Pa	1E+04	1E+04	5E+03	1E+04	1E+04	5E+03	-13	-13	-7	-13	-13	-5
Pb	3E+02	3E+02	1E+02	5E+03	5E+03	1E+03	-7	-7	-6	-7	-7	-6
Pd	4E+03	4E+03	4E+02	5E+03	5E+03	1E+03	-7	-7	-6	-7	-7	-6
Po	3E+02	3E+02	1E+02	3E+02	3E+02	1E+02	-7	-7	-6	-7	-7	-6
Pt	4E+03	4E+03	4E+02	5E+03	5E+03	1E+03	-7	-7	-6	-7	-7	-6
Pu	1E+04	1E+04	2E+03	1E+04	1E+04	2E+03	-12	-12	-7	-12	-12	-9
Ra	2E+02[(a)]	1E+02[(a)]	2E+02[(a)]	6E+03	6E+03	6E+02	-6	-6	-6	-7	-7	-7
Rb	2E+00	2E+01	1E+01	2E+00	2E+01	1E+01	NA	NA	NA	NA	NA	NA
Re	8E-01	8E-01	5E-01	1E+03	1E+03	1E+03	NA	NA	NA	-9	-9	-6
Rn	0E+00	0E+00	0E+00	0E+00	0E+00	0E+00	NA	NA	NA	NA	NA	NA
Sb	3E+02	3E+02	1E+02	3E+02	3E+02	1E+02	NA	NA	NA	NA	NA	NA
Se	3E+00	3E+00	3E+00	3E+02	3E+02	2E+02	NA	NA	NA	NA	NA	NA
Sm	6E+03	6E+03	6E+02	7E+03	7E+03	1E+03	-11	-8	-7	-11	-8	-7
Sn	4E+03	4E+03	2E+03	4E+03	4E+03	2E+03	-7	-7	-6	-7	-7	-6
Sr	9E+01[(a)]	2E+01[(a)]	9E+01[(a)]	1E+03	1E+03	1E+02	-5	-5	NA	-6	-6	-6
Tc	8E-01	8E-01	5E-01	1E+03	1E+03	1E+03	NA	NA	NA	-9	-9	-6
Te	3E+00	3E+00	3E+00	3E+02	3E+02	2E+02	NA	NA	NA	NA	NA	NA
Th	1E+04	1E+04	2E+03	1E+04	1E+04	2E+03	-12	-12	-7	-12	-12	-7
Tl	2E+02	2E+02	8E+01	2E+02	2E+02	8E+01	NA	NA	NA	NA	NA	NA
U	1E+03	5E+03	5E+03	5E+03	5E+03	5E+03	-6	-5	-6	-6	-7	-7
Y	6E+03	6E+03	6E+02	7E+03	7E+03	1E+03	-11	-8	-7	-11	-8	-7
Zn	4E+03	4E+03	4E+02	5E+03	5E+03	1E+03	-7	-7	-6	-7	-7	-6
Zr	1E+04	1E+04	2E+03	1E+04	1E+04	2E+03	-12	-12	-7	-12	-12	-7

[(a)] These values differ for reoxidized cementitious materials, *i.e.,* BFS-containing materials that have aged to the point that all their reduction capacity has been consumed (See Table 20).

Table 15. Special waste form distribution coefficients (*Kd* values) under ambient and cementitious leachate environments.

Constit-uent of Concern	Waste Form	*Kd* When Waste is Disposed in Sediment	*Kd* When Waste is Disposed in Concrete	References	SRS Document No.
		(mL/g)	(mL/g)		
I-129	F-Area Activated C	1E+05	9E+02	(Kaplan and Serkiz, 2000b)	WSRC-TR-2000-00308
I-129	H-Area Activated C	6E+04	3E+02	(Kaplan and Serkiz, 2000b)	WSRC-TR-2000-00308
I-129	F-Area CG-8	5E+01	3E+00	(Kaplan and Serkiz, 2000b)	WSRC-TR-2000-00308
I-129	H-Area CG-8	4E+02	1E+02	(Kaplan and Serkiz, 2000b)	WSRC-TR-2000-00308
I-129	H-Area Filtercake	7E+02	6E+02	(Kaplan and Serkiz, 2000b)	WSRC-TR-2000-00308
I-129	H-Area Dowex 21K	2E+04	2E+03	(Kaplan and Serkiz, 2000b)	WSRC-TR-2000-00308
I-129	F-WTU Dowex 21K	7E+03	3E+03	(Kaplan et al., 1999)	WSRC-TR-1999-00270
I-129	ETF Carbon	7E+03	6E+02	(Kaplan et al., 1999)	WSRC-TR-1999-00270
I-129	EDF GT-73	1E+04	3E+03	(Kaplan et al., 1999)	WSRC-TR-1999-00270
I-129	K&L Disassembly Basin Facilities Resins [a]	4E+03[b]	4E+03[b]	(Kaplan and Coffey, 2002)	WSRC-TR-2002-00349
I-129	SIR-1200	6E+03	6E+03	(Kaplan, 2001)	WSRC-TR-2001-00346
I-129	F-Area Ground Water Treatment Unit Filtercake	6E+01	1E+01	(Kaplan and Iverson, 2001)	WSRC-TR-2001-00253
C-14	K&L Disassembly Basin Facilities Resins [a]	2E+02	1E+02	(Kaplan and Coffey, 2002)	WSRC-TR-2002-00349
Tc-99	K&L Disassembly Basin Facilities Resins [a]	7E+02[b]	8E+02[b]	(Kaplan and Coffey, 2002)	WSRC-TR-2002-00349

[a] This is a mixed bed of resins, including a 42:58 cation:anion mass ratio of the cation resin CG-8, and the anion resin SBG-1. The tests were conducted, as was the case with the other measurements in this table, with spent resin, i.e., resin that had been used in production, actual waste resin that would be disposed.
[b] These were originally measured as “greater than” values.

Table 16. Distribution coefficients (*Kd* values, mL/g): Sandy Sediment Environment and Clay Sediment Environment.

Constituent of Concern	Sandy Sediment	Clayey Sediment	Comments/References[(a)]
Ar, ^{3}H, Kr, Rn,	0	0	Tritium & Noble Gases: No sorption experiments have been conducted on SRS sediments or other sediments with noble gases. Tritium is assumed to be primarily incorporated into water and the noble gases are assumed to be inert and not to interact with sediments.
Cl, N (nitrate, nitrite), F	1	8	Monovalent anions: Site-specific measurements of Cl *Kd* values were recently made (Seaman and Kaplan, 2010): sandy sediment *Kd* = 1.8 ± 1.1 mL/g and for a clayey sediment, the *Kd* was 8.5 ± 0.5 mL/g.
Cr	400	1000	Seaman and Kaplan (2010) measured Cr(VI) *Kd* values of 411 ± 84 mL/g in a sandy subsurface sediment and 1214 ± 149 mL/g in a clayey sediment (both soils had a pH of ~5). Using batch and column studies, Seaman et al. (1999) reported that Cr(VI) was strongly attenuated by SRS subsurface sediments. Fe-oxides within the soils used in the study were responsible for sorption because natural pH levels of ~5.5 were below the zero point of charge (pH ~8), giving the soils a net positive charge to attract the CrO_4^{2-} anions.
Ac, Am, Bi, Bk, Ce Cf, Cm, Es, Eu, Fm, Gd, Lu, Sm, Y	1000	9000	Trivalent Cations: Kaplan and Serkiz (2004) reported that SRS sandy sediment Ce(III) *Kd* = 1220 ± 1040 mL/g at pH 5.3; SRS clayey sediment Ce(III) *Kd* = 8697 ± 4980 mL/g at pH 5.3. Kaplan and Serkiz (2004) reported SRS sandy sediment Eu(III) *Kd* = 1168 ± 1159 mL/g at pH 5.3; SRS clayey sediment Eu(III) *Kd* = 9020 ± 3526 mL/g at pH 5.3. Both trivalent cations had very similar *Kd* values for a given sediment. Grogan (2008) measured Y *Kd* values in 27 SRS sediments collected from the E-Area SRS subsurface. Most of the *Kd* values were "greater-than values," that exceeded 3000 mL/g. Coutelot et al. (2020) conducted $Kd_{desorption}$ measurements (10 mM NaCl, 1/10 sediment-to-solution ratios, 30 days equilibration) using lysimeter samples (clayey sediment) that had been amended with ^{152}Eu (Lysimeter L26). The ^{152}Eu had been in contact with sediment for 4 yr and had an average (n = 10) $Kd_{desorption}$ = 4293 ± 2896 mL/g.
Al	1000	1000	Crapse et al. (2004) (Figure 33 and Table 4) made in situ measurements of Al solubility in a wide pH range from sediments collected from D-Area. At pH 3.18, Al porewater concentrations were at a maximum of 276,300 ppb, and then the concentration decreased to ~10 ppb at pH 7, and then at higher pH levels the Al concentrations started to rise again. At the pH of interest for the Sandy and Clayey sediment, pH 5.5, the Al concentrations (apparent solubility) were ~300 ppb. A comparable *Kd* value was 1300 mL/g (Al-solid = 402 ppm [Table 25 in Crapse et al. (2004) Al-liquid = 0.3ppm [Fig. 33 in Crapse et al. (2004) and Table 5). Theoretically, Al sorption is actually quite large in alkaline environments. Assumed species: Low pH: Al^{3+}, $Al(OH)^{2+}$, and $Al(OH)_3^0$; High pH: $Al(OH)_4^-$, and $Al(OH)_4^{2-}$.
Fe	200	400	Knox and Kaplan (2003) measured Fe K_d values of a subsurface sediment collected from TNX on the SRS. They conducted a sorption isotherm using one SRS loamy-textured sediment (K_d as a function of dissolved Fe(II) concentrations at ambient pH levels, pH 5.8). They did not take any precaution to exclude oxygen from their study, therefore the Fe(II) amendments almost certainly oxidized to Fe(III). They noted a rather flat response of K_d to Fe_{aq} concentrations from 0.1 to 0.21 µg/L with *Kd* values that were generally ~400 mL/g. Above 21 µg/L, Fe precipitation causing the apparent K_d values to increase precipitously to >2000 mL/g. Because of the minimal amount of relevant data. The observation of precipitation at µg/L Fe concentrations is indicative that the Fe(II) converting to Fe(III). But because the PA is interested in radio-Fe isotopes, sub-

Constituent of Concern	Sandy Sediment	Clayey Sediment	Comments/References[(a)]
			µg/L Fe concentrations, then *Kd* and not k_s *are appropriate.* The Fe K_d value assignments used this single measurement as an upper boundary for both sediment types.
Inorganic C	10	400	^{14}C is assumed to exist in the SRS subsurface primarily as HCO_3^-. Little carbonate minerals exists in the upper aquifers of the SRS due to the low pH and therefore HCO_3^- concentrations are not expected to be solubility controlled. Roberts and Kaplan (2008) found that ^{14}C-carbonate sorption to sediments had very slow kinetics; after 6 months, ^{14}C-carbonate sorption to SRS sediments had not come to steady state. *Kd* values in a sandy sediment were 1.5 ± 1.2 mL/g after 1 day and 8.6 ± 1.9 mL/g after 6 months. Similarly, *Kd* values in a subsurface clayey sediment were 27.6 ± 3.9 mL/g after 1 day and >372 after 6 months. While the sorption mechanism is not known, it may be attributed to the net positive charge of the pH ~5.5 SRS sediments (more specifically the Fe-oxide coatings on these sediments.
Cs, Fr, Rb	20	300	Monovalent (Group 1A): To develop better understanding of the underlying mechanisms responsible for the observed transport of Cs in the lysimeter experiments, a series of laboratory batch and column sorption experiments were conducted using conditions simulating RadFLEx, including identical sediment (clayey sediment) (Barber, 2017). In laboratory studies using lysimeter clayey sediments, he systematically evaluated effects on Cs sorption. Varying pH between 4 and 6 (background pH is 5.5) and ionic strength between 10 and 100 m*M* (background ionic strength is 0.1 mM) had minimal effect on Cs *Kd* values. Using sediments that had been in contact for 30 days with a five orders-of-magnitude ^{133}Cs concentration range, Barber (2017) detected minimal change in (ad)sorption *Kd* values when ^{133}Cs concentrations were <1.5 µg/L (*Kd* = 410.2, 352.0, 440.4, and 459.6 mL/g). But when ^{133}Cs concentration ranged between ≥1.5 and ≤134 µg/L ^{133}Cs, the *Kd* values progressively decreased from 459.6 to 39 mL/g. SRS PA conditions are expected to typically be <1.5 µg/L. Not surprisingly, desorption *Kd* value of the same samples followed similar trends, but the values were 2 orders-of-magnitude greater than the (ad)sorption *Kd* values. For the sediments amended with ^{133}Cs ≤1.5 µg/L, the $Kd_{desorption}$ were 27,200, 27,200, 26,700, 24,400 mL/g. When the sediments amended with ^{133}Cs concentrations ranging between ≥1.5 and ≤134 µg/L, the $Kd_{desorption}$ values progressively decreased from 24,400 to 18,400 mL/g. Using the same sediment, Barber (2017) conducted column studies and noted that after 128 pore-volumes effluent, the Cs center of mass in the column had migrated only 0.708 cm down the column. He concluded that: 1) *Kd* values of 200 mL/g grossly overestimated transport (meaning this *Kd* underestimated true (ad)sorption), 2) the desorption values of 27,000 mL/g were likely closer to the correct *Kd* value reflecting transport, and 3) that the soil Cs concentrations indicated that transport was controlled by more than the simple equilibrium *Kd* construct, included hysteresis with desorption and the presence of high-energy ("irreversible") sorption site. Additional modeling is planned to quantify these additional processes. Using the same clayey lysimeter sediment as Barber (2017), Montgomery et al. (2017) conducted a series of batch adsorption tests in support of the lysimeter program (clayey sediment) to provide insight into the role of organic ligands amendments on radionuclide *Kd* values. They measure Cs *Kd* values ranging from 4 to 245 mL/g, with an average of 108 mL/g. Finally, Coutelot et al. (2020) conducted some $Kd_{desorption}$ measurements (10 mM NaCl, 1/10 sediment-to-solution ratios, 30 days equilibration) from lysimeter (clayey sediment) samples that had been amended with ^{137}Cs (Lysimeter L26) and a second core that had been amended with a simulant Defense Waste Processing Facility (DWPF) glass contained Tank 50 waste, including ^{137}Cs. (The 10-cm^3 DWPF glass was buried 30-cm deep within a 60 cm long sediment core.) The former had been in contact with sediment for 4 yr and had an average (n = 10) $Kd_{desorption}$ = 2262 ± 390 mL/g, and the latter had been in contact with sediment for 26 years and had a $Kd_{desorption}$ (n = 1) of 2051 mL/g.

Constituent of Concern	Sandy Sediment	Clayey Sediment	Comments/References[(a)]
			Hoeffner (1985) reported that Cs sorption to SRS sediments is very pH dependent. Under ambient conditions (pH ~5.5), *Kd* values = 410 mL/g. Johnson (1995) (Figure 5-18 in citation) reported Cs *Kd* values of 800 mL/g in aged field samples recovered from F-Area, SRS (an acidic radionuclide plume) with initial Cs concentrations of 1E-8 M Cs at pH 5. In field observations (squeezed porewater out of aquifer sediment), he measured a *Kd* of 29 mL/g at pH 5. Johnson (1995; Figure 5-17 in citation), using subsurface F-area sediments, showed that the Cs sorption to SRS sediments was very pH dependent and that there was a steep increase in sorption as pH increased from 4.2 to 6.4, between which the *Kd* increased from about 5 to 95 mL/g. At pH 5.5 the *Kd* values ranged from 20 to 35 mL/g. Such field-desorption *Kd* values provide useful trends, but are difficult to extract quantitative information because of inherent problems in defining the solid phase "exchangeable fraction" of Cs used in the numerator of the *Kd* measurement (Krupka et al., 1999b). Findley (1998) conducted sequential extraction studies and reported that field contaminated sediments did not desorb Cs until extremely harsh acids were used, whereas in lab tests where Cs was added during adsorption (followed by desorption) tests, a majority of the Cs desorbed using relatively mild extractants. This suggests that Cs may become more strongly bound by SRS sediment with time. More recently, Barber (2017) noted significant increases in adsorption and desorption *Kd* values as contact time increased. This same finding has been reported for Hanford and Chernobyl sediments. In distilled water, Cs *Kd* values were as high as 1500 mL/g, underscoring the importance of using appropriate background electrolytes when conducting sorption experiments. Grogan et al. (2008) measured Cs *Kd* values in 27 sediments collected from E-Area SRS. They used SRS groundwater as a background solution. Mean was 13 ± 3.8 mL/g, ranging from 3.5 to 97 mL/g. The Upper Vadose Zone (dominated by clayey sediment) had a mean of 11.3 ± 3.0 mL/g; the Lower Vadose Zone (dominated by sandy sediment) had a mean of 5.6 ± 0.5 mL/g (In a zone containing mixed textured sediments, the Aquifer Zone, the mean *Kd* value was 21.2 ± 9.2 mL/g). Goto (2001) conducted >200 Cs sorption experiments with five SRS sediments of varying clay content. She showed a strong Cs-*Kd* dependency on Cs concentrations at environmental-relevant concentrations. The *Kd* values ranged from 226 ± 51 to 21 ± 7 mL/g at ambient pH levels; varying directly with clay content (Goto 2001; Table 5-3). Sediments with clay content of >10% had Cs *Kd* values >139 mL/g. Those with clay content <10% had *Kd* values of 73 to 15 mL/g. This series of studies provides the highest quality data, both in terms of providing understanding of how Cs binds to SRS soils and for providing quantitative information relative for the selection of best estimate *Kd* values. Based in part on the extensive desorption *Kd* values results conducted by Barber (2017) and Coutelot et al. (2020), which observed generally greater (ad)sorption *Kd* values than Goto (2001) and Montgomery et al. (2017), the recommended Cs *Kd* values previous reported by Kaplan (2016) of 10 mL/g for sandy sediment and 50 mL/g for clayey sediment were increased here to 20 mL/g for sandy sediment and 300 mL/g for clayey sediments. As noted above, these increases are supported by the renewed discovery of the much greater desorption vs. (ad)sorption *Kd* values and the presence of high-energy ("irreversible") sorption sites in our sediment, albeit there is a low concentration of these sites, perhaps <5% (Goto, 2001). Also, it is expected that dissolved radiocesium concentrations will be extremely low in most circumstances, thereby further supporting the need to increase sediment Cs *Kd* values from the previous recommended values. There has not been any recent research conducted with sandy sediments, only clayey sediments, therefore relatively smaller increases in recommended *Kd* values are reported here.
Tl	30	70	Seaman and Kaplan (2010) measured Tl(I) *Kd* values using SRS site specific sediments and simulated groundwater. Tl *Kd* values in the sandy sediment were 35 mL/g at pH 5.5 (background pH) and decreased to 20 mL/g as the pH decreased to 3

Constituent of Concern	Sandy Sediment	Clayey Sediment	Comments/References[(a)]
			and increased to >120 mL/g when the pH was increased above pH 7. In a clayey sediment, the Tl *Kd* value was about 90 mL/g at pH 5.5, and did not change greatly as the pH was decreased to 3, but increased sharply as the pH increased >7 to *Kd* = >120 mL/g. Together these results indicate that Tl does not behave geochemically like K.
Na, K	5	30	There has not been any Na or K sorption studies conducted with SRS sediments. Estimates were set lower than Cs sorption values because Na and K are also monovalent cations in the Group 1A in the Periodic Table, but they are strongly hydrated, weakening their outer-sphere sorption bonds to sediments. No studies showing the quantitative differences between Cs and Na/K were found in the literature to estimate better Na and K *Kd* values based on the large amount SRS Cs values.
Co	40	100	Hoeffner (1985) reported that: (1) a SRS sandy sediment (9% clay, pH ~4.7) had a Co *Kd* = 4.6 mL/g, (2) a SRS clayey sediment (23% clay, pH ~4.7) had a Co *Kd* = 29 mL/g; (3) Co *Kd* values in SRS sediments were independent of Co concentration between 1E-12 to 1E-6 M Co; (4) Co *Kd* values in SRS sediments decreased in the presence of high divalent cation concentrations but not in presence of high monovalent cation concentrations; (5) Co sorption had a strong pH dependency with a slight increase in *Kd* from pH 2 to 4.8 (background) then sharp increase in *Kd* between pH values of 4.8 to 7 (*Kd* = 20,000 mL/g), and then as pH increased to 9.5 the *Kd* steadily decreased to ~20 mL/g (thus concrete *Kd* values should be appreciably higher than background sediment *Kd* values (background pH *Kd* = 7 and cement pH *Kd* = 30) (*2*). Oblath et al. (1983) estimated *Kd* values of 10 to 20 mL/g based on SRS field lysimeters leachate ^{60}Co concentrations over a two-year period. Grogan et al (2008) measured Co *Kd* values in 27 sediments collected from E-Area SRS. Mean was 306 ± 117 mL/g, ranging from 33 to 2710 mL/g. The Upper Vadose Zone (dominated by clayey sediment) had a mean of 154 ± 37 mL/g; the Lower Vadose Zone (dominated by sandy sediment) had a mean of 54 ± 3 mL/g; Aquifer Zone (containing a mix of sandy and clayey sediments, including some of the Tan Clay layer, which has a high binding affinity for cations) had a mean of 535 ± 264 mL/g. Coutelot et al. (2020) conducted some $Kd_{desorption}$ measurements (10 mM NaCl, 1/10 sediment-to-solution ratios, 30 days equilibration) using lysimeter samples (clayey sediment) that had been amended with ^{60}Co (Lysimeter L26). The ^{60}Co had been in contact with sediment for 4 yr as part of the field lysimeter program (RadFLEx) and had an average (n = 15) $Kd_{desorption}$ = 29.0 ± 9.2 mL/g.
At, I	1	3	A review of iodine *Kd* values was recently conducted because a large number of recent studies had been completed to study not only the magnitude of iodine partitioning between groundwater and subsurface SRS sediment, but also what were the factors responsible for its geochemical behavior (Kaplan et al., 2013). In the report they recommend best estimate values of 1 mL/g for sandy sediments and 3 mL/g for clayey sediments, which are ~3x greater than best estimates reported in the previous *Kd* database (Kaplan 2010). These proposed *Kd* values reflect a much better understanding of iodine geochemistry in the SRS subsurface environment, which permits reducing the associated conservatism included in the original estimates to account for uncertainty. Among the key contributing discoveries supporting the contention that the *Kd* values should be increased are that: 1) not only iodide (I-), but also the more strongly sorbing iodate (IO_3^-) species exists in SRS groundwater (average total iodine = 15% iodide, 42% iodate, and 43% organo-iodine), 2) when iodine was added as iodate, the measured *Kd* values were 2 to 6 times greater than when the iodine was added as iodide, and perhaps most importantly, 3) higher desorption (10 to 20 mL/g) than (ad)sorption (all previous studies) *Kd* values were measured. The implications of this latter point is that the iodine desorption process would be appreciably slower than the (ad)sorption process, and as such would control the rate (and the PA *Kd* value) that iodine sorbed to and therefore migrated through the subsurface sediment. High desorption *Kd* values would result in the "effective *Kd*" for a reactive transport model being closer to the desorption *Kd* value

Constituent of Concern	Sandy Sediment	Clayey Sediment	Comments/References[(a)]
			(the rate limiting value) than the (ad)sorption *Kd* value. In summary, our understanding of ^{129}I geochemistry has greatly improved, reducing the uncertainty associated with the PA's conceptual model, thereby permitting us to reduce the conservatism presently incorporated in PA input values to describe ^{129}I fate and transport in the SRS subsurface environment. For iodide, the subsurface sediments had *Kd* values ranging from 1.1 to 33.7 mL/g; for iodate, the *Kd* values ranged from 2.4 to 60.9 mL/g (Emerson et al., 2014). Stone et al. (1985) reported iodide (I^-) *Kd* values based on column studies to be 0.6 mL/g, which was in the low range of *Kd* values they measured by the batch method, which ranged from 0.5 to 6.6 mL/g (texture of sediment is unknown). The column studies likely reflect non-equilibrium conditions and thus did not provide sufficient time for the iodide to sorb. Kaplan (2002) reported a similar *Kd* of 0.6 mL/g at pH ~5 in an upland sandy sediment and 1.2 mL/g in a wetland sediment at pH 5. Hoeffner (1985) reported appreciably higher *Kd* values in a sediment that contained 31% silt + clay content of 10, 5.35, and 3.62, mL/g for initial I^- concentration of 5, 50 and 500 µg/L I^-. Iodide sorption to a clayey subsurface SRS sediment (no fulvic acid added) and SRS uncontaminated groundwater was (units of mL/g): *Kd* = -0.2 ± 0.2 at pH 3.9, *Kd* = 0.1 ± 0.4 at pH 5.3, and 0.2 ± 0.1 at pH 6.7 (Kaplan and Serkiz 2006). Similar experimental setup, except to a sandy subsurface SRS sediment *Kd* values were always ~0 mL/g between pH 3.9 and 6.7 (Kaplan and Serkiz 2006). These latter studies had too much variability, making it impossible to discern whether the *Kd* values were significantly different than 0 mL/g. Powell et al. (2010) reported *Kd* values of SRS subsurface sandy soils after 8 days of contact; for iodide in contact with sandy sediment the *Kd* values were 8 mL/g and for clayey sediment, they were 9 mL/g. Similarly, iodate *Kd* values were 5 mL/g for sandy sediments and 40 mL/g for clayey sediments. Using three loamy sediments (texture that is in between a sand or a clay), iodide *Kd* values for three sediments ranged from 0.5 to 33.7 mL/g, and iodate *Kd* values ranged from 3.5 to 60.9 mL/g (Kaplan et al., 2010a).
Ag	10	30	Site-specific measurements of Ag *Kd* values were made (Seaman and Kaplan 2010): sandy sediment *Kd* = 10.6 ± 2.5 mL/g and for a clayey sediment, the *Kd* was 33.8 ± 13 mL/g.
Ni, Pd, Pt	7	30	Kaplan and Serkiz (2004) reported that SRS sandy sediment Ni *Kd* = 7 ± 2 mL/g at pH 5.3; SRS clayey sediment Ni *Kd* = 30 ± 1 mL/g at pH 5.3. Using 3 clayey sands (>19% clay) from the SRS, Neiheisel (1983) reported Ni *Kd* values of 115, 116, and 120 mL/g. The results from these two studies vary greatly. The lower, more conservative values will be used until additional work warrants using larger values.
Cu	50	70	Cu exists primarily in the +2 state through pH/Eh region of interest. Cu+ exists only under reducing & pH >6. CuS formed under reducing conditions. In oxidizing conditions, above pH 7, $Cu(OH)_2$ dominates; below pH 7, Cu^{2+} dominates. There have not been any *Kd* values measured in SRS subsurface sediments. In a fine sand (pH 8.3; OM. = 1.4%) had a Cu *Kd* value of 206 mL/g (Wong et al., 1993); this value is probably the upper limit of the *Kd* we may expect in the SRS subsurface due to the elevated organic matter concentrations and pH. Buchter et al. (1989) in a survey of 11 soils, reported that a soil ("Windsor": pH = 5.8, OM = 0.67%, silt + clay = 25%) like that of a clayey SRS sediment had a Cu *Kd* value of 77.1 mL/g. In the same study, the sediment most like a "sandy SRS sediment" ("Spodosal": pH 4.3; OM = 1.98%, silt + clay = 10%) had a Cu *Kd* value of 56 mL/g.
Cd, Zn	20	30	Grogan et al. (2008) measured Cd *Kd* values in 27 sediments collected from E-Area SRS; the mean was 89 ± 36 mL/g, ranging from 9 to 927 mL/g. The Upper Vadose Zone (dominated by clayey sediment) had a mean of 37 ± 8 mL/g; the Lower Vadose Zone (dominated by sandy sediment) had a mean of 16 ± 0.9 mL/g (Aquifer Zone 131 ± 53 mL/g, but it

Constituent of Concern	Sandy Sediment	Clayey Sediment	Comments/References[(a)]
			included some clay lenses from the semi-permeable Tan Clay layer and bias the *Kd* values to be larger). The best estimates were largely based on the data of Grogan et al. (2008) rounded to one significant figure.
Np, Pa	4	20	Np will exist primarily as NpO_2^+ (EPA, 2004). It has been shown that Np: (1) sorbs moderately to iron oxides and clays, (2) does not compete favorably with dissolved Ca or other divalent ions, and (3) sorption is strongly pH dependent (EPA, 2004). Extensive Np geochemical research has been conducted recently as part of the Radionuclide Field Lysimeter Experiment (RadFLEx) and associated laboratory experiments (Maloubier et al., 2017; Parker et al., 2020; Peruski et al., 2017a; Peruski et al., 2018a; Peruski et al., 2018c; Peruski et al., 2018d). Np from Np(V) sources at the RadFLEx facility readily leached from the vadose clayey sediments, whereas the amount of Np from Np(IV) leached orders of magnitude less (Peruski et al., 2018d). Parker et al. (2020) concluded that Np released into the effluent from field lysimeters amended with $Np(IV)O_2$ had oxidation of to the more mobile Np(V) aqueous species (Parker et al., 2020; Peruski et al., 2017a; Peruski et al., 2018a; Peruski et al., 2017c; Peruski et al., 2018d). From core samples recovered from a field lysimeter experiment, desorption *Kd* values of 34, 72, and 16 mL/g were measured in clayey sediments that were amended with Np(V) two years earlier (Kaplan et al., 2018; Peruski et al., 2018c). In a parallel set of experiments in which Np(IV) was the source, an oxidation state that is not generally expected in vadose zone sediments, desorption *Kd* values from lysimeter sediment cores samples were 810 and 1323 mL/g (Peruski et al., 2018d). Importantly, these results confirm expectations that Np(IV) binds more strongly to soils than Np(V). Finally, these field transport studies demonstrated the presence of mobile Np colloids. The nano-sized colloids were fragmentations from the original source NpO_2 solids placed in the lysimeter. Miller et al. (2009) measured *Kd* values in SRS sandy and clayey sediment of 4.26 ± 0.24 mL/g and 9.05 ± 0.61 mL/g, respectively. The latter represents the first Np *Kd* in a clayey sediment. Adding NOM resulted in increases in Np *Kd* values to 13 and 24 mL/g. In the presence of varying reductants, the *Kd* values increased slightly between 13 and 24 mL/g. These slight increases presumably resulted from partial reduction of Np(V) to Np(IV), the stronger sorbing form of Np. An important finding in this study was that Np had little tendency to reduce under to Np(IV) even under the most strongly reducing conditions expected under natural SRS conditions. A more recent SRS sediment Np *Kd* study was conducted by Powell et al. (2010), who reported sandy sediment *Kd* values 4.3 +/- 0.2 and 5.3 +/- 0.2 mL/g and for clayey sediment 9 +/1 0.6 and 10.0 +/- 0.3 mL/g. Furthermore, they demonstrated that 1) there very little Np was associated with mobile colloids, ~1%, 2) the addition of natural organic matter only moderately increased the *Kd* values, and 3) few if any conditions likely to exist in the SRS subsurface environment would likely promote Np(V) reduction to the more strongly binding (Np(IV) state. The Np sorption study using SRS sediments found in the literature was Sheppard et al. (1979). In this study, Np *Kd* values for a soil (pH = 5.1, cation exchange capacity = 2.5 meq/100 g, 3.6% silt, 0.5% clay, $CaCO_3$ = <0.2 mg/kg) were 0.25 and 0.16 mL/g. This sediment is lower in clay content and pH than our assumed typical sediments for the "Sandy Sediment" or "Clayey Sediment". The 4-year flow field lysimeter experiments, along with the desorption (vs. (ad)sorption) experiments provide important guidance for the selection of *Kd* values (Maloubier et al., 2017; Peruski et al., 2017a; Peruski et al., 2018a; Peruski et al., 2018c; Peruski et al., 2018d). These first-time desorption *Kd* measurements of Np from SRS sediments were much greater than previous (ad)sorption *Kd* values. This outcome is not surprising because the desorption process is the rate limiting process, and as such the more important values compared to adsorption *Kd* values for reactive transport PA purposes.

Constituent of Concern	Sandy Sediment	Clayey Sediment	Comments/References[(a)]
			Based on these high pedigree experiments, as well as earlier (ad)sorption laboratory studies, the recommended *Kd* values for the sandy and clayey sediments are 4 and 20 mL/g, respectively (an increase from 3 and 9 mL/g, respectively, as reported in the previous data package (Kaplan 2016).
Pu	1000	6000	A great deal of Pu sorption studies has recently been completed by SRNL and Clemson University (Fjeld et al., 2004; Kaplan et al., 2006; Kaplan et al., 2004a, b; Kaplan et al., 2001; Kaplan and Wilhite, 2001; Powell et al., 2004, 2005). Almond et al. (2012b) reviewed site specific Pu *Kd* values and concluded that there are a wide range of values. Their Pu *Kd* included 65 values derived from laboratory (ad)sorption experiments ranging in contact times between 1 and 33 days and included 34 measurements with sandy sediments and 31 measurements with clayey sediments. Looking at only measurements made at pH 4.5 to 7.0 (far field SRS conditions), the median Pu *Kd* in sandy sediment was1800 mL/g with a 95 percentile range between 210 and 20,000 mL/g. Similarly, for clayey sediment the median Pu *Kd* in sandy sediment was 8600 mL/g with a 95-percentile ranging from 1000 to 33,000 mL/g. Kaplan et al. (2004a), in a laboratory experiment using a clayey sediment showed that after 50-hr that 99% of the Pu added as Pu(V) had converted to Pu(IV) in the sediment/water system. Demirkanli et al. (2007) using computer simulation of a lysimeter study using clayey sediments reported that during a 24-yr simulation that 99.99% of the Pu existed as Pu(III/IV). Using X-ray adsorption spectroscopy, Kaplan et al. (2008b) did not detected any oxidized forms of Pu in SRS sediments that had been in field lysimeters for 11 years. The conclusion from these studies were that Pu exists in the SRS subsurface environment almost exclusively as the Pu(IV), the strong binding from of Pu, irrespective of the oxidation state that the Pu was introduced to the sediment. Recent studies at the Radionuclide Field Lysimeter Experiment (RadFLEx) using sediment (clayey texture) subsamples collected from a 3.4-year-old core that contained a $PuO_2(s)$ source (Lysimeter L44), revealed that Pu(IV) was strongly bound to the sediment with $Kd_{desorption}$ ranging from 10,853 to 41,166 mL/g (1:15 sediment:10mM-NaCl; triplicate; 14 day contact) (Maloubier et al., 2020; Maloubier et al., 2017; Peruski et al., 2017b). In another lysimeter core (L41) that was amended with $Pu(V)NH_4(CO_3)$ and had been left at the lysimeter RadFLEx facility for 3-yr, $Kd_{desorption}$ measurements ranged from 900 to 2400 mL/g (Maloubier et al., 2020; Maloubier et al., 2017; Peruski et al., 2018b). Pu from the Pu(V) source moved much further down the lysimeter than the Pu from the Pu(IV). They measured that most of the sediment bound Pu had been converted to Pu(IV); separate kinetic studies demonstrated that it took only hours for the Pu(V) to convert to Pu(IV) once it made contact with the lysimeter sediment (Maloubier et al., 2017). These recent lysimeter studies provide important mechanistic geochemical information from long-term flow conditions. Based on the critical review by Almond et al. (2012b) of (ad)sorption Pu *Kd* values, showing median values of 1800 mL/g for sandy sediments, it is recommended here that the Sandy Sediment *Kd* best value be increased from 650 (Kaplan 2016) to 1000 mL/g. No changes are recommended for the clayey sediment *Kd* value.
Th, Zr	900	2000	Tetravalent Cations: Kaplan and Serkiz (2004) reported that SRS sandy sediment had a Zr(IV) *Kd* = 991 ± 352 mL/g at pH 5.3; SRS clayey sediment had a Zr(IV) *Kd* = 1969 ± 561 mL/g at pH 5.3 (Kaplan and Serkiz 2004). Kaplan and Serkiz (2004) reported that SRS sandy sediment had a Th(IV) *Kd* = 245 ± 0 mL/g (the standard error is in fact zero) at pH 5.3; SRS clayey sediment Th(IV) *Kd* = 99 ± 48 mL/g at pH 5.3. The latter two Th(IV) data appears suspect in that greater sorption to sand than clay is inconsistent with basic principles of surface chemistry. This latter value will drive the uncertainty high and the "Conservative" estimates low. Thibault et al. (1990) in their *Kd* compilation of sorption values from throughout the

Constituent of Concern	Sandy Sediment	Clayey Sediment	Comments/References[(a)]
			world provide a very wide range of Th *Kd* values, with almost all values being >10,000 mL/g, however, a few values were as low as 35 mL/g.
Pb, Po, Sn	2000	5000	Divalent Soft Metals: Bibler and Marson (1992) reported that Pb *Kd* values for a SRS burial ground sediment (TF1, 40-60 mesh) was generally >10,000 mL/g, a second burial ground sediment (TF2 40-60 mesh) was 63 to 925 mL/g, and a sediment from near the ETF (40-60 mesh) facility had Pb *Kd* values generally >2,000,000 mL/g. It appears quite likely that all these experiments were conducted at concentrations above the solubility of Pb, and thus reflect precipitation more than adsorption; the experiments were conducted at an initial Pb concentration of 5 mg/L Pb^{2+}. Furthermore, the <40-mesh fraction of the sediment was not included in these experiments, thus greater sorption would likely have been measured with the entire sediment. In a compilation put together for groundwater modelers throughout the world, the estimated range of *Kd* values for sediments with a pH of 4 to 6.3 was 940 to 8,650 mL/g. Finally, these elements tend to have low solubility values. Solubility limits can easily be exceeded by these elements. Therefore it is especially important to consider using solubility constraints rather than *Kd* values when concentrations are slightly elevated for these elements.
Hg	800	1000	There has been two Hg^{2+} sorption study conducted with SRS sediments (Bibler and Marson, 1992; Kaplan and Iverson, 1999). The study by Bibler and Marson (1992) will not be discussed because they only used limited particle size fractions (40 to 60 mesh or 80 to 100 mesh sediment fractions) and they conducted their test using extremely high background ionic strength solutions, non-environmentally relevant levels, which would be expected to greatly influence sorption measurements. Kaplan and Iverson (1999) measured Hg^{2+} values of an SRS vadose zone sand and clay sediment samples, meant as end members of the types of sediments encountered at the SRS. The sand had *Kd* values ranging from 956 to 2452 mL/g, while the clay sample had *Kd* values 1296 to 8517 mL/g. *Kd* values measured in the clay sediment did not vary systematically with pH: at pH 3.1, 4.1, and 9.3 the Hg-*Kd* = 58, 1296 and 429 mL/g, respectively. Elevating Cl, a Hg complexing ligand known to reduce Hg sorption, concentrations by 0, 2, or 20 mg/L Cl^-, caused only marginal decreases in Hg *Kd*: 1296, 773, and 967 mL/g, respectively. Based on these data, Kaplan and Iverson (1999) concluded that the most likely *Kd* for this system was 800 mL/g for the sand and 1000 mL/g for the clay. The corresponding reasonably conservative *Kd* values for the sand and clay were 600 and 700 mL/g, respectively.
Ca, Sr	5	20	Alkaline Earth Elements (Group IIA): Kaplan and Serkiz (2004) reported that SRS sandy sediment Sr *Kd* = 5 ± 1 mL/g at pH 5.3; SRS clayey sediment Sr *Kd* = 17 ± 0 mL/g at pH 5.3. Hoeffner (1985) reported SRS sandy sediment (9% clay) Sr *Kd* = 3 mL/g, pH ~4.7; SRS clayey sediment (23% clay) Sr *Kd* = 9 mL/g, pH ~4.7; very strong pH effect on Sr *Kd* values on SRS sediments: for sandy sediment (9% clay) between pH 2 to 4.8 (background) *Kd* slightly increased from 4 to 19, then increased sharply from pH 4.8 to 6.0-7.0, where the *Kd* became 2000 mL/g, then the *Kd* decreased gradually to 100 mL/g as the pH increased to pH 11 (Hoeffner 1985). Prout (1958) study quantifying Sr sorption to SRS sediments is purposely not included here because of compromised experimental procedures. Sr sorption is almost entirely by cation exchange (EPA 1999), and as such, is readily reversible upon changes in groundwater chemistry. Another important environmental factor influencing Sr *Kd* values is the presence of native and stable Sr, which was shown to be 2100 and 3800 mg/kg in sandy and clayey SRS sediment, respectively (Powell et al. 2010). Depending on the ionic strength of the background solution (0.02 to 0.1 M NaCl), Powell et al. (2010) measure Sr *Kd* values between 5.8 and 6.0 mL/g in sandy soil and 8 and 32 mL/g in clayey sediment. Estimates in look-up table reflect the weak and readily-exchangeable sorption mechanism.

Constituent of Concern	Sandy Sediment	Clayey Sediment	Comments/References[(a)]
			Based on the results of Kaplan and Serkiz (2004) and Powell et al. (2010), the best clayey sediment value was estimated to be 17 mL/g; rounded to one significant figure is 20 mL/g.
Ba	8	30	Because the chemistry of elements in the IIA group of the periodic table (Be, Mg, Ca, Sr, Ba, and Ra) trend in a predictable manner in terms of aqueous chemistry and binding to soils (Chen and Hayes, 1999; Sposito, 1989), Powell et al. (2010) estimated Ba *Kd* values based on measured site-specific values of Sr and Ra. The theoretical trend is that as elements increase in atomic weight in this group, sorption increases. As such, Ba would be expected to have a *Kd* value greater than that of Sr, but less than that of Ra. They estimated the Ba *Kd* to be the average of the sandy and clayey sediment measurements: 20 mL/g for sandy sediment and 100 mL/g for clayey sediment. More recently, Coutelot et al. (2020) conducted Ba $Kd_{desorption}$ measurements (10 mM NaCl, 1/10 sediment-to-solution ratios, 30 days equilibration) using lysimeter samples (clayey sediment) that had been amended with ^{133}Ba (Lysimeter L26). The ^{133}Ba had been in contact with sediment for 4 yr as part of the field lysimeter program (RadFLEx) and had an average (n = 15) $Kd_{desorption}$ = 28.5 ± 3.7 mL/g. This is the first Ba *Kd* values measured with SRS sediments, and as such will have greater influence on estimated best values provided here for the PA. Kaplan (2016) in the earlier version of this document, provided the best estimate for sandy sediment of 20 mL/g and for clayey sediment of 100 mL/g. These best estimate values here reflect the logic of IIA group chemistry based on periodicity as well as the new measurements reported by Coutelot et al. (2020).
Ra	30	200	Recently *Ra* values were measured using SRS sandy and clayey sediments in a solution of similar ionic strength as SRS groundwater (~0.02 M NaCl) (Powell et al. 2010). In the sandy sediment the *Kd* values were 30 ± 0.3 mL/g, in clayey sediment the Ra *Kd* values were 185 ± 26 mL/g. Based on these measurements and to be geochemically consistent with the known trend (Chen and Hayes, 1999; Sposito, 1989) that *Kd* values increase in the order of: Sr < Ba < Ra, the recommended values of Ra *Kd* values were selected. Therefore the trends for Sr, Ba, and Ra *Kd* values for sandy sediments are 5, 20, and 30 mL/g, respectively, and for clayey sediments are 20, 100, and 200 mL/g, respectively.
Mo, Nb, Se, Te	1000	1000	Selenate (SeO_4^{2-}) sorbs strongly to SRS sediments between the pH values of 3.9 and 6.7 (Kaplan and Serkiz 2006). With 0 mg/L C from fulvic acid added to SRS groundwater, selenate *Kd* values for a clayey subsurface SRS sediment were 1041±0.7 mL/g at pH 3.9; 1041± 0.4 mL/g at pH 5.3, and 1041±0.3 mL/g at pH 6.7 (Kaplan and Serkiz 2006). The authors remarked that there appeared to be an upper sorption limit reached yielded such similar *Kd* values as a function of pH. Under similar experimental conditions but using a subsurface sandy sediment, selenate *Kd* values were 1041± 0 mL/g at pH 3.9, 1311± 384 mL/g at pH 5.3, and 601± 65 mL/g at pH 6.7 (Kaplan and Serkiz 2006). The sandy sediment, but not the clayey sediment, showed the characteristic decrease in *Kd* values as the pH increased. Consistent with the large *Kd* values reported by Kaplan and Serkiz (2006), more recently Seaman and Chang (2013) reported Se *Kd* values to a clayey SDU-6 sediment of >1400 mL/g. There is little Nb sediment sorption data. Recently, Soderlund et al. (2015) reported that *Kd* values tended to decrease with increasing pH (typical of anions). At pH 7 *Kd* values for a soil in contact with a simulated soil solution was ~10,000 mL/g and at pH 5.5 (closer to SRS groundwater pH values), *Kd* values were >100,000 mL/g. The *Kd* value change with pH was attributed to changes in the speciation of Nb, where the speciation became more negatively charged at high pH values: below pH 6 was $Nb(OH)_5$; pH 6-9 was $Nb(OH)_6^-$; and pH >9 was $Nb(OH)_7^{2-}$. They also reported *Kd* values of 500,000 mL/g for pure kaolinite, the dominant mineral in SRS clay-size fraction. Echevarria et al. (2005) also reported extremely high Nb *Kd* values for three soils of >1000 mL/g after 1 day of contact with amended Nb. In previous geochemical data packages

Constituent of Concern	Sandy Sediment	Clayey Sediment	Comments/References[(a)]
			(Kaplan, 2010) , it was assumed that Nb was an anion, and geochemically behaved more like Cl^- or NO_3^-. These studies indicate that Nb, in fact, sorbs very strongly to soils.
Mn	20	200	Thibault et al. (1990) report Mn *Kd* values for sand textured sediments of 14, 18, 24, 29, 30, 50, 70, 71,150, 2000 mL/g, and for clay sediments of 250, 2100, and 10,000 mL/g. Willett and Bond (1995) used highly weathered soils similar to those found on the SRS and reported *Kd* values of 4 (pH 5), 5 (pH 6), and 9.5 (pH 7) mL/g. The increase Mn sorption with pH was attributed to the tendency for Mn to hydrolyze at elevated pH levels. However, the soils used by Willett and Bond (1995) had much lower Fe-oxide concentrations than SRS sediments, which would underestimate the Mn sorption potential of SRS sediments. Given the lack of site specific information, the recommended best estimates are towards the lower range identified in Thibault et al. (1990), but greater than those reported by Willett and Bond (1995) .
As	100	200	Crapse et al. (2004) measured in situ As *Kd* values in D-Area, SRS, by collecting porewater/sediment paired samples along a pH gradient. The As *Kd* values varied by 3 orders of magnitude along the transect and did not vary in a consistent manner with pH. At pH 5.5, the *Kd* values varied from about 30 to 20,000 mL/g (Crapse et al. (2004); Figure 45). Also, note that Sb below can be considered a chemical analog.
Sb	3000	3000	Oxidizing: Sb(III) as $HSbO_2^0$ and $Sb(OH)_3^0$. Sb sorption studies have been conducted with SRS burial ground sediments with deionized water or groundwater (Hoeffner 1985). They indicate Sb sorbs strongly to our sediment, with a near linear decrease in log*Kd* values and pH. The decrease in sorption at the more basic pH levels may be a result of formation of anionic Sb complexes, such as $Sb(OH)_4^-$ and SbO_2^-. Between pH 5 and 6, the five measured *Kd* values were between 3000 and 4000 mL/g. At pH 10.5, the Sb *Kd* value was 22 mL/g. SRS lysimeter studies indicate that a small amount of Sb is in a mobile anionic form (Hoeffner 1985). The literature indicates there have been very few Sb sorption studies conducted. Ames and Rai (1978) reviewed Sb sorption and concluded that over the pH range of 4 to 8 that Sb exists as a neutral and complexed species. In high pH and high ionic strength systems, Sb *Kd* values were very low, 0 to 2 mL/g (*38*). When Ca concentrations were high, such as in a concrete system, Sb appeared to coprecipitate with $CaCO_3$, yielding Kd values in the range of 17 to 122 mL/g. Beneath leaking high level waste tanks in Hanford, Sb was found to migrate rapidly through the subsurface sediment (at the same rate as Co and ruthenium) Ames and Rai (1978). The high mobility may be attributed to the tendency of Sb to form complex or hydrolyzed species which are neutral or negatively charged. Recently, Seaman and Chang (2013) measured Sb *Kd* values of >1200 mL/g for SDU-6 SRS sediments, providing additional support that Sb sorbs strongly to SRS sediments.
Re, Tc	0.6	1.8	Tc exists as the anion TcO_4^- s in oxidized systems, such as the vadose zone and the aquifer. Hoeffner (1985) reported correlation between clay content in SRS sediments and Tc *Kd*: <10% clay *Kd*=0.17 mL/g, ~10% clay *Kd* = 0.14 mL/g, ~10% clay *Kd* = 0.23 mL/g, 11% clay *Kd*=0.10 mL/g, 30% clay *Kd*=0.33 mL/g, 43% clay *Kd*=1.31 mL/g, 45% clay *Kd* = 1.16 mL/g. Kaplan (2005) reported TcO_4^- sorption to an SRS sediment occurred only when the pH was <4.3; the *Kd* values to this sandy subsurface sediment increased from 0 at pH 4.3 to ~0.11 at pH 3.7. Sorption studies with ReO_4^- to a clayey subsurface SRS sediment in SRS groundwater as a function of pH all had a *Kd* of ~0 mL/g: -0.6 ± 0.6 mL/g at pH 3.9; -0.3 ± 0.1 mL/g at pH 5.3; -0.1 ± 0.3mL/g at pH 6.7 (Kaplan and Serkiz 2006). Similar studies conducted with sandy subsurface SRS sediment showed no sorption between the pH of 3.9 and 6.7: *Kd* = -0.4 ± 0.3mL/g at pH 3.9, *Kd* = -0.2 ± 0.4mL/g at pH 5.3, and *Kd* = 0 ± 0.2mL/g at pH 6.7 (Kaplan and Serkiz 2006). The variability in these latter studies was quite high due to the limited number of replicates, only two replicates. Montgomery et al. (2017) conducted a series of batch adsorption tests in

Constit-uent of Concern	Sandy Sedi-ment	Clayey Sedi-ment	Comments/References[(a)]
			support of the lysimeter program (clayey sediment) to provide insight into the role of organic ligands amendments on radionuclide *Kd* values. They measure Tc *Kd* values ranging from -3.0 to 1.1 mL/g, with an average of -0.2 mL/g. However, they indicate that Tc or Re sorption is very limited to these SRS sediments. Kaplan et al. (2008a) measured Tc *Kd* values in 26 sediments collected from E-Area SRS. The mean was 3.4 ± 0.5 mL/g and ranged from -2.9 to 11.2 mL/g. The 95-percentile range was 2.4 to 4.4 mL/g. The Upper Vadose Zone and Lower Vadose Zone, which consist primarily of clayey and sandy sediments, respectively, did not have significantly differently *Kd* values, which is inconsistent with Hoeffner (1985). The recommended value originates from the median value of 47 Tc Kd values, which includes the 26 *Kd* values from E-Area reported by Kaplan et al. (2008a): the median value for clayey sediment = 1.8 mL/g and for sandy sediment = 0.6 mL/g (Kaplan 2009).
U	300	400	Dong et al. (2012) conducted an in-depth study of U binding to SRS subsurface sediment. They concluded that the Fe-oxyhydroxide coating the soil particles were responsible for most of the U binding to these soils and that there was a strong pH dependency of U binding to soils. At pH 5.5 (background), U *Kd* values for a sediment with higher levels of clay were ~3000 mL/g, and for a sandier sediment, the *Kd* value was ~700 mL/g. Seaman and Kaplan (2010) measured U(VI) *Kd* values using SRS site specific sediments and simulated groundwater. U(VI) *Kd* values in the sandy sediment were ~450 mL/g at pH 5.5 (background pH) and remained largely constant between pH 3 to 9. When the pH was raised above pH 10.5, the *Kd* values raised sharply to ~800 mL/g. In a clayey sediment, the U *Kd* values followed similar trends, but the *Kd* values were larger. Between pH 3 and 9 the *Kd* values were largely constant at 500 mL/g; when the pH was raised above pH 10.5, the *Kd* value increased to >23,000 mL/g. Barnett et al. (2002) reported a *Kd* value of ~300 mL/g for a clayey SRS sediment. However, like Dong et al. (2012) they reported much greater changes in *Kd* values with changes in pH values than was reported by Seaman and Kaplan (2010). Finally, Montgomery et al. (2017) conducted a series of batch adsorption tests in support of the lysimeter program (clayey sediment) to provide insight into the role of organic ligands amendments on radionuclide *Kd* values. They measure U *Kd* values ranging from 785 to 849 mL/g, with an average of 813 mL/g.

Table 17. Distribution coefficients (*Kd* values, mL/g): Oxidizing Cementitious Environment.

Constituent of Concern	Oxidizing Cement Stage I[a]	Oxidizing Cement Stage II[a]	Oxidizing Cement Stage III[a]	Comments/References[a]
Ar, Kr, Rn	0	0	0	Until studies are conducted to prove otherwise (such as tritium; see below), it will be necessary to assume their *Kd* values = 0 mL/g.
Re, Tc	0.8	0.8	0.5	TcO_4^- adsorption to oxidized cementitious material has been measured between 1 and 10 mL/g (Allard et al., 1984). Kaplan and Coates (2007) measured TcO_4^- *Kd* values in Ca(OH)-saturated and $CaCO_3$-saturated solutions in ground, 40-yr old concrete, simulating 1st/2nd and 3rd Stages, respectively. The measured *Kd* values under oxidizing condition were 0.8 and 1.4 mL/g, respectively. Lilley et al. (2009) reported TcO_4^- *Kd* values measured under oxidizing conditions of 3.30 mL/g to a 50 year-old aged cement; 5.08 mL/g to a Saltstone Vault 2 (25% slag) cementitious sample; and 4.77 & 2.75 mL/g to two Saltstone simulant samples. Almond and Kaplan (2011) conducted leaching studies under reducing and oxidizing conditions with Vault 4, Cell E samples from the Saltstone Disposal Facility. Under oxidizing conditions, a *Kd* value of 12 mL/g was measured. It was not substantiated whether the samples were fully oxidized (i.e., that all the reduction capacity was oxidized) during this study and therefore, it is possible that had the study been conducted over a much longer period, that greater Tc release, or lower *Kd* values would have been measured. Baker et al. (2000) measured Tc(VII) *Kd* values of <1 mL/g for NRVB (Nirex Reference Vault Backfill: 25% OPC, 10% Limestone, 30% hydrated lime, 35% water) cementitious materials at pH 12.8. Serne et al. (1992) conducted a large number of diffusion tests involving Tc(VII) and nitrate in cement waste forms. Seven effective diffusion (D_{eff}) values were measured on a slag-free blend (CRW); the average D_{eff} for Tc was 5×10^{-9} cm^2/s and for NO_3^- was 3×10^{-8} cm^2/s. Assuming NO_3^- has a $Kd = 0$ mL/g, $D_{eff} = D_0/R_f$ (D_0 = diffusion coefficient in the absence of any solids) and $R_f = 1 + Kd$*density/porosity, then Tc *Kd* in these tests were ~5 mL/g. All of the D_{eff} values reported by Westsik et al. (2013) and Um et al. (2016) were conducted with slag-containing formulations, and were therefore not considered here. After a comprehensive review of the cement literature, Ochs et al. (2016) concluded that TcO_4^- K_d values do not change between Stages I, II, and III, and a best estimate is 1 mL/g for all three stages. The recommended values listed here account for the observation that most TcO_4^- sorption studies in the literature or measured using SRS materials reported non-zero TcO_4^- *Kd* value.
^3H	0	0	0	A great deal of recent research has been conducted using careful measurements of tritium sorption to cement (Ochs et al., 2016; Tits, 2003; Wieland and Van Loon, 2003). Through the use of batch sorption and diffusion experiments they measured similar *Kd* value, 0.8 ± 0.2 mL/g and 0.8 ± 0.1 mL/g, respectively. In Wieland and Van Loon's (2003) look-up table for cement *Kd* values, they suggest using a value of 1 mL/g for tritium. However, there is also a great deal of data indicating that tritium does not sorb and that experimental evidence indicating sorption can be attributed to errors in mass balance (reviewed by Krupka et al. 2004). That is, during diffusion tests or batch sorption test, researchers incorrectly assign tritium existing in the concrete/cement pore water as "sorbed tritium" during their mass balance calculations (*Kd* calculations).

Constit-uent of Concern	Oxidizing Cement Stage I[a]	Oxidizing Cement Stage II[a]	Oxidizing Cement Stage III[a]	Comments/References[a]
Cl, F	0	10	1	Ochs et al. (2016) recently completed a review of Cl *Kd* values and reported that about ¾ of the values were >1 mL/g and about half were >10 mL/g. They observed that iodine (also a monovalent halide) *Kd* values were about an order of magnitude greater in Stage II (pH 12.5) than in Stage I (pH >12.5). They also concluded that stable Cl^- in repository environments can be quite high, ~1 mM Cl (Bayliss et al., 1991; Pointeau et al., 2008) and may greatly diminished Cl *Kd* values. This latter observation would be especially relevant to Cl uptake during the 1st Stage. Evans (2008) reported 5 different processes involved in Cl uptake by cement systems: including coprecipitation, chemisorption onto Ca-sulfate (C_3S) phases, formation of Friedel's salts, surface complexation, binding to CSH gel. Based on diffusion studies with French sulfate-resistant cement Cl *Kd* values were 25 mL/g (Sarott et al., 1992) and noted that Cl was retarded with respect to NO_3^-. Atkins and Glasser (1992) also reported measurable amounts of Cl sorption to cement, but it was not possible to calculate a *Kd* using the data provided in the paper. Cl *Kd* to cement powder after 24 h contact time = 0.8 mL/g (Atkins and Glasser, 1992).
Cr	10	10	1	CrO_4^{2-} immobilization as a result of carbonation (the natural process by which concrete becomes coated with $CaCO_3$ mineral phases) has been documented (Macias et al., 1997). CrO_4^{2-} can also be substituted for sulfate in ettringite (Gougar et al., 1996) and can participate in ion-exchange with OH^-. It is anticipated that divalent CrO_4^{2-} will not be as readily exchanged by monovalent anions, such Cl^- and F^-. Ochs et al. (2002) reported CrO_4^{2-} K_d values were between 10 and 100 mL/g when put in contact with various non-reducing cement pastes. They developed a predictive model of CrO_4^{2-} uptake by correlating *Kd* values to cement sulfate concentrations. It is very likely that CrO_4^{2-} *Kd* values should be much greater than the recommended values of 10 mL/g, but additional measurements are necessary under appropriate SRS conditions to confirm this before it is possible to recommend larger values. During Stage III the *Kd* values were reduced to 1 mL/g because system pH levels eventually decreases to background levels of pH 5.5; a pH level that would promote carbonate mineral dissolve and the release of co-precipitated Cr.
N (nitrate, nitrite)	0	0	0	Nitrate and nitrite are assumed to be non-reactive (non-sorbing) to cementitious materials.
At, I	8	10	4	Iodine can exist as either iodide (I^-) or iodate (IO_3^-) in nature. Based on thermodynamic considerations, iodine is expected to exist as a mixture of iodate and iodide under oxidizing conditions and only as iodide under reducing conditions. This is important because iodide sorbs less than iodate to cementitious materials (Evans 2008; Allard et al. 1984). I-*Kd* measured on 7 types of concrete samples increased gradually over 3-mo, then leveled off at 25 to 130 mL/g (Allard et al., 1984; Dayal et al., 1989). Iodide sorption to cement is highly reversible when chloride is in the aqueous phase, suggesting that iodide is very weakly bound to cement surfaces and not precipitated onto the surface of the cement (Atkins and Glasser, 1992). The impact of chloride concentrations on iodine sorption is important because chloride generally exists in much greater concentrations, ~10^{-5} M, than iodine, which exist at

Constit-uent of Concern	Oxidizing Cement Stage I[a]	Oxidizing Cement Stage II[a]	Oxidizing Cement Stage III[a]	Comments/References[a]
				concentrations closer to ~10^{-8}M (Wang et al., 2009). Increasing pH >12.5 resulted in decreased iodide sorption, which was likely caused by a decrease in the number of surface positive-charged site. (Atkins and Glasser, 1992). Iodide sorption increased with increased Ca/Si ratios of CSH (Atkins and Glasser, 1992), (which is at its maximum during Stage II and initial part of Stage III). Recommended *Kd* values are lower in Stage I because of high concentration of aqueous salts. Iodide sorbed stronger to cement than Cs (Allard et al., 1984). A recent review of I cement *Kd* values showed that in Stage I, when the pH range was >12.5, that I *Kd* generally varied between 10 and 300 mL/g (Ochs et al. 2016). Jakob et al. (1999) reported I *Kd* values that ranged between 10 and 50 mL/g, based on diffusion tests. Allard et al. (1984) suspected that the high sorption of iodine on cements was due to iodine existing as iodate, the stronger sorbing species. Pointeau et al. (2008) noted that *Kd* values to hardened cement increased by an order of magnitude as experimental conditions changed from those representing Stage I to those representing Stage II. As the pH decreased further, to values expected during Stage III and CSH phase (the most iodine reactive phases) concentrations continue to decrease, the I *Kd* decreased again. Kaplan and Coates (2007) measured iodide *Kd* values in Ca(OH)-saturated and $CaCO_3$-saturated solutions in ground, 40-yr old SRS concrete, simulating Stage I&II, and Stage III, respectively. The measured *Kd* values were 14.8 and 14.4 mL/g, respectively. Finally, Serne et al. (1992) measured effective diffusion coefficients, $D_{eff,}$ in reducing and oxidizing cementitious waste formulations. The oxidized samples had D_{eff} values of 1E-10 to 3E-9 cm^2/s and the reduced samples had D_{eff} values 2 E-8 to 8E-8 cm^2/s. The oxidized but not the reduced samples were retarded with respect to the D_{eff} of Na. Recently, there have been reports of iodine, primarily in the form of iodate being incorporated in grout (Aimoz et al., 2012a; Aimoz et al., 2012b; Atkins and Glasser, 1992; Avalos et al.; Gillispie et al., 2020; Guo et al., 2020; Reigel and Hill, 2016). Possible sorption sinks in cement include aluminoferrite monosulfate, ettringite (aluminoferrite tri-sulfate), and calcium-silicate-hydrate phases. For sorption onto aluminoferrite monosulfate and ettringite, I^-/IO_3^- substitutes for SO_4^{2-} Using X-ray absorption fine structure (EXAFS), Guo et al. (2020) showed that minimal I^- was incorporated into ettringite (0.05%), whereas IO_3^- exhibited a high affinity for ettringite via anion substitution for SO_4^- (96%). Bonhoure et al. (2002) used I K-edge X-ray absorption spectroscopy to demonstrate that calcium-silicate-hydrate phases was not an especially important uptake-controlling phase for IO_3^-. Their findings supports earlier finding that the aluminoferrite monosulfate and ettringite are much more efficient scavenger for I^- than calcium-silicate-hydrate phases (Atkins and Glasser, 1992). Recently, Avalos et al. (2021) further noted that aqueous IO_3^- can be immobilized into calcite as it coprecipitates on the surfaces of cementitious materials, especially when pH <10. Given these geochemical considerations, of pH, ionic strength, and changes in solid phase mineralogy, iodine *Kd* values are expected to be greatest during Stage II. After a detailed review of the literature, Krupka et al. (2004) recommended "reasonably conservative" *Kd* values for the Hanford IDF for Stages I, II, and III of 10, 5, and 1 mL/g, respectively. More recently, Flach et al. (2016) recommended I *Kd* values for the Hanford IDF of 4, 8, and 2 mL/g for Stages I, II, and III, respectively.

Constit-uent of Concern	Oxidizing Cement Stage I[a]	Oxidizing Cement Stage II[a]	Oxidizing Cement Stage III[a]	Comments/References[a]
				Flach et al. (2016) indicated that especially conservative values were necessary because at the time of writing, the composition of the cementitious waste form was not selected and there was a lot of uncertainty associated with the iodine speciation in the wide range of waste sources being proposed for the IDF. Ochs et al. (2016) recommended best I *Kd* values for Stages I, II, and III of 1, 10, and 1 mL/g, respectively for both oxidizing and reducing cementitious conditions. The slightly lower values recommended by Ochs et al. (2016) than recommended here can be attributed in part to Ochs et al. (2016) not distinguishing between reducing and oxidizing conditions, as is done here. Also, Ochs et al. (2016) provide "conservative estimates," where these are "best estimates." Tests conducted under oxidizing conditions, measured non-zero I *Kd* values, generally between 10 and 300 mL/g. As will be discussed below (Table 18), recommended I *Kd* values under reducing conditions are 0, 2, and 0 mL/g for Stages I, II, and III, respectively. Additionally, the best values reported here are also based on site-specific data noted above by Kaplan and Coates (2007).
Inorganic C[c]	2000	5000	50	^{14}C chemistry is especially complicated in cementitious environments and is not well characterized by the *Kd* construct. It is influenced by carbon dioxide in the gas/water/solid phase equilibrium, isotopic exchange, adsorption, precipitation, and coprecipitation. Inorganic C exists in pH environments >10 almost exclusively as CO_3^{2-} and as at pH decreases below pH 10, an increasing percentage of HCO_3^- is present (Allard et al., 1984). The three parameters influencing ^{14}C concentrations the most in cementitious environments is the large amount of stable $^{12}CO_3^{2-}$ present in the system (isotopic exchange, solubility (dissolved Ca concentrations), and pH. The total dissolved C concentration is about 8 µM and 300 µM at pH 12.5 and 13.5, respectively (Stage I) (Wang et al. 2009). When portlandite dissolves and the pH drops below 12.5, Ca concentrations will be regulated by the solubility of CSH phases of decreasing Ca/Si ratio. As the Ca/Si ratio drops, Ca concentration in solution drops also and the dissolved C concentration will increase. Studies that demonstrate that steady state was achieved ($^{14}CO_3^{2-}$ sorption kinetics is slow) reported very large *Kd* values: for concrete and cement paste, *Kd* = 1600 to 10,000 mL/g (Allard et al., 1981); for sulfur-resistant portland cement, *Kd* = 6000 mL/g (Bayliss et al., 1988); for crushed concrete, *Kd* = 1850 mL/g (Hietanen et al., 1985); for mortar grains, 30,000 mL/g (Matsumoto et al., 1995); for OPC (0% BFS) and CSH phases, *Kd* = 2000 and 1800 to 3900 mL/g, respectively (Noshita et al., 1988). The *Kd* values adopted here are based on the rational offered by Evans (2008), Jacques et al. (2008), and Wang et al. (2009). They concluded that the effective *Kd* for $^{14}CO_3^{2-}$ is equal to the ratio of the quantity of CO_3^{2-} in the cement to the solubility limit of $CaCO_3$ in the pore solution. There are two important conclusions from this work. First, $^{14}CO_3^{2-}$ sorption to cementitious materials is best represented by a solubility term and secondly, the release of $^{14}CO_3^{2-}$ into the aqueous phase is independent of the $^{14}CO_3^{2-}$ inventory. In addition to simply setting the *Kd* values based on solubility calculations, they further refined the *Kd* values by assuming that only 10% of the CO_3^{2-} was assessable for isotopic exchange (because some CO_3^{2-} would be buried within the calcite mineral and not in contact with the aqueous phase). Jacques et al. (2008) later estimated this "assessable percentage" to be

Constit-uent of Concern	Oxidizing Cement Stage I[a]	Oxidizing Cement Stage II[a]	Oxidizing Cement Stage III[a]	Comments/References[a]
				23% based on additional theoretical rigor. Jacques et al. (2008) reported *Kd* values using this technique of between 1000 to 5000 mL/g in Stage I (pH 13.5 to 12.2), 5000 mL/g in Stage II (pH 12.2), and 5000 to 2000 mL/g in Stage III (pH 12.2 to 9). Based on these recommendations by Jacques et al. (2008), Wang et al. (2009) adopted for Stage I, II, and III, *Kd* values of 2000, 5000, and 2000 mL/g, respectively. For this report, the best estimate *Kd* values for Stage I and II were taken directly from Wang et al. (2009). For Stage III, the best estimate *Kd* value was decreased from their recommended 2000 mL/g to 50 mL/g because Wang et al. (2009) assumed the final pH in Stage III was pH 9, whereas SRS background pH is pH 5.5, which is expected to support lower porewater CO_3^{2-} concentrations and carbonate phases are expected to dissolve at pH levels below 7.5. Early during Stage III, sorption is expected to be very high (~5000 to 50000 mL/g; Wang et al. 2009), and much later in Stage III, once only calcite remains, ^{14}C-carbonate sorption is expected to be much lower (~1 mL/g; Allard et al. 1981).
Ac, Al, Am, Bk, Bi, Ce, Cf, Cm, Es, Eu, Fe, Fm, Gd, Lu, Sm, Y	6000	6000	600	Trivalent cation *Kd* values for concrete consistently exceed those for sediments. Am *Kd* values of > 10,000 mL/g were reported by Ewart et al. (1992). Am *Kd* value of 12,000 mL/g were estimated based on diffusion tests in cement (Bayliss et al., 1991). Am *Kd* values ranged from 2,500 to 35,000 mL/g for seven fresh concrete blends (Allard et al., 1984; Hoglund et al., 1985). Am *Kd* for 65-yr old concrete sample were 10,000 mL/g (Allard et al., 1984; Hoglund et al., 1985). Fresh cement Am *Kd* were 2000 mL/g for 24-h contact time (Kato and Yanase, 1993). Eu *Kd* of 2,400 mL/g were measured after a contact time of only 24-h (Kato and Yanase, 1993). These very large *Kd* values likely reflect precipitation reaction that occurred during the sorption measurements. Kaplan and Coates (2007) measured Am(III), Ce(III), and Y(III) *Kd* values in Ca(OH)-saturated and $CaCO_3$-saturated solutions in ground, 40-yr old concrete recovered from the SRS, simulating Stages I&II and III, respectively. The measured Am(III) *Kd* values were 6,031 and 4,112 mL/g, respectively. The measured Ce(III) *Kd* values were 6,003 and 4,652 mL/g, respectively. Both sets of *Kd* values were quite similar. Y(III) *Kd* values were 4,830 mL/g in Ca(OH)-saturated solution (Stages I & II), and 4,738 mL/g in $CaCO_3$-saturated solution (Stage III). By way of comparison, Ochs et al. (2016), after an exhaustive review of the literature relevant to the Belgium proposed repository, recommended Am(III) *Kd* values for Stage I of 10,000 mL/g, Stage II of 10,000 mL/g, and for Stage III of 10,000 mL/g.
Ag, Cd, Co, Cu, Pd, Pt, Zn	4000	4000	400	Selected Monovalent and Divalent Transitions Metals: Using SRS materials, Kaplan and Coates (2007) measured Cd(II) and Co(II) *Kd* values in Ca(OH)-saturated and $CaCO_3$-saturated solutions in ground, 40-yr old concrete, simulating Stages I&II, and Stage III, respectively. The measured Cd(II) *Kd* values were 9,907 mL/g and 3,180 mL/g, respectively. The measured Co(II) *Kd* values were 4,343mL/g in Ca(OH)-saturated solutions and 3,994 mL/g in $CaCO_3$-saturated solutions. Using an actual aged saltstone core sample recovered the Saltstone Disposal Facility, Almond et al. (2012b) reported desorption Co *Kd* values using a cement leachate simulate under bench top oxidizing conditions of 5,600 mL/g, and under inert glovebag conditions of 1,700 mL/g. Aqueous Ag concentrations are likely to be controlled by $AgCl_{(s)}$ solubility because Cl^- concentrations will be especially high in Saltstone and during Stage I of cement evolution; $AgCl_{(s)}$ solubility at pH 12 is 10^{-6}M during Stages II and III, and

Constit-uent of Concern	Oxidizing Cement Stage I[a]	Oxidizing Cement Stage II[a]	Oxidizing Cement Stage III[a]	Comments/References[a]
				about 10^{-5}M during Stage I, when the pH is >12.5 (Ochs et al. 2016). No reliable Ag sorption to cementitious materials studies were found in the literature. Similarly, no reliable Pd sorption data was found in the literature.
Ni	70	400	400	Seven studies were identified from the literature that included Ni sorption to cement or cement phases (Aggarwal et al., 2000; Hietanen et al., 1984; Holgersson et al., 1998; Jakob et al., 1999; Pilkington and Stone, 1990; Wieland et al., 2000; Wieland et al., 2006). But in all cases, distinction between reversible sorption and solubility controls were not made, and as such, the measured *Kd* values are compromised. For example, Hietanen et al (1984) reported *Kd* values that ranged from 500 to 3000 mL/g, Kato and Yanase (1993) reported a Ni *Kd* value of 1500 mL/g, and Pilkington and Stone (1990) reported *Kd* values that ranged from 500 to 3000 mL/g. Evans (2008) summarized that possible uptake mechanism on cement phases for Ni include: ettringite accommodating Ni at the divalent metal site in the crystal structure, non-electrostatic sorption on CSH, co-precipitation or surface complexation via hydroxyl groups, and precipitation by solubility limiting processes. Thus, there are several competing processes influencing *Kd* values of which Ni solubility of various Ni solid-solution phases control aqueous Ni concentrations (Evans, 2008). Considering stable Ni cement concentrations and converting pH-dependent (Stage dependent) solubility term into *Kd* values, Ochs et al. (2016) recommended *Kd* values: 65, 400, and 400 mL/g for Stage I, II, and III, respectively.
Ba, Ra	200[b]	100[b]	200[b]	Ra sorbs to cementitious materials in a near identical manner as Sr, primarily cation exchange (Tits et al., 2004). However, Ra *Kd* values to cementitious materials are consistently greater than those of Sr (Tits et al., 2004; Ochs et al. 2016). Related, CSH has a selectivity coefficient of Ra to Ca (the preferential uptake of dissolved Ra when dissolve Ca is also present) of ~5, whereas the Sr to Ca selectivity coefficient is 1. Therefore, recommended Ra *Kd* values are greater than those for Sr. When aqueous Ca concentrations are at their highest during Stage II, recommended Ra *Kd* values are at their lowest. Bayliss et al. (1991) and Berry et al. (1988a) measured Ra *Kd* values onto ordinary Portland cement and as a function of Ra concentration. They reported *Kd* values that ranged from 50 to 530 mL/g. Ochs et al. (2016) recommended Ra *Kd* values of 300, 160, and 800 mL/g for Stages I, II, and III, respectively. It is recommended here that Ba and Ra *Kd* values for Stages I, II, and III be 200, 100, and 200 mL/g, respectively. Regarding the footnotes in columns 2, 3, and 4, the presence of sulfur can greatly increase *Kd* values of alkaline earth metals (Ba, Ra, and Sr). BFS contributes sulfur to cementitious waste forms. BFS exists in many SRS cementitious material formulations, including saltstone and materials used for tank disposition, and most formulations used for LLW disposal (except those for Components-in-Grout and Intermediate Level Vault (Section 5.0). Almond and Kaplan (2011) measured very high apparent *Kd* values for Ba from an actual saltstone core sample recovered from the Saltstone Disposal Facility: >15,000 mL/g under oxidizing conditions, and 7400 mL/g under inert gas conditions. While radionuclide immobilization in the presence of slag is commonly attributed to the reduction process, for

Constit-uent of Concern	Oxidizing Cement Stage I[a]	Oxidizing Cement Stage II[a]	Oxidizing Cement Stage III[a]	Comments/References[a]
				the alkaline earth metals, additional immobilization results from the formation of a sulfate/sulfide precipitate. Barium sulfate is highly insoluble in water (k_s = 10^{-10} M; Barium sulfide has only a slightly higher solubility value of k_s = 5 x 10^{-10} M). These latter results using site specific materials are especially representative of conditions expected in cementitious systems containing BFS, either reduced or oxidized, where larger concentrations of sulfur exist in the waste form. As the saltstone undergoes oxidation, the sulfide converts to sulfate, which is also highly effective at immobilizing the alkaline metal earth elements. Therefore, larger *Kd* values are warranted for these elements in OPC/BFS-blends than in OPC blends. For reoxidized cementitious materials containing slag, it is recommended that *Kd* values for **Stages I, II, and III of 6000, 6000, and 600 mL/g,** respectively, be used.
Sr	90[b]	20[b]	90[b]	Stable Sr, exists in very high concentrations with respect to radiostrontium in cements, ranging from 100 to 1000 ppm, ~10^{-3} M. The presence of large amounts of an isotope is expected to influence radiostrontium geochemical behavior. Wieland et al. (2007) showed that radiostrontium was reversibly and linearly sorbed to cement. Furthermore, they showed that radiostrontium and stable Sr had similar *Kd* values; stable Sr had *Kd* values between 80 to 110 mL/g and ^{85}Sr had *Kd* values of 100 to 120 mL/g. They also noted that varying natural Sr concentrations did not influence radiostrontium *Kd* values. Several researchers (Evans, 2008; Tits et al., 2004; Tits et al., 2006) concluded that CSH phases in hardened Portland cement sorbed Sr^{2+} via cation exchange. More specifically, the silanol groups (≡SiO^-) are responsible for Sr exchange sites. Therefore, as the Ca:Si ratio of CSH decreases during the 3rd Stage, Sr sorption increases (Ochs et al. 2016). Wieland et al. (2007) showed that the CSH phases have equal affinities for Ca and Sr, i.e., they have selection coefficient = ~1. Some Sr-cementitious material *Kd* values follow. Sr *Kd* values were influenced by aqueous Ca concentrations, which steadily decreases during the 2nd Stage while CSH phases loses Ca and the Ca:Si ratio steadily decreases (Sugiyama and Fujita, 1999; Tits et al., 2004). Presumably the Ca^{2+} competes with the Sr^{2+}; consequently, Sr *Kd* values would tend to increase during the 3rd Stage. In pH environments of >12.5 (Stage I): Wieland et al. (2007) reported *Kd* values of 80 to 110 mL/g for sulfur resistant Portland cement and between and 300 to 400 mL/g for CSH phases; Tits et al. (2004) reported *Kd* values of 100 to 4000 for CSH phases. In pH environments of ~12.5 (Stage II): Kaplan and Coates (2007) reported Sr *Kd* value of 28.1 mL/g in 40-yr old concrete with a $CaOH_2$-saturated background solution. Wieland et al. (2008) reported a *Kd* value of 28 mL/g to CSH phases in an alkali-free background solution; Hietanen et al. (1985) reported *Kd* values of 1 to 5 for concrete samples. For pH environments of 10.5 to 12 (3rd Stage): Suiyama and Jujita (1999) reported *Kd* values between 5 to 170 mL/g for OPC/BFS and 50 to 2000 mL/g for CSH of varying Cs:Si ratios. Kaplan and Coates (2007) reported a *Kd* of 39 mL/g for 40-years old SRS concrete with a $CaCO_3$-saturated background solution. In summary, it appears that Sr *Kd* values decreased during Stage II as a result of competing elevated aqueous Ca levels (Tits et al., 2004). Because CSH slowly decreases the Ca:Si ratios during Stage II (competing aqueous Ca concentrations decrease), it is expected that Sr *Kd* values will increase again during Stage III. By way of comparison, Ochs et al. (2016) recommended Sr *Kd* values of 100, 30, and

Constit-uent of Concern	Oxidizing Cement Stage I[(a)]	Oxidizing Cement Stage II[(a)]	Oxidizing Cement Stage III[(a)]	Comments/References[(a)]
				100 mL/g for Stages I, II, and III, respectively. It is recommended here that Sr *Kd* values for slag-free cementitious materials (e.g., Components-In-Grout and Intermediate Level Vault) be 90, 20, and 90 mL/g for Stages I, II, and III, respectively. Regarding the footnotes in columns 2, 3, and 4, the presence of sulfur can greatly increase *Kd* values of alkaline earth metals (Ba, Ra, and Sr). BFS contributes sulfur to cementitious waste forms. BFS exists in many SRS cementitious material formulations, including saltstone and materials used for tank disposition, and most formulations used for LLW disposal (except those for Components-in-Grout and Intermediate Level Vault (Section 5.0). The presence of large amounts of stable Sr is expected to be especially important in systems with high sulfur concentrations, as exists in BFS-blends. When sulfate concentrations are high, $SrSO_4$ precipitates. $SrSO_4$ has a solubility of 3.2×10^{-7} M (strontium sulfite solubility product is even lower, $SrSO_3$ $k_s = 4 \times 10^{-8}$ M). Almond and Kaplan (2011) measured very high apparent Sr *Kd* values in an actual saltstone core sample recovered from the Saltstone Disposal Facility: 5728 mL/g under oxidizing conditions, and 737 mL/g under inert gas conditions. For reoxidized cementitious materials containing slag, it is recommended that *Kd* values for **Stages I, II, and III of 1000, 1000, and 100 mL/g,** respectively, be used.
Ca	90	20	90	There have not been any tracer concentration levels sorption studies conducted with Ca, consequently *Kd* estimates are based on Sr uptake studies (as described above). One important difference between Ca and Sr, is that Ca likely does not bond with or precipitate with S as much as with Sr. This can be attributed to the much greater concentrations of Ca (thereby overwhelming the capacity of S to complex it) and the weaker complexation between Ca and S than between Sr and S.
Sn	4000	4000	2000	Sn exists in cementitious environments in the +4 state (Wieland and Van Loon, 2003) and as such readily hydrolyses. Using sulfate resistant Portland cement, Sn *Kd* values were >30,000 mL/g; this likely reflected some precipitation (Wieland and Van Loon, 2003). Kaplan and Coates (2007) measured Sn *Kd* values in Ca(OH)-saturated and $CaCO_3$-saturated solutions in ground, 40-yr old concrete, simulating Stages I & II, and III, respectively. The measured *Kd* values were 3,900 and 3,360 mL/g, respectively.
Cs, Fr, K, Rb	2	20	10	Cs K_d values in hardened HTS cement discs, pH 13.3 were close to 3 mL/g (Sarott et al., 1992). Wieland and Van Loon (2003) reviewed Cs K_d values of various cementitious materials and reported a very narrow range: from 0.2 to 5.0 mL/g. It is recommended here that Stage I K_d values should be decreased compared to Stage II and III because high ionic strength likely results in competitive exchange (desorption). This has been shown experimentally (Wieland and Van Loon, 2003). Kaplan and Coates (2007) measured Cs^+ *Kd* values in Ca(OH)-saturated and $CaCO_3$-saturated solutions in ground, 40-yr old concrete, simulating Stages I&II, and III, respectively. The measured K_d values were 21 and 17.6 mL/g, respectively. Using an actual aged saltstone core sample recovered the Saltstone Disposal Facility, Almond and Kaplan (2011) reported desorption K_d values using a cement leachate simulate under bench top oxidizing conditions of

Constit-uent of Concern	Oxidizing Cement Stage I[(a)]	Oxidizing Cement Stage II[(a)]	Oxidizing Cement Stage III[(a)]	Comments/References[(a)]
				18 mL/g, and under inert glovebag conditions (reducing conditions) of 21 mL/g. Thus, there was little difference in measured *Kd* values between oxidizing and reducing cementitious material conditions. The recommended values here are largely in agreement with the previous values selected by Krupka et al. (2004) and Ochs et al. (2016). Krupka et al. (2004) recommended "reasonably conservative" Cs K_d values for oxidizing cement for Stages I, II, and III of 2, 20, and 20 mL/g, respectively. Ochs et al. (2016) in a detailed review of the general literature recommended best Cs K_d values for Stages I, II, and III of "insufficient data", 2, and 20 mL/g, respectively.
Tl	200	200	80	Seaman and Kaplan (2010) measured Tl *Kd* values of an agent cement using a saturated $Ca(OH)_2$ solution to simulate a Stage II system and a saturated-$CaCO_3$ solution to simulate a Stage III system; the *Kd* values were 198 ± 2 and 201 ± 0.3 mL/g, respectively. Measurements made with BFS formulations were near identical to these values, 193 to 195 mL/g. These values are the only Tl *Kd* values found in SRS reports or the broader literature.
Na	0	0	0	Sodium is in the 1A group of elements with Cs, Fr, Tb, and K, but it would be expected to sorb appreciably less strongly due to its strong energy of hydration (water molecules are tightly bound to the Na^+, thereby not permitting the metal ion to come into direct contact with the cementitious material surface). There are extremely high stable Na concentrations present in these systems, especially in the case of saltstone waste forms, which will promote cation exchange with the radioactive sodium.
Nb	1000	1000	500	Nb aqueous speciation under oxidizing and reducing cementitious conditions is likely $Nb^v(OH)_7^{2-}$ (Wang et al. 2009). Due to the lack of thermodynamic data, Sn stability constants have been used in such calculations as a chemical analogue of Nb behavior (Wang et al. 2009). Pilkington and Stone (1990) measured Nb_2O_5 solubility in BFS/OPC leachate at 2E-7 M. Baker et al. (1994) measured Nb solubility values in cementitious leachate between pH 9 to 12 of 1E-8 M; above pH 12, the solubility increased to has high as 1E-6 M. Talerico et al. (2004) suggested that Ca concentrations, especially high during Stage II, may promote Nb precipitation by forming Ca-Nb-oxide phases. Measurements showed that the solubility of Nb salts is probably lower than Nb_2O_5, in the range of $5E\text{-}9^9$ to 5E-8 M, depending on pH and Ca concentrations ((Baker et al., 1994; Berner, 2002). Such low solubility values likely impact Nb releases from cementitious wasteforms. Pilkington and Stone (1990) measured Nb *Kd* values ranging from 500 to 80,000 mL/g on different cement blends at pH 12 to 13. Baker et al. (1994) reported *Kd* values of 40,000 mL/g in pH 12.2 saline solutions. Ochs et al. (2016) reported Nb *Kd* values for various cement pastes and CSH phases of 100,000 mL/g for Stage I conditions, 240,000 mL/g for Stage II conditions, and 40,000 to 70,000 mL/g for Stage III conditions. CSH phases were shown to be the dominant solid phase controlling Nb uptake (Baker et al., 1994). Therefore, Stage III *Kd* values likely are lower than the other stages because CSH concentrations during this stage continue to decrease with time. The mechanism of Nb sorption in not known and therefore introduces some uncertainty to estimated *Kd* values. But sorption is very strong and appears to involve a combination of sorption and solubility, depending on aqueous conditions.

Constit-uent of Concern	Oxidizing Cement Stage I[a]	Oxidizing Cement Stage II[a]	Oxidizing Cement Stage III[a]	Comments/References[a]
Np, Pa	10,000	10,000	5,000	Neptunium sorption to aged SRS cement samples were conducted by Miller et al. (2009). They used an ICP-MS which permitted them much lower detection limits than conventional radiometric analytical methods and as a result, much lower *Kd* values were measured. They added Np(V) at varying concentrations to ground 50 year old cement samples and measured constant aqueous Np concentration at 1e-12 M, indicating solubility controls. Six triple Np Kd values were measure with ground aged concrete, all were >100,000 mL/g. Previous measurements by Kaplan and Coates (2007) measured lower *Kd* values, but were running up against the analytical limits of the instruments. These radionuclides are assumed to exist in the +5 oxidation state. Np sorption test to 7 different 65-yr old cements using cement pore water reached steady state after 30 days, *Kd* values ranged from 1500 to 9500 mL/g (Allard et al., 1984; Hoglund et al., 1985). As is the case with all large *Kd* values, these values may reflect some precipitation occurring during the adsorption measurement. Kaplan and Coates (2007) measured NpO_2^- and PaO_2^- *Kd* values in Ca(OH)-saturated and $CaCO_3$-saturated solutions in ground, 40-yr old concrete, simulating Stages I&II, and III, respectively. The measured NpO_2^- *Kd* values were 1,652 and 1,318 mL/g, respectively. The measured PaO_2^- *Kd* values were 1,630 and 1074 mL/g, respectively. Ochs et al. (2016) reported that there was insufficient data in the literature (even though he acknowledged the work of Allard et al. (1984) and Hoglund et al. (1985)) to provide recommended *Kd* values. This was in part because Np(V) has been shown to quickly undergo reduction to Np(IV) within 6 months of being added to a cementitious material without BFS added (Zhao et al., 2000). Additional spectroscopy research related to the impact of redox on Np binding to cementitious materials has been reported (Gaona et al., 2011; Tits et al., 2014). However, they did make recommended Np(IV) *Kd* values of 30,000, 30,000, and 30,000 for Stages I, II, and III, respectively. It is assumed here that the very high Np *Kd* values noted in this review to cements without BFS in the formulation can be attributed to the added Np(V) converting to Np(IV) once added to the highly alkaline conditions of the cement. In turn the Np(IV) forming sparingly soluble phases and also sorbed to the cementitious material surfaces.
Se, Te, Mo	3	3	3	For selenate, relatively weak sorption was observed on hardened cement paste, but strong sorption was observed on ettringite. A series of experiments with different selenate/sulfate ratios demonstrated that selenate replaces sulfate in the ettringite structure and allowed development of an empirical solid-solution model relating the sorption of selenate to the sulfate concentration in the solid and solution. This is consistent with the findings of Baur and Johnson (2003). Based on a literature review by Ochs et al. (2010), Se(VI) is preferentially taken up by the sulfate-aluminate minerals (ettringite, monosulfate), and that selenite and selenate can substitute for sulfate ions. Potentially this could result in either or both Se species appearing in the Al_2O_3-Fe_2O_3-tri (Aft) and Al_2O_3-Fe_2O_3-tri (AFm) phases of cement by lattice substitution as well as their sorption on CSH. Thus, sorption of selenate would be favored by a high content of sulfate-aluminate minerals and a low aqueous concentration of competing sulfate ions. There are much fewer selenate than selenite cementitious material uptake studies. Lothenbach et al. (1999) measured selenate uptake in > 40 experimental conditions across a wide range of pH levels and

Constit-uent of Concern	Oxidizing Cement Stage I[a]	Oxidizing Cement Stage II[a]	Oxidizing Cement Stage III[a]	Comments/References[a]
				contact times to various cement phases and cement formulations of varying ages. While uptake by ettringite (a sulfate containing mineral) was high (*Kd* = 50 – 70 mL/g), uptake to various hardened cement paste samples ranged from 0 to 18 mL/g (Lothenbach et al. (1999); Samples designated Fresh CEM and Aged CEM). Ochs et al. (2002) did not notice a change in Se *Kd* values between pH 10 and 13; therefore, Kd values were kept the same for all three stages. Regarding Mo, the only aqueous species relevant to a cement system is the molybdate, $Mo^{VI}O_4^{2-}$. In slag cements, however, sufficient sulfide could be present to form $MoS_{2(s)}$. Only one study was found regarding Mo uptake by cementitious materials. Kato et al. (2002) reported *Kd* values between 4 and 70 mL/g for molybdate uptake by hardened cement paste between pH 12.1 and 12.5. These *Kd* values are consistent with those of selenate, SeO_4^{2-}, a chemical analogue, which has the same oxidation state of +6, charge of -2, and structure with 4 oxygen atoms. However, Se is not necessarily a good analogue for Mo under reducing conditions, because the latter likely does not undergo reduction to +4 under cementitious conditions. In the absence of site specific *Kd* values, the recommended best estimate *Kd* values used here were taken from Ochs et al. (2016). They recommended Se and Mo *Kd* values of 3, 3, and 3 mL/g for oxidizing cement during Stages I, II, and III, respectively.
Mn	100	100	10	No site-specific measurements have been reported. These recommended values were taken from Bradbury and Sarott (1995).
As, Sb	300	300	100	Almond and Kaplan (2011) measured As desorption from core-samples recovered from the Saltstone Disposal Facility under oxidizing conditions, on the bench top, and reported a *Kd* value of 318 mL/g. This is the first As *Kd* measurement made with site-specific cementitious materials. Previously, As *Kd* values were based on the assumption that As (as AsO_4^{3-}) behave like phosphate (PO_4^{3-}). (It is noted that Almond and Kaplan (2011) recommend that the best estimate for As *Kd* for reducing systems be set to 320 mL/g. Given the paucity of data, a more conservative value is suggested here.)
Hg, Pb, Po	300	300	100	Soft divalent cations : Bayliss et al. (1991) conducted a series of sorption experiments with Pb and crushed sulfate resisting Portland cement and ordinary Portland cement/blast furnace slag pastes with an Eh of +50 to -500 mV. The main findings were that sorption was concentration and cement composition dependent. Data strongly suggested solubility controls on Pb aqueous concentrations. Bradbury and Sarott (1995) suggested *Kd* values of 500, 500, & 500 mL/g for these three stages, respectively. Kaplan and Coates (2007) measured Hg *Kd* values in three cementitious materials (50 year old aged concrete sample recovered from a demolition site, saltstone sample, and a highly oxidized saltstone sample) in which $^{230}Hg^{2+}$ was spiked to a suspension of ground material, permitted to equilibrate, and then desorption K_d values were measured under atmospheric conditions. In the non-reducing aged cement, K_d values ranged from 289 to 568 mg/L; in the saltstone sample (again, measured under oxidizing conditions), the K_d values ranged from 1095 to 1173 mg/L. In the highly oxidized saltstone

Constit-uent of Concern	Oxidizing Cement Stage I[a]	Oxidizing Cement Stage II[a]	Oxidizing Cement Stage III[a]	Comments/References[a]
				samples, the K_d value was 841 mL/g. More recently, Bannochie (2015) reported Hg speciation measurements of SRS Tank 50 samples and the TCLP results when that solution was used to make a laboratory saltstone sample. The Tank 50 sample had 126 mg/L total Hg, the saltstone had a total Hg concentration of about 50.4 mg/kg Hg, and the TCLP (conducted in oxidizing conditions) had a total Hg concentration of 0.151 mg/L. As a first approximation, a K_d value based on these values is 334 mL/g. The likely K_d would be greater under reducing conditions. The key finding by Bannochie (2015) was that 80% of the leached Hg from the TCLP tests was in the methyl-Hg form, demonstrating the importance of speciation on Hg leaching from cementitious materials. It is unknown what the Hg speciation is in Hanford secondary solid waste. Especially low K_d values are recommended here because of the uncertainty regarding the waste form and status of the Hg in the various types of solid secondary waste. Furthermore, solubility controls are likely very important in predicting Hg leaching given the highly reactive nature of Hg towards solids and in high sulfur concentration environments. The recommended values here are less than those generally reported in the literature because there is a wide range of sources of Hg in solid waste. In regard to saltstone, the impact of varying Hg species (Bannochie, 2015) on sorption is not clear, and therefore some conservatism needs to be accounted for in the recommended *Kd* values.
Pu,Th, Zr	10,000	10,000	2000	Concrete containing reducing agents (blast furnace slag, BFS) did not have greater Pu *Kd* values than those that did not contain BFS. High *Kd* values are attributed more to low solubility of Pu in high pH systems, than to adsorption/absorption processes. Using three 65-yr-old crushed concrete samples and seven fresh concrete samples, Th-*Kd* values were 2,500 to 5,500 mL/g (Allard et al., 1984; Hoglund et al., 1985). Th- *Kd* values were consistently less than Am *Kd* values, greater than U- *Kd* values, and very similar to Np and Pu *Kd* values (Allard et al., 1984; Hoglund et al., 1985). Pu- *Kd* values ranged from 1,000 to 12,000 mL/g (Allard et al., 1984; Hoglund et al., 1985). Using a sulfate resistant Portland cement, Th *Kd* values were measured to be 100,000 mL/g (Wieland and Van Loon 2003). Kaplan and Coates (2007) measured Pu *Kd* values added as Pu(VI) but likely reduced to Pu(IV) in Ca(OH)-saturated and $CaCO_3$-saturated solutions in ground, 40-yr old concrete, simulating $1^{st}/2^{nd}$ and 3^{rd} Stages, respectively; the measured *Kd* values were 100,000 and 92,000 mL/g, respectively. Pu(V/VI) would likely not remain in this oxidation state for long, even under normal oxidizing conditions, before it would reduce to Pu(IV). Using an actual aged saltstone core sample recovered the Saltstone Disposal Facility and simulated cement leachate, Almond and Kaplan (2011) reported desorption Pu *Kd* values under bench top oxidizing conditions of 4600 mL/g, and under inert glovebag conditions of >2500 mL/g.
U	1000	5000	5000	Ochs et al. (2016), recommended U(VI) K_d values for Stages I, II, and III of 2,000, 30,000, and 30,000 mL/g, respectively. The two primary factors controlling U(VI) sorption to cementitious materials is aqueous Ca and pH conditions (Ochs et al. 2016). There are few studies in which U oxidation state were systematically investigated. The only exception is the study by Bayliss et al. (1996), in which both U(IV) and U(VI) sorption were measured in otherwise identical conditions. No

Constit-uent of Concern	Oxidizing Cement Stage I[a]	Oxidizing Cement Stage II[a]	Oxidizing Cement Stage III[a]	Comments/References[a]
				major differences in K_d were reported. Harfouche et al. (2006) used EXAFS to identify U(VI) incorporated into CSH phases. Several authors have reported the formation of calcium urinate (Evans, 2008; Wellman et al., 2007). Wellman et al. (2007) reported that U(VI) precipitates in concrete without BFS as insoluble uranyl-oxyhydroxide phases initially, and over time these phases transform to uranyl-silicate phases and then ultimately to uranyl phosphate phases as long as adequate phosphate is present. Together these results indicate that solubility is an important controlling process in the release of aqueous U. Pointeau et al. (2004) reported that U uptake by degraded cement and CSH was linear between 10^{-13} to 10^{-7} M. This suggests two things, sorption is linear in this range and that CSH is the phase controlling U sorption. Sorption on silanol groups ($\equiv SiO^-$) that changed with variable charge (pH) and Ca:Si ratios were reported to be important factors controlling U uptake. They noted increases in U K_d values with decreasing pH, which was in part attributed to the coincidental release of Ca to the aqueous phase. Between pH 12.2 to 10 (within the pH range of the 3rd Stage), the measured U *Kd* values increased from 30,000 to 150,000 mL/g. More recently, Pointeau et al. (2008), reported that during the 1st and 2nd Stage, U K_d values in hardened cement paste ranged from 1,000 to 4,000 mL/g. It was not until the portlandite was dissolved (the start of the 3rd Stage), that U *Kd* values increased significantly by at least an order of magnitude. The observed increase in *Kd* with degradation of cement towards lower pH and lower Ca concentration range seems to be consistent with the theory that Ca is competing with sorbing sites on cement for uranium. Similarly, Tits et al. (2008) measured U *Kd* values of CSH phases over a wide range of pH values and reported values in the range of 1000 to 1,000,000 mL/g. It is noteworthy that while the values reported by Tits et al. (2008) were similar to those of Pointeau et al. (2004), they used different cementitious materials: CSH and hardened cement paste, respectively. Because pH and aqueous Ca concentrations change in a systematic manner, it is not possible to separate their respective influences on U uptake (Ochs et al. 2016). Also, opposing observations have been noted regarding the influence of Ca on U uptake: some experiments report that Ca compete with U for sorption sites, whereas other experiments indicate that Ca promote the precipitation of U-Ca solid solution endmembers. Regarding U oxidation state, Bayliss et al. (1996) measured U(IV) and U(VI) sorption under otherwise identical conditions. No major differences in K_d were reported. Evans (2008) concluded that sorption to silanol groups ($\equiv SiO^-$) likely controls uptake at total U concentration less than 10^{-6} to 10^{-5} molar, beyond which solubility of either $CaUO_4$ (Tits et al. 2008) or CaU_2O_7 (Valsami-Jones and Ragnarsdöttir, 1997) control aqueous U concentrations. Ochs et al. (2016) recommended K_d values of 2000, 30,000, and 30,000 mL/g for Stages I, II, and III, respectively. Because the formulation of the IDF cementitious waste forms have not been finalized, lower *Kd* than those recommended by Ochs et al. (2016) were selected to account for this uncertainty. It is anticipated that much of the pessimistic-bias built into these recommended best estimates will be eliminated once measurements are conducted under site specific conditions.
[a] The age of each of the stages is facility specific because it depends on the amount of water that passes through the cementitious material (see Section 4.4).				

Constit-uent of Concern	Oxidizing Cement Stage I[a]	Oxidizing Cement Stage II[a]	Oxidizing Cement Stage III[a]	Comments/References[a]
[b] The presence of sulfur can greatly increase *Kd* values of alkaline earth metals (Ba, Ra, and Sr). *Kd* values for these elements are higher in cement systems containing BFS, a source of sulfur. A second set of recommended best estimate *Kd* values are provided in the "Comments/Reference" column for these elements. [c] Inorganic carbon geochemistry is complicated. The use of only the *Kd* value without the associated solubility value in a cementitious environment will greatly overestimate the true mobility of C through this environment. An excellent review of inorganic C chemistry and its impact of ^{14}C attenuation in cementitious materials is presented in Wang et al. (2009).				

Table 18. Distribution coefficients (*Kd* values, mL/g): Reducing Cementitious Environment.

Constituent of Concern	Reducing Cement Stage I[(a)]	Reducing Cement Stage II[(a)]	Reducing Cement Stage III[(a)]	Comments/References
^{3}H, Ar, As, C, Ca, Cl, Cs, F, Fr, K, Kr, Mn, N, Na, Nb, Ni, Po, Pu, Rb, Rn, Sb, Sn, Sr, Th, Tl, Zr				Use same *Kd* values as reported in Table 17 for Oxidizing Cementitious Solids. No changes in *Kd* values are recommended because the constituents of concern are either not redox sensitive or there is not any information available to indicate if the *Kd* values varies and to what extent it varies.
Ag, Cd, Co, Cu, Pb, Pd, Pt, Zn	5000	5000	1000	Selected transitions monovalent and divalent metals: Kaplan and Coates (2007) measured Cd and Co *Kd* values in Ca(OH)-saturated and $CaCO_3$-saturated solutions in ground, SRS reducing grout, simulating 1st/2nd and 3rd Stages, respectively. The measured Cd *Kd* values were 297,000 and 17,500 mL/g, respectively. The measured Co *Kd* values were 15,000 and 6,500 mL/g, respectively. It is likely the sulfides are forming strong bonds to these transition metals, perhaps forming sulfide precipitates.
Ac, Al, Am, Bi, Bk, Ce, Cf, Cm, Es, Eu, Fe, Fm, Gd, Lu, Sm, Y	7000	7000	1000	Trivalent Cations: Kaplan and Coates (2007) measured Am, Ce, and Y *Kd* values in Ca(OH)-saturated and $CaCO_3$-saturated solutions in ground, SRS reducing grout, simulating 1st/2nd and 3rd Stages, respectively. The measured Am *Kd* values were 42,900 and 17,000 mL/g, respectively. The measured Ce *Kd* values were 104,000 and 4,560 mL/g, respectively. The measured Y *Kd* values were 64,800 and 5,300 mL/g, respectively. It is likely the sulfides were forming strong bonds to multivalent cations, perhaps forming sulfide precipitates. Sorption to trivalent cations under reducing conditions and with reducing grout had higher *Kd* values than under oxidizing conditions.
Tc, Re	1000	1000	1000	Under reducing conditions, it is recommended that Tc(IV) sorption be characterized with a solubility term; *Kd* values are provided here to offer alternative modeling approaches and to accommodate any potential numerical models that cannot use k_s values. $Tc^{VII}O_4^-$ gets reduced to Tc^{4+}, which like other tetravalent cations sorbs strongly to surfaces. Lukens et al. (2005) conducted fundamental studies using SRS slag and grout mixtures. In their study, they added Tc(VII) to a reducing grout and using X-ray Absorption Spectroscopy, specifically, XANES, they observed the slow transformation of Tc(VII) to $Tc^{VII}O_2$-H_2O to $Tc^{IV}S_x$. This process was monitored in the grout over a course of 45 months. Arai and Powell (2015), used XANES to showed that while Tc(VII) existed in Saltstone samples after 29 days, no Tc(VII) was present after 117 days (Arai and Powell, 2014, 2015). They also observed that, as the samples aged, that there was a growing percentage of the Tc in association with S as TcS_x. See a discussion of Tc solubility values under reducing conditions in Table 21. The high *Kd* values selected for these conditions reflect in part the low solubility of Tc under these conditions. Lilley et al (2009) measured $Tc^{VII}O_4^-$ sorption to two SRS Saltstone simulants containing 45% slag but did not reach steady state. In one experiment they measured a *Kd* of 18 mL/g and in the other a *Kd* of 3660 mL/g. Estes et al. (2012) measure Tc *Kd* values for four types of cement recovered from the SRS in an inert glove bag. After 319 days, two formulations containing BFS had *Kd* values ranging between 2001 and 8300 mL/g (samples Vault 2 and TR545). Seaman et al. (2018) measured effective diffusivity values of Tc in saltstone over a range of curing times (2 – 20 mo), Tank 50 simulants, and sources of BFS; values were consistently three orders-of-magnitude slower than the conservative tracer, NO_3^-, 5E-11 cm^2/s vs. 5E-8 cm^2/s, respectively.

Constit-uent of Concern	Reducing Cement Stage I[(a)]	Reducing Cement Stage II[(a)]	Reducing Cement Stage III[(a)]	Comments/References
				Furthermore, they concluded, based on thermodynamic modeling considerations that the Tc solid phase controlling solubility was likely TcO_2-$2H_2O$(*s*) or TcO_2-$1.6H_2O$(*s*) (Seaman and Coutelot, 2017; Seaman et al., 2018; Seaman et al., 2019) There have been several reviews of Tc uptake by reducing cementitious materials (Icenhower et al., 2010; Kaplan et al., 2011; Ochs et al., 2016; Pabalan et al., 2009; Ridge, 2015; Westsik et al., 2013; Westsik Jr et al., 2014). (Additional relevant discuss is present in Table 21.) Ochs et al. (2016) recommended best Tc(IV) K_d values for the reducing cementitious waste forms at the Belgium proposed repository of 3000, 3000, and 3000 mL/g for Stages I, II, and III, respectively.
Hg	500	500	100	Immobilization of Hg from various industrial sources into cementitious waste forms has been studied extensively (Razzell, 1990; Svensson and Allard, 2007, 2008; Svensson et al., 2006). Mercury does not form sufficiently insoluble (hydr)oxides, and a sulfur source needs to be added to promote the formation of the sparingly soluble HgS phase. While many researchers have pointed to cinnabar, a crystalline form of HgS, as a natural analogue for the HgS phase in cementitious materials controlling Hg solubility, this may be an oversimplification because there are many less crystalline and meta-stable forms of the mineral, resulting in a wide range of solubilities. Furthermore, redox status of the waste monolith is a crucial parameter for the formation of HgS. In samples where only slag was used as a sulfur source, Svensson and Allard (2008) reported D_a values of 1.5E-15 to 3.7E-14 cm^2/s. In the same trial with slag-free formulations (OPC and sand), the D_a values were 3.8E-14 to 1.8E-11 cm^2/s (based on long-term test results). Given that a conservative element, such as Na, may have a D_a value in the order of 1E-8 cm^2/s, these studies indicate that Hg is strongly bound by cementitious materials, and that reducing conditions may be expected to decrease D_a values (increase sorption) by at least an order of magnitude. Another important general conclusion from this work is that Hg D_a values vary greatly with the speciation of Hg in the waste form. If HgS is not likely formed, e.g., Hg(0) and Hg(II) are present, than D_a values may increase (are more readily leached) to 1E-9 to 1E-11 cm^2/s. More recently, Bannochie (2015) reported Hg speciation measurements of SRS Tank 50 samples and the TCLP results when that solution was used to make in the laboratory a saltstone sample. The Tank 50 sample had 126 mg/L total Hg, the saltstone had a total Hg concentration of about 50.4 mg/kg Hg, and the TCLP (conducted in oxidizing conditions) had a total Hg concentration of 0.151 mg/L. As a first approximation, a K_d value based on these values is 334 mL/g. This K_d value would have been greater had it been measured under reducing conditions. The key finding by Bannochie (2015) was that 80% of the leached Hg from the TCLP tests was in the methyl-Hg form, underscoring the importance of speciation on Hg leaching. In summary, the presence of sulfides in reducing cementitious waste forms is extremely effective at immobilizing ionic forms of Hg, with *Kd* values >10,000 mL/g, based on the extremely low solubility values of various Hg-sulfide phases. However, because the Hg speciation in solid waste or in saltstone is not known. While a majority of the Hg is expected to exist in the strongly immobilized ionic form (*e.g.*, Hg^{2+}), full speciation of Hg in the solid waste and saltstone is not known, therefore additional pessimistic-

Constit-uent of Concern	Reducing Cement Stage I[a]	Reducing Cement Stage II[a]	Reducing Cement Stage III[a]	Comments/References
				bias needs to be added to the recommended best estimate values. It is recommended that the best estimates be 500, 500, and 100 mL/g for Stages I, II, and III, respectively. The Stage III value is lowered to account for loss of sulfur from the cementitious material and the conversion of sulfide to sulfate. It is very likely that once additional research is carried out with site specific samples, that much of this conservatism can be removed.
Ba, Ra	6000	6000	600	Barium sulfate is highly insoluble in water ($k_s = 10^{-10}$ M; Barium sulfide has only a slightly higher solubility value of $k_s = 5 \times 10^{-10}$ M). Almond and Kaplan (2011) measured very high apparent *Kd* values for Ba from an actual saltstone core sample recovered from the Saltstone Disposal Facility: >15,000 mL/g under oxidizing conditions, and 7400 mL/g under inert gas conditions. While radionuclide immobilization in the presence of slag is commonly attributed to the reduction process, for Ba, immobilization is likely the result of the formation of a sulfate/sulfide precipitate. These latter results using site specific materials are especially representative of conditions expected under disposal conditions. Therefore, larger *Kd* values are warranted for Sr (and Ba) OPC/BFS-blends than in traditional OPC blends.
Sr	1000	1000	100	Stable Sr, exists in very high concentrations with respect to radiostrontium in cements, ranging from 100 to 1000 ppm. The presence of large amounts of stable Sr is expected to be especially important in systems with high sulfur concentrations, as exists in BFS-blends. When sulfate concentrations are high, $SrSO_4$ precipitates. $SrSO_4$ has a solubility of 3.2×10^{-7} M (strontium sulfite solubility product is even lower, $SrSO_3$ $k_s = 4 \times 10^{-8}$ M). Almond and Kaplan (2010) measured very high apparent Sr *Kd* values in an actual saltstone core sample recovered from the Saltstone Disposal Facility: 5728 mL/g under oxidizing conditions, and 737 mL/g under inert gas conditions. Similarly, Reigel and Hill (2016) measured appreciably lower apparent Sr *Kd* values in an actual saltstone core sample recovered from the Saltstone Disposal Facility: ~40 mL/g under oxidizing conditions, and ~50 mL/g under inert gas conditions. The cause for the discrepancy of these results compared to earlier results and literature results is not known. While radionuclide immobilization in the presence of slag is commonly attributed to the reduction of the radionuclide to a less mobile oxidation state, in the case of Sr (and Ba), the presence of sulfur, the reducing agent, is responsible for immobilization through the formation of sulfate/sulfide precipitates. These latter results using site specific materials are especially representative of conditions expected under disposal conditions. Therefore, larger *Kd* values are warranted for Sr (and Ba) OPC/BFS-blends than in traditional OPC blends.
Cr	1000	1000	1000	Under reducing conditions, it is recommended that Cr(III) sorption be characterized with a solubility term; K_d values are provided here to offer alternative modeling approaches and to accommodate any potential numerical models that cannot use k_s values. Kindness et al. (1994) reported that <0.01 ppm Cr leached from a well cured OPC/BFS monolith prepared with water and spiked with 5000 ppm Cr(III). Using these values, a K_d value is >500,000 mL/g, and an apparent solubility value, solubility values of <2E-7 mol/L. Bajt et al. (1993) observed XAS spectra of the reduction of Cr(VI) in SRS reducing grout to Cr(III). Rai et al. (1987) measured the solubility of Cr(III) at varying pH and ionic strengths and as varying solid phases. Evans (2008) reported that Cr(III) is structurally incorporated into numerous cement phases, including

Constit-uent of Concern	Reducing Cement Stage I[(a)]	Reducing Cement Stage II[(a)]	Reducing Cement Stage III[(a)]	Comments/References
				hydrogarnet, and CSH phases, where the Cr^{3+} replaces octahedrally coordinated Al^{3+}. Polettini and Pomi (2003) reported that Cr^{3+} could substitute into Si sites of CSH. Westsik et al. (2013) reported Cr apparent diffusion coefficients for 26 Cast Stone (BFS-cement) samples with a wide range of formulations. Cr apparent diffusion coefficients (10^{-12} to 10^{-14} cm^2/sec) were 4 to 6 orders-of-magnitude slower than nitrate, nitrite, and Na (assumed to be conservative tracers with no retardation; 10^{-8} cm^2/s), indicative of significant retardation. Cr effective diffusion rates were also 2 to 4 orders-of-magnitude lower than Tc. Assuming reversible and linear sorption is responsible for the Cr retention to the Cast Stone, the D_e value are inversely related to retardation factor, which in turn is directly related to K_d (i.e., $D_e = D_0/R_f$). Cr K_d values may be as much as 6 orders of magnitude greater than nitrate/nitrite/Na K_d values, and 2 to 4 orders of magnitude greater than Tc K_d values. While this work suggests that Cr *Kd* values may by >10,000 mL/g, lower values are recommended here to account for wide range of sources and forms of Cr in the solid and liquid waste on the SRS.
At, I	0	2	0	Three studies have shown that I *Kd* values under reducing conditions are much less than under oxidizing condition. Westsik et al. (2013) and Serne et al. (1992) showed that I had diffusion coefficients similar to nitrate, nitrite and Na, suggesting that no I retardation occurred. Atkins and Glasser (1992) showed that I *Kd* values for reducing cement was 5 mL/g and for OPC-cement was 40 mL/g. Similarly, Allard et al. (1984) report I *Kd* values of 3 mL/g for slag-containing cements and for slag-free cement (ordinary Portland cement) they reported an I *Kd* value of 125 mL/g. It is likely that part of the reason for the differences between I *Kd* values can be attributed to changes in I speciation; reducing conditions will have a greater percentage of iodide, the weakly sorbing species, and oxidizing conditions with have a greater percentage of iodate, the more strongly sorbing species and the species most likely to coprecipitate in various CSH phases. Reigel and Hill (2016) measured desorption ^{129}I *Kd* values in an inert glovebag of saltstone cores recovered from the Saltstone Disposal Facility of -1, 5, 4, and 2 mL/g under conditions that would most closely approximate those of Stage II. These latter *Kd* measurements represent the highest pedigree data. Kaplan and Coates (2007) measured on the benchtop (exposed to air) iodide I^- (iodide) *Kd* values in $Ca(OH)_2$ saturated and $CaCO_3$-saturated solutions in ground, SRS reducing grout, simulating Stages I&II, and Stage III, respectively. The measured I^- *Kd* values were 6.2 and 11 mL/g, respectively. The best estimate *Kd* value in Stage I is set to 0 mL/g because of high ionic strength and low redox. *Kd* values in the 2nd stage are slightly increased to capture the results from actual Saltstone samples noted above (Reigel and Hill, 2016). In Stage III, the *Kd* value is reduced again because all CSH phases have been exhausted and cementitious leachates have elevated ionic strength. Recent effective diffusivity measured of saltstone made with different sources of BFS by Seaman et al. (2018) indicated that ^{129}I was not retained by the grout, more specifically, that ^{129}I effective diffusivity was similar to that of nitrate, 10^{-8} to 10^{-9} cm^2/s.
Np, Pa	10,000	10,000	5000	Np(V) added to cementitious materials without BFS under goes oxidation state transformation to more strongly binding species, Np(VI) and Np(IV) (Gaona et al., 2011; Tits et al., 2014; Zhao et al., 2000). These transformed oxidation states are likely responsible for the unexpectedly high *Kd* values noted in the

Constit-uent of Concern	Reducing Cement Stage I[a]	Reducing Cement Stage II[a]	Reducing Cement Stage III[a]	Comments/References
				literature. These XANES and EXFS studies have shown that that the Np formed sparingly soluble phases, co-precipitated, and also sorbed to the cementitious material surfaces. Kaplan and Coates (2007) measured Np(V) and Pa(V) (often considered chemical analogues) *Kd* values in $Ca(OH)_2$ –saturated and $CaCO_3$-saturated solutions in ground, SRS reducing grout, simulating Stages I & II, and Stage III, respectively. It is not clear whether each element underwent reduction to the +4 species, based on thermodynamic considerations alone, they would be expected to have been reduced. The Np *Kd* values in the $Ca(OH)_2$ solution were 3,949 m/g and in the $CaCO_3$ solution was 2,779 mL/g. .) The Pa *Kd* values in the $Ca(OH)_2$ solution was 9,890 mL/g and in the $CaCO_3$ solution was 8,049 mL/g. Kaplan et al. (2008a) using reducing DDA simulant Saltstone (25 wt-% slag) and Vault 2 concrete (10% slag) measured Np(V) *Kd* values that were all "greater than values". Commutatively, the *Kd* values were >4218 mL/g. Lilley et al. (2009) measured 10 cementitious Np *Kd* values >1E6 mL/g, using varying types of solids (50-year old cement, two SRS Saltstone simulants, and Vault 2 Cement), and contact times of 1 or 4 days, and 3 NpO_2^- concentrations. They demonstrated that solubility was controlling sorption. (See discussion in apparent solubility look-up tables.) Ochs et al. (2016) recommended Np(IV) *Kd* values of 30,000, 30,000, and 30,000 for Stages I, II, and III, respectively.
Se, Mo, Te	300	300	200	Se may exist as either Se(IV) or Se(0) under reducing conditions (Ochs et al., 2010). Selenite sorbed appreciably on nearly all hardened cement paste minerals, as well as to harden cement paste. The sorption mechanism is not known but appears to include a combination of substitutions into sulfate containing phases, such as ettringite, and surface complexation, ligand exchange, and adsorption. Twenty-seven cementitious formulations (varying water/solid, silica fume %, and clay concentration) were used to measure selenite (SeO_3^{2-}) *Kd* values from an alkaline solution *Kd* values ranging from 250 to 930 mL/g (Johnson et al. 2000). Several researchers have measured selenite *Kd* values for various formulations of hardened cement paste formulations: Johnson et al. (2000) measured >570 mL/g (included slag in formulation), Pointeau et al. (2008) measured *Kd* values >1000 mL/g after 1000 days of curing, and Mace et al. (2007) measured *Kd* values of >3250 mL/g. In a review of Se *Kd* values, Ochs et al. (2010) reported little difference as a function of pH between 9 and 13, therefore it is reasonable to keep the same *Kd* values the same for all three Stages. Regarding Mo, the only aqueous species relevant to a cement system is the MoO_3^{2-}. In slag cements, however, sufficient sulfide could be present to form MoS_2.
Pu	10,000	10,000	2000	Kaplan and Coates (2007) measured Pu(VI) *Kd* values in $Ca(OH)_2$-saturated and $CaCO_3$-saturated solutions in ground, SRS reducing grout, simulating Stages I&II, and Stage III, respectively. The Pu(VI) likely reduced to Pu(IV). The measured Pu *Kd* values were 5760 and 11055 mL/g, respectively. In the same study, Kaplan and Coates (2007) also measured Sn (tin) sorption, also a tetravalent cation. It had a *Kd* of 71,762 mL/g in $Ca(OH)_2$ and 5520 mL/g in the $CaCO_3$ solutions. Using SRS DDA simulated Saltstone, Kaplan et al. (2008d) measured a *Kd* of 12,176 mL/g in $Ca(OH)_2$ saturated solution and a *Kd* of 165,570 mL/g in a $CaCO_3$ saturated solution. The first solution was design to simulate Stages I&II aqueous

Constit-uent of Concern	Reducing Cement Stage I[(a)]	Reducing Cement Stage II[(a)]	Reducing Cement Stage III[(a)]	Comments/References
				conditions, whereas the second solution was to simulate Stage III. Pu(VI) was added but it likely reduced to Pu(IV) during the course of the measurement. Ochs et al. (2016) recommended using Pu(IV) *Kd* values of 5000, 30,000 and 30,000 mL/g for Stages I, II, and III, respectively.
U	5000	5000	5000	Precipitation and coprecipitation are important U immobilization processes under oxidizing and reducing cementitious conditions. Most studies of U immobilization have been conducted with non-reducing grout. The only exception is the study by Bayliss et al. (1996) in which both U(IV) and U(VI) sorption were measured in otherwise identical conditions. They reported no major differences in U(IV) and U(VI) *Kd* values. Another indication of the strong U binding potential of potential BFS-containing cementitious materials was reported by Cantrell et al. (2016), where they concluded that the best U effective diffusion coefficients, D_a, value for Cast Stone is <6E-16 cm^2/s (which is approximately equivalent to *Kd* value >1,000,000 mL/g), which was the slowest noted diffusion of all radionuclides investigated. As part of an extensive review of the literature, Ochs et al. (2016) concluded that there were no significant differences between recommended U K_d values for the three cement stages; for Stages I, II, and III, they recommended 30,000, 30,000, and 30,000 mL/g, respectively. The recommended values here have been set lower than those recommended by Ochs et al. (2016) to capture the uncertainty associated with the disposal of U as possibly several different species (e.g., U speciation in saltstone versus in solid waste).

[(a)] The age of each of the stages is facility specific because it depends on the amount of water that passes through the cementitious material (see Section 4.4).

Table 19. Distribution coefficients (*Kd* values, mL/g): Reoxidizing cementitious materials (*i.e.,* oxidized BFS-cementitious materials).

Constituent of Concern	Reoxidizing Cement[(a)] Stage I[(b)]	Reoxidizing Cement Stage II	Reoxidizing Cement Stage III	Comments/References
All constituents of concern except Ba, Ra, and Sr				Used *Kd* values noted in Table 17 for oxidizing cementitious materials.
Ba, Ra	6000	6000	600	The presence of sulfur can greatly increase *Kd* values of alkaline earth metals (Ba, Ra, and Sr). BFS contributes sulfur to cementitious waste forms. BFS exists in many SRS cementitious material formulations, including saltstone and materials used for tank closure, and most formulations used for several solid LLW disposal (Section 5.0). Almond and Kaplan (2011) measured the solubility of Ba from a core sample recovered from the SRS Saltstone Disposal Facility using simulated cementitious leachate. Under oxidizing conditions, the solubility was $<1.9 \times 10^{-7}$ M Ba and under reducing conditions, the solubility was 3.9×10^{-7} M Ba. This same data expressed as apparent *Kd* values was >15,000 mL/g under oxidizing conditions, and 7400 mL/g under inert gas conditions. While radionuclide immobilization in the presence of slag is commonly attributed to the reduction process, for the alkaline earth metals, additional immobilization results from the formation of a sulfate/sulfide precipitate. Barium sulfate is highly insoluble in water ($k_s = 10^{-10}$ M; Barium sulfide has only a slightly higher solubility value of $k_s = 5 \times 10^{-10}$ M). These latter results using site specific materials are especially representative of conditions expected in cementitious systems containing BFS, either reduced or oxidized, where larger concentrations of sulfur exist in the waste form. As the saltstone ages, *i.e.,* undergoes oxidation, the sulfide converts to sulfate, which is also highly effective at immobilizing the alkaline metal earth elements. Therefore, larger *Kd* values are warranted for these elements in OPC/BFS-blends than in OPC type blends. For reoxidized cementitious materials containing slag, it is recommended that *Kd* values for Stages I, II, and III of 6000, 6000, and 600 mL/g, respectively, be used.
Sr	1000	1000	100	The presence of large amounts of stable Sr is expected to be especially important in systems with high sulfur concentrations, as exists in BFS-blends. When sulfate concentrations are high, $SrSO_4$ precipitates. $SrSO_4$ has a solubility of 3.2×10^{-7} M (strontium sulfite solubility product is even lower, $SrSO_3$ $k_s = 4 \times 10^{-8}$ M). Almond and Kaplan (2011) measured very high apparent Sr *Kd* values in an actual saltstone core sample recovered from the Saltstone Disposal Facility: 5728 mL/g under oxidizing conditions, and 737 mL/g under inert gas conditions. For oxidized cementitious materials containing slag, it is recommended that *Kd* values for Stages I, II, and III of 1000, 1000, and 100 mL/g, respectively, be used.

[(a)] Reoxidized cementitious materials are cementitious materials that include BFS in their formulation and have aged to the point that their reduction capacity has been exhausted. Unlike redox sensitive radionuclides, such as Tc, I, Np, and Pu (as noted in Table 19), that have different *Kd* values based on the redox status of the cementitious material, Ba, Ra, and Sr have large *Kd* values to cement formulations including BFS, irrespective of the redox status because they form strong bond to the sulfur in BFS, regardless of whether the S is oxidized or reduced.

[(b)] The age of each of the stages is facility specific because it depends on the amount of water that passes through the cementitious material (see Section 4.4).

Table 20. Apparent solubility values (k_s, mol/L) for the Oxidizing Cementitious Environment.

Constit-uent of Concern	Oxidizing Cement k_s Stage I [a]	Oxidizing Cement k_s Stage II[a]	Oxidizing Cement k_s Stage III[a]	Comments/References
^{3}H, Ar, As, At, Cl, Cr, Cs, F, Fr, I, K, Kr, Mn, Mo, N, Na, Nb, Pu, Rb, Re, Rn, Sb, Se, Tc, Te, Tl	NA	NA	NA	No solubility constrains are assumed to exist with these radionuclides.
C[b]	10^{-5}	10^{-6}	10^{-5}	**Solubility, *ks:*** For a cement dominated repository environment, at relatively low flow or stagnant groundwater flow conditions, the near field, alkaline chemical conditions are likely to exert control on calcite solubility and thus inhibit ^{14}C release from the waste form. The solubility will be primarily controlled by natural carbonate concentrations, not ^{14}C-carbonate concentrations. Natural carbonate concentrations, in turn will be largely controlled by pH. Based on thermodynamic calculations, Bradbury and Sarott (1995) calculated the concentration of aqueous and solid phase natural carbonate concentrations as a function of pH. These values were used in this table. Krupka et al. (2004) came up with similar results. For young concrete, they assumed that portlandite controls Ca concentrations to 10^{-3} M and CO_3^{2-} at 10^{-6} M (Krupka et al., 2004). Ca concentrations are set by the solubility of calcite to "fix" the carbonate concentration. For aged cement the Ca is controlled at 10^{-2} M by some undefined reactions (Krupka et al. 2004). Subsurface C chemistry in a cementitious environment has been reviewed (Dayal et al., 1989; Dayal and Reardon, 1992) and modeling gaseous ^{14}C in cementitious environments in the SRS subsurface has been discussed by Kaplan (2005). ***Kd* values [c]**: As discussed in Section 6.1 and shown in Table 17, the paired *Kd* value associated with these k_s values for Stages I, II, and III, are 2000, 5000, and 50, respectively.
Ac, Al, Am, Bk, Bi, Ce, Cf, Cm, Es, Eu, Fe, Fm, Gd, Lu, Sm, Y	10^{-11}	10^{-8}	10^{-7}	**Solubility, *ks:*** <u>All +3 oxidation state:</u> <u>Young Concrete</u>: Am solubility in concrete rinsate at pH 12 = 8e-11 M, at pH 13 = 1e-11 to 7e-12 M Am (Ewart et al., 1992). Solid phase controlling solubility assumed to be $Am(OH)_3$ or $Am(OH)CO_3$ (Brady and Kozak, 1995; Ewart et al., 1992; Ochs et al., 2016). Using a variety of cements and contact times of 100 days under oxidizing conditions measured Am solubility average was 1e-11 M (Allard et al., 1984). Experiments with sulfate resistant Portland cement consistently had Eu concentrations <1e-11 M. Time-resolved laser fluorescence spectroscopy (TRLFS) showed that Eu was incorporated within CSH and another fraction had properties suggesting it was within a

Constit-uent of Concern	Oxidizing Cement k_s Stage I [a]	Oxidizing Cement k_s Stage II[a]	Oxidizing Cement k_s Stage III[a]	Comments/References
				structure like $Eu(OH)_3$ (Atkins et al., 1993). Similarly, Cm was shown to be incorporated into the structure of calcium-silicate-hydrate (CSH) gels (Wieland and Van Loon, 2003). Moderately Aged Concrete: Am solubility in concrete rinsate (no solid phase) at pH 10 to 11 was 1e-8 to 1.5e-10 M Am (Ewart et al., 1992). ***Kd* values [c]**: As discussed in Section 6.1 and shown in Table 17, the paired *Kd* value associated with these k_s values for Stages I, II, and III, are 6000, 6000, and 600, respectively.
Ag, Cd, Co, Cu, Pd, Pt, Zn	10^{-7}	10^{-7}	10^{-6}	**Select Monovalent and Divalent Transitions Metals** **Solubility, k_s:** Solid phase assumed to control solubility is $Co(OH)_2$ (Allard et al. 1984; Wieland and Van Loon, 2003). Experiments with sulfate resistant Portland cement had Co solubility values of 5e-8 and 2e-7 M at pH 13.3 (Wieland and Van Loon, 2003). The solubility of $Co(OH)_2$ was calculated to be 6.5e-5 M (Wieland and Van Loon, 2003; Ochs et al. 2016). Calculated values are considered less reliable than experimental values. Experiments and calculations have also been done with aged cement end members under alkaline cement conditions (Ewart et al., 1992; Brady and Kozak, 1995; Krupka and Serne 1998). Several experiments show solubility controls (Ewart et al., 1992; Brady and Kozak, 1995; Krupka and Serne 1998). Solubility controls of Ni are shown by (Atkins et al., 1993; Hietanen et al., 1985; Pilkington and Stone, 1990). ***Kd* values [c]**: As discussed in Section 6.1 and shown in Table 17, the paired *Kd* value associated with these k_s values for Stages I, II, and III, are 4000, 4000, and 400, respectively.
Ni	10^{-7}	10^{-7}	10^{-6}	**Solubility, k_s:** Ni concentrations consistently in range of 5e-8 to 2e-7 M regardless of the solid/liquid ratio (Wieland and Van Loon, 2003; Ochs et al. 2016). ***Kd* values [c]**: As discussed in Section 6.1 and shown in Table 17, the paired *Kd* value associated with these k_s values for Stages I, II, and III, are 70, 400, and 400, respectively.
Hg, Pb, Po	10^{-7}	10^{-7}	10^{-6}	**Solubility, k_s:** For a discussion about the basis for selecting the k_s value, see above in this table the discussion for Ag, Cd, Co, Cu, Pd, Pt, Zn. ***Kd* values [c]**: As discussed in Section 6.1 and shown in Table 17, the paired *Kd* value associated with these k_s values for Stages I, II, and III, are 300, 300, and 100, respectively.
Sn	10^{-7}	10^{-7}	10^{-6}	**Solubility, k_s:** For a discussion about the basis for selecting the k_s value, see above in this table the discussion for Ag, Cd, Co, Cu, Hg, Ni, Pb, Pd, Po, Pt, Sn, and Zn. ***Kd* values [c]**: As discussed in Section 6.1 and shown in Table 17, the paired *Kd* value associated with these k_s values for Stages I, II, and III, are 4000, 4000, and 200, respectively.
Np, Pa	10^{-13}	10^{-13}	10^{-7}	**Solubility, k_s:** Neptunium sorption to aged SRS cement samples were conducted by Miller et al. (2009). They used an ICP-MS which permitted them much lower detection limits than conventional radiometric analytical methods and as a result, much lower *Kd* values were measured. They added Np(V) at varying concentrations to ground 50-year old cement samples and measured constant aqueous Np concentration at 1e-13 M, indicating solubility controls. Oxidation state of radionuclides is +5. Assume that NpO_2^+ and PaO_2^+ is the

Constit-uent of Concern	Oxidizing Cement k_s Stage I [a]	Oxidizing Cement k_s Stage II[a]	Oxidizing Cement k_s Stage III[a]	Comments/References
				controlling solid. There is empirical data in Ewart et al. (1992) that predicts much lower concentrations than thermodynamic predictions (Eward et al., 1992; Brady and Kozak, 1995; Krupka and Serne, 1998). Allard et al. (1984) added Np(V) to a variety of cements & measured solubility after 100 days of 4e-9 M. Solubility of Np(IV) is ~1e-8 M for pH 9.75 through pH 12.6 (*3*). Thus, according to Allard et al. (1984) and Ewart et al (1992) solubility of Np is about the same in concrete whether it is in +4 or +5 state. Miller et al (2009) had appreciably better detection limits than Ewart et al. (1992) and the former were working with aged material whereas the latter were working with fresh materials. ***Kd* values [c]**: As discussed in Section 6.1 and shown in Table 17, the paired *Kd* value associated with these k_s values for Stages I, II, and III, are 10,000, 10,000, and 5000, respectively.
Ra	10^{-6}	10^{-6}	10^{-6}	**Solubility, k_s:** Ra solubility has been measured under a wide range of geochemical conditions, and it's tendency to coprecipitate under environmental conditions with other alkaline metal earths has been the subject of several studies (Grandia et al., 2008; Monnin and Galinier, 1988; Ochs et al., 2016). At moderate sulfate concentrations, several alkaline earth metals (Sr, Ba, and Ra) have been shown to precipitate as *X*-SO_4 phases. ***Kd* values [c]**: As discussed in Section 6.1 and shown in Table 17, the paired *Kd* value associated with these k_s values for Stages I, II, and III, are 200, 100, and 200 mL/g, respectively. Note that when the system involves a slag-amended cement that has aged and has since re-oxidize (as is the case with aged saltstone or grout in tank disposition) the Ra has a paired *Kd* value of Stages I, II, and III, of 6000, 6000, 600 mL/g, respectively.
Ba	10^{-5}	10^{-5}	NA	**Solubility, k_s:** Ba, Ca, and Sr solubility has been measured under a wide range of geochemical conditions, and it's tendency to coprecipitate under environmental conditions with other alkaline metal earths has been the subject of several studies (Grandia et al., 2008; Monnin and Galinier, 1988; Ochs et al., 2016). At moderate sulfate concentrations, several alkaline earth metals (Sr, Ba, and Ra) have been shown to precipitate as *X*-SO_4 phases. ***Kd* values [c]**: As discussed in Section 6.1 and shown in Table 17, the paired *Kd* value associated with these k_s values for Stages I, II, and III, are 200, 100, and 200, respectively. Note that when the system involves a slag-amended cement that has aged and has since re-oxidize (as is the case with aged saltstone or grout in tank disposition) the Ra has a paired *Kd* value of Stages I, II, and III, of 6000, 6000, 600 mL/g, respectively.
Sr	10^{-5}	10^{-5}	NA	**Solubility, k_s:** Ba, Ca, and Sr solubility has been measured under a wide range of geochemical conditions, and it's tendency to coprecipitate under environmental conditions with other alkaline metal earths has been the subject of several studies (Grandia et al., 2008; Monnin and Galinier, 1988; Ochs et al., 2016). At moderate sulfate concentrations, several alkaline earth metals (Sr, Ba, and Ra) have been shown to precipitate as *X*-SO_4 phases.

Constit-uent of Concern	Oxidizing Cement k_s Stage I [a]	Oxidizing Cement k_s Stage II[a]	Oxidizing Cement k_s Stage III[a]	Comments/References
				***Kd* values [c]**: As discussed in Section 6.1 and shown in Table 17, the paired *Kd* value associated with these k_s values for Stages I, II, and III, are 90, 20, and 90, respectively. Note that when the system involves a slag-amended cement that has aged and has since re-oxidize (as is the case with aged saltstone or grout in tank disposition) the Ra has a paired *Kd* value of Stages I, II, and III, of 1000, 1000, 100 mL/g, respectively.
U	10^{-6}	10^{-5}	10^{-6}	**Solubility, k_s:** Solubility controlling phases are likely U(VI) hydrous oxide [schoepite] and uranophase [calcium U(VI) silicate] (Brady and Kozak 1995; Ochs et al. 2016). Brady and Kozak (1995) calculated a solubility of 10^{-8} M U(VI). Ochs et al. (2016) calculated U(VI) solubility at pH >12.2 was in the order of 10^{-13} M, and between pH 10 and 12.2, U(VI) solubility was $<10^{-12}$ M. King and Hobbs (2015) recently noted that U solubility under oxidizing conditions simulating tank disposal, measured solubility values of 1.1E-4 to 1.4E-4 M. These are rather unique conditions that are generally not representative of most LLW SRS disposal conditions. ***Kd* values [c]**: As discussed in Section 6.1 and shown in Table 17, the paired *Kd* value associated with these k_s values for Stages I, II, and III, are 1000, 5000, and 5000, respectively.

[a] The age of each of the stages is facility specific because it depends on the amount of water that passes through the cementitious material (see Section 4.4).
[b] Inorganic carbon geochemistry is complicated. The use of only the *Kd* value without the associated solubility value in a cementitious environment will greatly overestimate the true mobility of C through this environment. An excellent review of inorganic C chemistry and its impact of ^{14}C attenuation in cementitious materials is presented in Wang et al. (2009).
[c] All k_s values have associated *Kd* values, where aqueous solute concentrations are controlled by the k_s value above the critical solubility value and by the *Kd* value above the critical solubility value. This is discussed in Section 6.1 and depicted in Figure 1 – Bottom.

Table 21. Apparent solubility values (k_s; mol/L) for the Reducing Cementitious Environment.

Constituent of Concern	Reducing Cement k_s Stage I[a]	Reducing Cement k_s Stage II[a]	Reducing Cement k_s Stage III[a]	Comments/References
^{3}H, Ac, Ag, Al, Am, Ar, As, At, Bi, Bk, C, Ca, Cd, Ce, Cf, Cl, Cm, Co, Cs, Cu, Es, Eu, Fr, F, Fe, Fm, Gd, Hg, I, Lu, K, Kr, Mn, Mo, N, Na, Nb, Ni, Pb, Pd, Po, Pt, Pu(V/VI), Rb, Rn, Sb, Se, Sm, Sn, Te, Tl, Th, Y, Zn, Zr,				These constituents of concern are assumed to have the same apparent solubility values and distribution coefficients as for the Oxidizing Cementitious (Table 20**Error! Reference source not found.**). Redox is not expected to influence apparent solubility values for these radionuclides.
Ba, Ra	10^{-7}	10^{-7}	10^{-7}	**Solubility (k_s) & *Kd*:** The presence of sulfur can greatly increase *Kd* values of alkaline earth metals (Ba, Ra, and Sr). BFS contributes sulfur to cementitious waste forms. BFS exists in many SRS cementitious material formulations, including saltstone and materials used for tank disposition, and most formulations used for solid LLW disposal (except those for Components-in-Grout and Intermediate Level Vault grout filled materials (Section 5.0). Almond and Kaplan (2011) measured the solubility of Ba from a core sample recovered from the SRS Saltstone Disposal Facility using simulated cementitious leachate. Under oxidizing conditions, the solubility was <1.9 x 10^{-7} M Ba and under reducing conditions, the solubility was 3.9 x 10^{-7} M Ba. This same data expressed as apparent *Kd* values was >15,000 mL/g under oxidizing conditions, and 7400 mL/g under inert gas conditions. While radionuclide immobilization in the presence of slag is commonly attributed to the reduction process, for the alkaline earth metals, additional immobilization results from the formation of a sulfate/sulfide precipitate. Barium sulfate is highly insoluble in water (k_s = 10^{-10} M; Barium sulfide has only a slightly higher solubility value of k_s = 5 x 10^{-10} M) (Angus and Glasser, 1985). These latter results using site specific materials are especially representative of conditions expected in cementitious systems containing BFS, either reduced or oxidized, where larger concentrations of sulfur exist in the waste form. As the saltstone undergoes oxidation, the sulfide converts to sulfate, which is also highly effective at immobilizing the alkaline metal earth elements. Therefore, larger *Kd* values are warranted for these elements in OPC/BFS-blends than in OPC type blends. For reoxidized cementitious materials containing slag, it is recommended that *Kd* values for Stages I, II, and III of 6000, 6000, and 600 mL/g, respectively, be used. ***Kd* values [b]**: As discussed in Section 6.1 and shown in Table 18, the paired *Kd* value associated with these k_s values for Stages I, II, and III, are 6000, 6000, and 600 mL/g, respectively.
Sr	10^{-6}	10^{-6}	10^{-6}	**Solubility, k_s:** $SrSO_4$ has a solubility of 3.2 x 10^{-7} M (strontium sulfite solubility product is even lower, $SrSO_3$ k_s = 4 x 10^{-8} M). $SrCO_3$ is generally the controlling solubility phase. However, Sr may coprecipitate as $(Ca,Sr)CO_3$ which has an even lower solubility value (Angus and Glasser, 1985). But solubility controls are only important at pH <11, *i.e.*, in the absence of $Ca(OH)_2$ and high ratios of calcium-silicate-hydrate gel. Therefore, coprecipitation is unlikely in the paste matrix, but may occur at the cement/leachate interface. For this reason, Atkins and

Constituent of Concern	Reducing Cement k_s Stage I[a]	Reducing Cement k_s Stage II[a]	Reducing Cement k_s Stage III[a]	Comments/References
				Glasser (1992) recommend a minimum Sr solubility of ~2e-5 M. Almond and Kaplan (2011) measured the Sr solubility from a core sample recovered from the SRS Saltstone Disposal Facility using simulated cementitious leachate. Under oxidizing conditions, the solubility was 7.8E-7 M Sr and under reducing conditions, the solubility was 6.0E-6 M Sr. This solubility value is likely to decrease even further if coprecipitation occurs (Ochs et al., 2016). No solubility data is provided for "Aged Cement in the 3rd Stage" because it is believed that it will likely not precipitate in this stage. ***Kd* values [b]**: As discussed in Section 6.1 and shown in Table 18, the paired *Kd* value associated with these k_s values for Stages I, II, and III, are 1000, 1000, and 100 mL/g, respectively.
Tc(IV), Re(IV)	10^{-9}	10^{-9}	10^{-6}	**Solubility, k_s:** Two recent Tc solubility values were made on actual aged Saltstone cores recovered from the Saltstone Disposal Facility; as such, these measurements represent values with high pedigree. Actual saltstone solubility values measured under largely reducing conditions (in both cases some O_2 was detected in the glovebag) were 2E-10 M (Almond and Kaplan, 2011) and 3E-8 M (Reigel and Hill, 2016). There were also three experimental Tc solubility values measured under reducing conditions with simulated saltstone samples. A flow-through experiment showed that Tc solubility ranged from 2E-6 to 1E-7 M in saltstone leachate (pH was 12.66 and Eh was -0.38 V) (Cantrell and Williams, 2012). In a batch experiment conducted in an inert environment with simulated saltstone, Tc solubility after 319 days was between 9E-9 and 5E-10 M in a simulated saltstone leachate of pH ~11.8 and Eh -0.44 V (Estes et al., 2012). In the same study but using reducing vault concrete (a slag-containing cement), Estes et al. (2012) measured a solubility in the pH 10.9 and Eh -0.40 V leachate of 4.5E-10 M Tc. Um et al. (2016), using a hydrated lime, 35% OPC, and 45% BFS formulation, reported a Tc solubility of 4.3E-9 M. Thermodynamic modeling captured the data trends and the magnitude of these experimental data from the SRS reasonably well (Li and Kaplan, 2012). The Tc solubility during Stage III has a lower solubility to account for the general transformation of Tc into a more soluble phase (as observed through spectroscopy; (Arai and Powell, 2015; Lukens et al., 2005; Um et al., 2013) as the Eh of the system gradually becomes increasingly oxidized and the solid phase Tc speciation transitions to more soluble species. Um et al. (2016) measured Tc(IV) solubility in a reducing grout formulation, LSW waste (20% hydrated lime, 35% OPC, 45% BFS) and reported a best values of 3.4×10^{-9} M. Pinkston (2013) reviewed and conducted thermodynamic calculation related to some early experiments, but did not review results from actual Saltstone Disposal Facility studies. Bayliss et al. (1991) adsorbed Tc onto Portland cement or concrete in an anoxic glove box with 0.05 M dithionite in 1.5 M NaCl (simulating Stage I) for 28 days in 50:1 water:crushed cement: K_d = 5000 mL/g and measured Tc solubility was 10^{-11} M. Assuming Tc_2S_7 as the solubility controlling phase, it was calculated that reducing grout used in the SRS saltstone program would maintain Tc at a concentration of 1.4×10^{-20} M (2.4E-8 pCi/L)

Constit-uent of Concern	Reducing Cement k_s Stage I[a]	Reducing Cement k_s Stage II[a]	Reducing Cement k_s Stage III[a]	Comments/References
				(MMES, 1992). Allard et al. (1984) calculated that reducing concrete would maintain Tc at a concentration <1E-10 M. The selected represented the lower range of values in the literature. The only lower solubility values were reported by Cantrell and Williams (2012), however, their flow through test may not have been at steady state. EPA 1315 Leaching studies with Tc-amended saltstone indicate that after 2 months, Tc solubility was about 4E-9 M (Seaman et al., 2019). SDU-2A cores had similar Tc apparent solubility values of 2E-9 M (Seaman et al., 2019). ***Kd* values [b]**: As discussed in Section 6.1 and shown in Table 18, the paired *Kd* value associated with these k_s values for Stages I, II, and III, are 1000, 1000, and 1000 mL/g, respectively.
Cr	10^{-7}	10^{-7}	10^{-6}	**Solubility, k_s:** Bajt et al. (1993) observed XAS spectra of the reduction of Cr(VI) in SRS reducing grout to Cr(III). Rai et al. (1987) measured the solubility of Cr(III) at varying pH and ionic strengths and as varying solid phases (at elevated pH environments, he reported Cr(III) solubilities of <1E-8 M. Kindness et al. (1994) reported that <0.01 ppm Cr leached from a well cured OPC/BFS monolith prepared with water and spiked with 5000 ppm Cr(III). Using these values from Kindness et al. (1994), the K_d value is >500,000 mL/g, and an apparent solubility value, k_s, is <2E-7 mol/L. ***Kd* values [b]**: As discussed in Section 6.1 and shown in Table 18, the paired *Kd* value associated with these k_s values for Stages I, II, and III, are 1000, 1000, and 1000 mL/g, respectively.
Np(IV), Pa(IV)	10^{-13}	10^{-13}	10^{-5}	**Solubility, k_s:** Lilley et al (2009) measured Np(V) Kd values in Vault 2 cement containing 25% slag and two SRS Saltstone samples under reducing and oxidizing conditions. In oxidizing conditions, they measured 10^{-12} M solubility. Under reducing conditions, they measured 10^{-13} M solubility values. One of the main reasons they were able to measure such low levels was because they used an ICP-MS rather than conventional radiometric analytical methods. Under reducing conditions, both Np and Pa are reduced from +5 to +4. In the tetravalent form they would be expected to sorb very strongly or be insoluble. Assume that metal hydroxide is the controlling solid. The empirical laboratory data generated by Ewart et al. (1992) is much lower than thermodynamic predictions (Neck and Kim, 2001; Ochs et al., 2016). Berry et al. (1988b) reported that Pa sorbed very strongly, but due to experimental problems (sorption to glassware and filters) was unable to come up with reliable cement sorption values. It is assumed that the cementitious materials remain reducing throughout all three stages. ***Kd* values [b]**: As discussed in Section 6.1 and shown in Table 18, the paired *Kd* value associated with these k_s values for Stages I, II, and III, are 10,000, 10,000, and 5000 mL/g, respectively.
Pu	10^{-12}	10^{-12}	10^{-9}	**Solubility, k_s:** Lilley et al (2009) measured Pu(V) Kd values in Vault 2 cement containing 25% slag and 2 Saltstone samples under reducing and oxidizing conditions. In both oxidizing and

Constit-uent of Concern	Reducing Cement k_s Stage I[a]	Reducing Cement k_s Stage II[a]	Reducing Cement k_s Stage III[a]	Comments/References
				reducing conditions he measured 10^{-12} M solubility levels. The Pu(V) presumably quickly reduced to Pu(IV) (or perhaps less likely Pu(III)) in these experiments. Pu(IV) solubility measured by adding Pu(IV) spike into concrete rinsate under reducing conditions without solid phase and adjusting pH: from 9 to 11 the solubility was 1E-10 to 5E-11; essentially not changing (Brady and Kozak, 1995; Ochs et al., 2016). Assumed $Pu(OH)_4$ controlled solubility. Based on thermodynamic calculations, solubility limits under reducing cementitious conditions were estimated to be less than 10^{-9} to 10^{-10} M Pu (*9*). It is assumed that the cementitious materials remain reducing throughout all three stages. Lilley et al (2009) measured Pu(V) Kd values in Vault 2 cement containing 25% slag and 2 Saltstone samples under reducing and oxidizing conditions. In both oxidizing and reducing conditions he measured 10^{-12} M solubility levels. Pu(combo) is a single geochemical parameter for Pu taking into account its many oxidation states. For this system, all Pu is assumed to exist in the +4 oxidation state. King and Hobbs (2015) recently noted that Pu solubility under reducing conditions simulating tank disposal, measured solubility values of <1.6E-12 to 4.6E-10 M. These are rather unique conditions that are generally not representative of most LLW SRS disposal conditions. ***Kd* values [b]**: As discussed in Section 6.1 and shown in Table 18, the paired *Kd* value associated with these k_s values for Stages I, II, and III, are 10,000, 10,000, and 2000 mL/g, respectively.
U	10^{-6}	10^{-7}	10^{-7}	**Solubility, k_s:** U(IV) solubility measured by adding U(IV) spike into concrete rinsate under reducing conditions without solid phase and adjusting pH: from 5 to 13 the solubility was 8E-7 to 2E-7 M; essentially not changing over that entire pH range (Ewart et al., 1992). This wide pH range suggests that the solubility concentration limits does not change as a function of cement Stage. Assumed UO_2(crystal) and UO_2(amorph) were the solubility controlling phases. Based on thermodynamic calculations, solubility limits of U under reducing cementitious conditions were estimated to be less than 10^{-9} to 10^{-10} M U(IV) (Brady and Kozak, 1995; Ochs et al., 2016). It is assumed that the cementitious materials remain reducing throughout all three stages. King and Hobbs (2015) recently noted that U solubility under reducing conditions simulating tank disposal, measured solubility values of 1.9E-7 to 2.5E-5 M. These are rather unique conditions that are generally not representative of most LLW SRS disposal conditions. ***Kd* values [b]**: As discussed in Section 6.1 and shown in Table 18, the paired *Kd* value associated with these k_s values for Stages I, II, and III, are 5000, 5000, and 5000 mL/g, respectively.

[a] Discussion of the age of each of the stages is facility specific because it depends on the amount of water that passes through the cementitious material (see Section 4.4).

[b] All k_s values have associated *Kd* values, where aqueous solute concentrations are controlled by the k_s value above the critical solubility value and by the *Kd* value above the critical solubility value. This is discussed in Section 6.1 and depicted in Figure 1 – Bottom.

.

Table 22. Cementitious Leachate Impact Factors, $f_{CementLeach}$ (Eq. 6).

Element	$f_{CementLeach}$ (Unitless)	Analog	Comments [a]
Ac	1.5	Eu	trivalent
Ag	3.2	Sr	Because Sr is not a good analog (Sr is a hard base and Ag is much softer), assumed half the impact factor
Al	1.5	Eu	trivalent
Am	1.5	Eu	trivalent
Ar	1	None	inert
As	1.4	Se	oxyanion
At	0.1	I	monovalent anion
Ba	3	Sr	hard divalent cation
Bi	1.5	Eu	trivalent
Bk	1.5	Eu	trivalent
C	5	C	carbonate
Ca	3	Sr	hard divalent cation
Cd	3	Sr	hard divalent cation
Ce	1.5	Eu	trivalent
Cf	1.5	Eu	trivalent
Cl	0.1	Cl	monovalent anion
Cm	1.5	Eu	trivalent
Co	3.2	Sr	Because Sr is not a good analog (Sr is a hard base and Co is much softer), assumed half the impact factor
Cr	1.4	Se	oxyanion
Cs	1	Cs	hard monovalent cation
Cu	3.2	Sr	Because Sr is not a good analog (Sr is a hard base and Cu is much softer), assumed half the impact factor
Es	1.5	Eu	trivalent
Eu	1.5	Eu	trivalent
F	0.1	Cl	monovalent anion
Fe	1.5	Eu	trivalent
Fm	1.5	Eu	trivalent
Fr	1	Cs	hard monovalent cation
Gd	1.5	Eu	trivalent
H	1	H	no impact on ^{3}H chemistry, set impact fact to 1.
Hg	3.2	Sr	Because Sr is not a good analog (Sr is a hard base and Hg is much softer), assumed half the impact factor
I	0.1	I	monovalent anion
K	1	Cs	hard monovalent cation
Kr	1	None	inert
Lu	1.5	Eu	trivalent
Mo	1.4	Se	oxyanion
Mn	1.4	Se	oxyanion
N	0.1	I	monovalent anion
Na	1	Cs	hard monovalent cation
Nb	1.4	Se	oxyanion

Element	$f_{CementLeach}$ (Unitless)	Analog	Comments [a]
Ni	3.2	Sr	Because Sr is not a good analog (Sr is a hard base and Ni is much softer), assumed half the impact factor
Np	1.5	Np	Assume NpO_2^-
Pa	1.5	Np	Assume PaO_2^-
Pb	3.2	Sr	Because Sr is not a good analog (Sr is a hard base and Pb is much softer), assumed half the impact factor
Pd	3.2	Sr	Because Sr is not a good analog (Sr is a hard base and Pd is much softer), assumed half the impact factor
Po	2	Pu	Tetravalent, Pu is only a marginal analog
Pt	3.2	Pu	Ni analog
Pu	2	Pu	Pu is Solubility controlled at pH >9
Ra	3	Sr	hard divalent cation
Rb	1	Cs	hard monovalent cation
Re	0.1	Tc	monovalent anion, ReO_4^-
Rn	1	None	Inert
Sb	1.4	Se	Oxyanion
Se	1.4	Se	Assumed dominate phase SeO_4^{2-}
Sm	1.5	Eu	trivalent
Sn	3	Sr	Sn is actually a soft divalent metal, whereas Sr is a hard metal therefore, not a good analog match
Sr	3	Sr	hard divalent cation
Tc	0.1	Tc	Monovalent oxyanion
Te	1.4	Se	Assumed dominate phase TeO_4^{2-}
Th	2	Pu	Pu is predominantly +4 in sediments
Tl	1	Cs	Cs is a hard-monovalent cation; Tl is appreciably softer, not a good analog
U	3	Sr	hard divalent cation
Y	1.5	Eu	trivalent
Zn	3	Sr	hard divalent cation
Zr	2	Pu	Tetravalent, Pu is only a marginal analog

[a] All data in this table in based on experimentation conducted with offsite material (Cantrell et al. 2007). Cementitious Leachate Impact Factors are discussed in more detail in Section 4.4.5 and 4.4.6, in particular Table 2.

7.0 FUTURE RESEARCH AND DATA NEEDS

In the process of collecting data for this geochemical data package, several data needs were identified. Identifying data needs is part of the PA maintenance program, which provides a vehicle to update PA calculations when new or improved data become available or when new information is learned that requires additional modeling scenarios to be conducted. The following is a list of the key geochemical areas that require additional research.

1. *Kd* Values for Cementitious Leachate Impacted Sediment Environments: Measure *Kd* values for key constituents of concern under conditions simulating cementitious leachate sediment environments (Sections 4.4.5 and 4.4.6).
2. Solubility controls in cementitious waste forms: Many elements, besides Tc, may be best represented as controlled by solubility, especially in oxidizing and/or reducing cementitious materials. In many cases, besides being more accurate of the geochemistry occurring in the cementitious waste forms, it would reduce conservatism. Specific elements that almost certainly would be better represented by solubility as opposed to sorption controls include, but not limited to Ba, Cr, Np, Pa, Pb, Pu, Sr, and U.
3. Reactive Transport Modeling: Although *Kd* and apparent solubility values are convenient for use in transport models, they are not robust parameters applicable to the evolving geochemical conditions expected over the duration of the PA calculations (Sections 3.1 and 3.3). For this reason, it is necessary to rely on site-specific and condition-specific experiments to provide insight into how the constituents of concern interact with the solid phase. A reactive transport model requires that important ancillary aqueous solutes, such as pH or dissolved organic carbon concentrations be modeled along with the radionuclide concentrations. Changes in the concentrations of these ancillary parameters are known to greatly influence the mobility of many constituents of concern. The present PA attempts to estimate the impact of these ancillary parameters by organizing the *Kd* values into Conceptual Environments, but a more elegant and robust approach would be to model the spatial and temporal changes of key ancillary parameters that may in turn influence how constituents of concern interact with the solid phase. There are several software programs presently available to accomplish this, but they would need to be parameterized for SRS conditions.
4. C-14 Geochemistry in Cementitious and Natural SRS Subsurface Environments: There is little information about inorganic C chemistry under natural SRS subsurface conditions. Given the importance of C-14 to risk calculations, additional attention should be directed at understanding how C-14 interacts with sediments at varying pH levels and in the presence of natural organic matter. The latter is especially important for composite analyses or where cellulose degradation products may be present.
5. Impact of Corrosion Products on Constituents of Concern Immobilization in Cementitious Systems: All cementitious waste disposal systems include either iron structural support, such as rebar, or are incased in iron structures, such as in tanks. Few studies exist that provide insight into the long-term geochemical (as oppose to structural) impact of iron corrosion on constituent of concern immobilization in cementitious systems. It is anticipated that while greater flow rates will exist in an aged cementitious system, that the presence of iron as mixed-oxides in the system may greatly increase the immobilization of some radionuclides, such as Pu and U.

8.0 REFERENCES

Aggarwal, S., Angus, M. J., and Ketchen, J. (2000). "Sorption of radionuclides onto specific mineral phases present in repository cement," Rep. No. NSS/R312. AEA Technology, United Kingdom.

Aimoz, L., Kulik, D. A., Wieland, E., Curti, E., Lothenbach, B., and Maeder, U. (2012a). Thermodynamics of AFM-(I_2,SO_4) solid solution and of its end-members in aqueous media. *Applied Geochemistry* **27**, 2117-2129.

Aimoz, L., Wieland, E., Taviot-Gueho, C., Dahn, R., Vespa, M., and Chrakov, S. V. (2012b). Strutural insight into iodide uptake by AFm phases. *Environmental Science and Technology* **46**.

Allard, B., Eliasson, L., Hoglund, S., and Andersson, K. (1984). "Sorption of Cs, I and Actinides in Concrete Systems," Rep. No. SKB/KBS Technical Report, SKB/KBS-TR 84-15 SKB, Stockholm, Sweden.

Allard, B., Torstenfelt, B., and Andersson, K. (1981). Sorption studies of $H^{14}CO_3^-$ on some geologic media and concrete. *Materials Research Society Symposium Proceedings*, 465-472.

Almond, P. M., and Kaplan, D. I. (2011). "Distribution coefficients (K_d) Generated from a Core Sample Collected from the Saltstone Disposal Facility," Rep. No. SRNL-STI-2010-00667, Savannah River National Laboratory, Aiken, SC.

Almond, P. M., Kaplan, D. I., Langton, C. A., Stefanko, D. B., Spencer, W. A., Hatfield, A., and Arai, Y. (2012a). "Method Evaluation and Field Sample Measurements for the Rate of Movement of the Oxidation Front in Saltstone," Rep. No. SRNL-STI-2012-00468, Savannah River National Laboratory, Aiken, SC.

Almond, P. M., Kaplan, D. I., and Shine, E. P. (2012b). "Variability of Kd values in cementitious materials and sediments," Rep. No. SRNL-STI-2011-00672, Savannah River National Laboratory, Aiken, SC.

Ames, L. L., and Rai, D. (1978). "Radionuclide interactions with soil and rock media. Volume 1: Processes influencing radionuclide mobility and retention, element chemistry and geochemistry, and conclusions and evaluation," Rep. No. EPA 520/6-78-007A. U.S. Environmental Protection Agency, Washington DC.

Angus, M. J., and Glasser, F. P. (1985). The Chemical Environment in Cement Matrices. *Mat. Res. Soc. Symp. Proc.* **50**, 547-556.

Arai, Y., and Powell, B. A. (2014). "Examination of Tc, S, and Fe Speciation within Saltstone." Savannah River Remediation, Aiken, SC.

Arai, Y., and Powell, B. A. (2015). "Examination of Tc, S, and Fe Specation within Saltstone.," Rep. No. SRRA042328. Clemson University, Clemson, SC.

Atkins, M., and Glasser, F. P. (1992). Application of portland cement-based materials to radioactive waste immobilization. *Waste Management* **12**, 105-131.

Atkins, M., Glasser, F. P., Moroni, L. P., and Jack, J. J. (1993). "Thermodynamic Modeling of Blended Cements at Elevated Temperatures (50-90°C). ," Rep. No. DoE/HMIP/RP/94.011. UK Nirex Ltd., Harwell, UK.

Atkinson, A., Everett, N., and Guppy, R. (1988). "Evolution of pH in a Radwaste Repository: Internal Reactions Between Concrete Constituents," Rep. No. AERE-R12939. UKAEA, Harwell, UK.

Avalos, N. M., Varga, T., Mergelsberg, S. T., Silverstein, J. A., and Saslow, S. A. Behavior of iodate substituted ettringite during aqueous leaching. *Applied Geochemistry* **125**, 104863.

Avalos, N. M., Varga, T., Mergelsberg, S. T., Silverstein, J. A., and Saslow, S. A. (2021). Behavior of iodate substituted ettringite during aqueous leaching. *Applied Geochemistry* **125**, 104863.

Baes, C. F., and Mesmer, R. E. (1976). "Hydrolysis of cations," Wiley.

Bajt, S., Clark, S. B., Sutton, R. S., Rivers, M. L., and Smith, J. V. (1993). Synchrotron X-ray microprobe determination of chromate content using X-ray Absorption Near-Edge Structure. *Analytical Chemistry* **65**, 1800-1804.

Baker, S., Baston, G. M. N., Manning, M. C., McCrohon, R., and Williams, S. (2000). "The Aqueous Solubility Behviour of Selenium, Technetium and Tin," Rep. No. AEAT/R/ENV/0233. AEA Technology, Harwell, Didcot UK.

Baker, S., McCrohon, R., Oliver, P., and Pilkington, N. J. (1994). The sorption of niobiium, tin, iodine and chlorine onto nirex reference vault backfill. *Mat. Res. Soc. Symp. Proc.* **333**, 719-724.

Bannochie, C. J. (2015). "Results of Preliminary Hg Speciation Testing on 4Q14 Tank 50, 1Q15 Tank 50, and SRNL 14-day TCLP Leachate," Rep. No. SRNL-L3100-2015-00054 Rev 0. Savannah River National Laboratory, Aiken, SC.

Barber, K. K. (2017). Evaluation of Aging Proccesses Controlling Cesium Transport Through Savannah River Site Soils. M.S. Thesis, Clemson University, Clemson, SC.

Barnett, M. O., Jardine, P. M., and Brooks, S. C. (2002). U(VI) adsorption to heterogeneous subsurface media: Application of a surface complexation model. *Environmental Science and Technology* **36**, 937-942.

Baur, I., and Johnson, C. A. (2003). Sorption of Selenite and Selnate to Cement Minerals. *Environ. Sci. & Technol* **37**, 3442-3447.

Bayliss, S., Ewart, F., Howse, R., Smith-Briggs, J., Thomason, J., and Willmott, H. (1988). The Solubility and Sorption of Lead-210 and Carbon-14 in a Near-Field Environment. *In* "Scientific Basis for Nuclear Waste Management" (M. Adted and R. Westerman, eds.), Vol. 11, pp. 33-39. Material Research Society, Pittsburgh, PA.

Bayliss, S., Haworth, A., McCrohon, R., Moreton, A. D., Oliver, P., Pilkington, N. J., Smith, A. J., and Smith-Briggs, J. L. (1991). Radioelement Behavior in a Cementitious Environment. *In* "Scientific Basis for Nuclear Management XV - Materials Research Society Symposium Proceedings" (C. G. Sombret, ed.), Vol. 257, pp. 641-648. Materials Research Society, Pittsburgh, PA.

Bayliss, S., McCrohon, R., Oliver, P., Pilkington, N. J., and Thomason, H. P. (1996). "Near-field Sorption Studies: January 1989 to June 1991," Rep. No. NSS/R277, AEA-ESD-0353.

Berner, U. R. (1992). Evolution of Pore Water Chemistry during Degradation of Cement in a Radioactive Waste Repository Environment. *Waste Management* **12**, 201-215.

Berner, U. R. (2002). "Project Opalinus Clay: Radionuclide concentration limits in the cementitious near-field of an ILW repository," Rep. No. 02-26. PSI, Villigen, Switzerland.

Berry, J., Ewart, F. T., Howse, R. M., Lane, S. A., Pilkington, N. J., Smith-Briggs, J., and Williams, S. J. (1988a). The solubility and sorption of radium and tin in a cementitious near-field environment. *Mat. Res. Soc. Symp. Proc.* **127**, 879-885.

Berry, J., Hobley, J., Lane, S., Littleboy, A., Nash, M., Oliver, P., Smith-Briggs, J., and Williams, S. (1988b). "The solubility and sorption of protactinium in the near-field and far-field environment of a radioactive waste repository," Rep. No. NSS/R122. UK Nires Ltd, Harwell, UK.

Bethke, C., and Yeakel, S. (2009). "Geochemist's Workbench: Release 8.0 Reference Manual."

Bibler, J. P., and Marson, D. B. (1992). "Behavior of Mercury, Lead, Cesium, and Uranyl Ions on Four SRS Soils," Rep. No. WSRC-RP-92-326. Westinghouse Savannah River Company, Aiken, SC.

Bonhoure, I., Scheidegger, A. M., Wieland, E., and Dähn, R. (2002). Iodine species uptake by cement and CSH studied by I K-edge X-ray absorption spectroscopy. *Radiochimica Acta* **90**, 647-651.

Bower, H. (1991). Simple Derivation of the Retardation Equation and Application to Preferential Flow and Macrodispersion. *Ground Water* **29**, 41-46.

Bradbury, M. H., and Sarott, F. A. (1995). "Sorption Databases for the Cementitious Near-field of a L/ILW Repository for Performance Assessment." Paul Scherrer Institut, Villigen Switzerland.

Brady, P. V., and Kozak, M. W. (1995). Geochemical Engineering of Low Level Radioactive Waste in Cementitious Environments. *Waste Management* **15**, 293-301.

Buchter, B., Davidoff, B., Amacher, M. C., Hinz, C., Iskandar, I. K., and Selim, H. M. (1989). Correlation of Freundlich Kd and n Retention Parameters with Soils and Elements. *Soil Science* **148**, 370-379.

Buesseler, K. O., Kaplan, D. I., Dai, M., and Pike, S. (2009). Source-dependent and source-independent controls on plutonium oxidation state and colloid associations in groundwater. . *Environmental Science & Technology* **43**, 1322-1328.

Cantrell, K. J., Westsik, J. H., Serne, R. J., Um, W., and Cozzi, A. D. (2016). "Secondary Waste Cementitious Waste Form Data Package for the Integrated Disposal Facility Performance Assessment," Rep. No. RPT-SWCS-006, Rev. A. Pacific Northwest National Laboratory, Richland, WA.

Cantrell, K. J., and Williams, B. D. (2012). "Equilibrium Solubility Model for Technetium Release from Saltstone Based on Anoxic Single-Pass Flow Through Experiments," Rep. No. PNNL-21723. Pacific Northwest National Laboratory, Richland, WA.

Cantrell, K. J., Zachara, J. M., Dresel, P. E., Krupka, K. M., and Serne, R. J. (2007). "Geochemical Processes Data Package for the Vadose Zone in the Single-Shell Tank Waste Management Areas at the Hanford Site," Rep. No. PNNL-166663. Pacific Northwest National Laboratory, Richland, WA.

Chen, C.-C., and Hayes, K. F. (1999). X-ray absorption spectroscopy investigation of aqueous Co(II) and Sr(II) sorption at clay-water interfaces. *Geochimica et Cosmochimica Acta* **63**, 3205-3215.

Chung, C.-W., Um, W., Valenta, M. M., Sundaram, S., Chun, J., Parker, K. E., Kimura, M. L., and Westsik, J. H. (2012). Characteristics of Cast Stone cementitious waste form for immobilization of secondary wastes from vitrification process. *Journal of Nuclear Materials* **420**, 164-174.

Corapcioglu, M. Y., and Jiang, S. (1993). Colloid-facilitated groundwater contaminant transport. *Water Resources Research* **29**, 2215-2226.

Coutelot, F., Estes, S. L., and Powell, B. A. (2020). "Partitioning of cesium-137 and other gamma-emitting radionuclides to SRS sediments recovered from the Field Lysimeter Experiments at the Savannah River Site," Rep. No. SRRA021685-000012. Clemson University, Anderson, SC.

Crapse, K. P., Serkiz, S. M., Pishko, A., McKinsey, P. C., Brigmon, R. L., Shine, E. P., Fliermans, C., and Knox., A. S. (2004). "Monitored Natural Attenuation of Inorganic Contaminants Treatability Study Final Report. ," Rep. No. WSRC-TR-2004-00124, Rev. 0. Westinghouse Savannah River Company, Aiken, SC.

Dai, M., Kelley, J. M., and Buesseler, K. O. (2002). Sources and migration of plutonium in groundwater at the Savannah River Site. *Environmental Science and Technology* **36**, 3690-3699.

Davis, J. A., Coston, J. A., Kent, D. B., and Fuller, C. C. (1998). Application of the surface complexation concept to complex mineral assemblages. *Environmental Science Technology* **32**, 2820–2828.

Davis, J. A., and Kent, D. B. (1990). Surface complexation modeling in aqueous geochemistry. *In* "Review in Mineralogy: Mineral-Water Interface Geochemistry" (M. F. Hochella and A. F. White, eds.), pp. 177-260. Mineralogy Society of America, Washington, DC.

Davis, J. A., Meece, D. E., Kohler, M., and Curtis., G. P. (2004). Approaches to surface complexation modeling of uranium(VI) adsorption on aquifer sediments. *Geochem. Cosmochem.* **68**, 3621-3641.

Dayal, R., Johnston, H., and Zhou, Z. (1989). "Reactor Operating Waste Disposal Program, 1989 Progress Report," Rep. No. 89-226-K. Ontario Hydroelectic, Ltd., Ontario, Canada.

Dayal, R., and Reardon, E. J. (1992). Cement-based engineered barriers for carbon-14 isolation. *Waste Management* **12**, 189-200.

Demirkanli, D. I., Molz, F. J., Kaplan, D. I., Fjeld, R. A., and Coates, J. T. (2007). Modeling plutonium transport through sediment containing plutonium sources of various oxidation states: An 11-year lysimeter study. *Abstracts of Papers of the American Chemical Society* **233**.

Denham, M. E. (2006). "Thermodynamic and mass balance analysis of expansive phase precipitation in saltstone," Rep. No. WSRC-TR-2006-00035. Washington Savannah River Company, Aiken, SC.

Denham, M. E. (2007). "Conceptual model of waste release from the contaminated zone of closed radioactive waste tanks," Rep. No. WSRC-STI-2007-00544, Savannah River National Laboratory, Aiken, SC.

Denham, M. E. (2009). "Conceptual Model of Waste Release from the Contaminated Zone of Closed Radioactive Waste Tanks." Savannah River National Laboratory, Aiken, South Carolina.

Denham, M. E., and Millings, M. R. (2012). "Evolution of chemical conditions and estimated solubility controls on radionuclides in the residual waste layer during post-closure ageing of High-Level Waste Tanks," Savannah River National Laboratory, Aiken, SC.

Dong, H., Kukkadapu, R. K., Fredrickson, J. K., Zachara, J. M., Kennedy, D. W., and Kostandarithes, H. M. (2003). Microbial reduction of structural Fe (III) in illite and goethite. *Environmental Science & Technology* **37**, 1268-1276.

Dong, W., Tokunaga, T. K., Davis, J. A., and Wan, J. (2012). Uranium (VI) adsorption and surface complexation modeling onto background sediments from the F-Area Savannah River Site. *Environmental Science & Technology* **46**, 1565-1571.

Echevarria, G., Morel, J. L., and Leclerc-Cessac, E. (2005). Retention and phytoavailability of radioniobium in soils. *Journal of Environmental Radioactivity* **78**, 343-352.

Emerson, H. P., Xu, C., Feng, Y., Lilley, M., Kaplan, D. I., Santschi, P. H., and Powell, B. A. (2014). Geochemical controls of iodine transport in Savannah River Site subsurface sediments. *Chemical Geology* **45**, 105-113.

EPA (2004). "Understanding Variation in Partition Coefficient, Kd, Values. Volume III: Review of Geochemistry and Available K_d Values for Americium, Arsenic, Curium, Iodine, Neptunium, Radium, and Technetium," US EPA, Washington, DC.

Estes, S. L., Kaplan, D. I., and Powell, B. A. (2012). "Technetium sorption by cementitious materials under reducing conditions," Rep. No. SRNL-STI-2012-00596, Savannah River National Laboratory, Aiken, SC.

Evans, N. (2008). Binding mechanisms of radionuclides to cement. *Cement and Concrete Research* **38**, 543-553.

Ewart, R., Smith-Briggs, J. L., Thomason, H. P., and Williams, S. J. (1992). The solubility of actinides in a cementitious near-field environment. *Waste Management* **12**, 241-252.

Findley, M. (1998). Characterizing the Environment Availability of Trace Metals in Soils at the Savannah River Site, Clemson University, Clemson, SC.

Fjeld, R. A., Serkiz, S. M., McGinnis, P. L., Elci, A., and Kaplan, D. I. (2004). Modeling the Effect of Surface-Mediated Reduction of Pu(V) to Pu(IV) on Plutonium Transport Behavior. *J. Contam. Hydrol* **67**, 79-94.

Flach, G. P., Kaplan, D. I., Nichols, R. L., Seitz, R. R., and Serne, R. J. (2016). "Solid Secondary Waste Data Package Supporting the Hanford Integrated Disposal Facility Performance Assessment," Rep. No. SRNL-STI-2016-00175, Rev. 0. Savannah River National Laboratory, Aiken, SC.

Fredrickson, J. K., Zachara, J. M., Kennedy, D. W., Kukkadapu, R. K., McKinley, J. P., Heald, S. M., Liu, C., and Plymale, A. E. (2004). Reduction of TcO_4^- by sediment-associated biogenic Fe(II). *Geochimica et Cosmochimica Acta* **68**, 3171-3187.

Gaona, X., Dähn, R., Tits, J., Scheinost, A. C., and Wieland, E. (2011). Uptake of Np (IV) by C–S–H phases and cement paste: an EXAFS study. *Environmental Science & Technology* **45**, 8765-8771.

Gillispie, E. C., Mergelsberg, S. T., Varga, T., Webb, S. M., Avalos, N. M., Snyder, M. M., Bourchy, A., Asmussen, R. M., and Saslow, S. A. (2020). Competitive TcO_4^-, IO_3^-, and CrO_4^{2-} Incorporation into Ettringite. *Environmental Science & Technology*.

Goto, M. (2001). Development of a Quantitative Model for Binding Cesium to SRS Soils, Georgia Institute of Technology, Atlanta, GA.

Gougar, M., Scheetz, B., and Roy, D. (1996). Ettringite and C□ S□ H Portland cement phases for waste ion immobilization: A review. *Waste Management* **16**, 295-303.

Grandia, F., Merino, J., and Amphos, J. B. (2008). "Assessment of the radium-barium co-precipitation and its potential influence on the solubility of Ra in the near-field." SKB, Stockholm, Sweden.

Greenwood, N. N., and Earnshaw, A. (1998). "Chemistry of the Elements," Butterworth Heinemann, Oxford.

Grindrod, P. (1993). The impact of colloids on the migration and dispersal of radionuclides within fractured rock. *J. Contam. Hydrol* **13**, 167-181.

Grogan, K. P. (2008). Spatial Variability of Radionuclide Distribution Coefficients at the Savannah River Site and the Subsurface Transport Implications, Clemson University, Clemson, South Carolina.

Grogan, K. P., Fjeld, R. A., Kaplan, D. I., DeVol, T., and Coates, J. D. (2010). Distributions of Radionuclide Sorption Coefficients (K_d) in Subsurface Sediments and Their Implications to Transport. *Journal of Environmental Radioactivity* **101**, 874-853.

Grogan, K. P., Fjeld, R. A., Kaplan, D. I., Shine, G. P., DeVol, T. A., Coates, J., and Seaman, J. C. (2008). "Distribution of Sorption Coefficients (K_d Values) in the SRS Subsurface Environment," Rep. No. WSRC-STI-2008-00285. Savannah River National Laboratory, Aiken, South Carolina.

Guo, B., Xiong, Y., Chen, W., Saslow, S. A., Kozai, N., Ohnuki, T., Dabo, I., and Sasaki, K. (2020). Spectroscopic and first-principles investigations of iodine species incorporation into ettringite: Implications for iodine migration in cement waste forms. *Journal of Hazardous Materials* **389**, 121880.

Haas, J. R., Shock, E. L., and Sassani, D. C. (1995). Rare earth elements in hydrothermal systems: estimates of standard partial molal thermodynamic properties of aqueous complexes of the rare earth elements at high pressures and temperatures. *Geochimica et Cosmochimica Acta* **29**, 4329-4350.

Harbour, J. R., Hansen, E. K., Edwards, T. B., Williams, V. J., Eibling, R. E., Best, D. R., and Missimer, D. M. (2006). "Characterization of slag, fly ash and portland cement for saltstone," Rep. No. WSRC-TR-2006-00067, Savannah River National Laboratory, Aiken, SC.

Harfouche, M., Wieland, E., Dähn, R., Fujita, T., Tits, J., Kunz, D., and Tsukamoto, M. (2006). EXAFS study of U (VI) uptake by calcium silicate hydrates. *Journal of Colloid and Interface Science* **303**, 195-204.

Henderson, A. D., and Demond, A. H. (2007). Long-term performance of zero-valent iron permeable reactive barriers: a critical review. *Environmental Engineering Science* **24**, 401-423.

Herbelin, A. L., and Westall, J. C. (1999). "FITEQL: A Computer Program for the Determination of Chemical Equilibrium Constants from Experimental Data. Version 4.0," Rep. No. Report 99-01. Oregon State University, Corvallis, OR.

Hietanen, R., Alaluusua, M., and Jaakkola, T. (1985). "Sorption of caesium, strontium, iodine, nickel and carbon in mixtures of concrete, crushed rock and bitumen," Rep. No. YJT-85-38. University of Helsinki, Helsinki, Sweden.

Hietanen, R., Kamarainen, E.-L., and Aluusua, M. (1984). "Sorption of Cesium, Strontium, Iodine, Nickel and Carbon in Concrete." Nuclear Waste Commission of Finnish Power Companies, Helsinki, Finland.

Hoeffner, S. L. (1985). "Radionuclide Sorption on Savannah River Plant Burial Groumd Soil: A Summary and Interpretation of Laboratory Data.," Rep. No. DP-1702, E. I. Dupont de Nemours & Co., Aiken, SC.

Hoglund, S., Eliasson, L., B. Allard, K. A., and Torstenfelt, B. (1985). Sorption of some Fission Products and Actinides in Concrete Systems. *Mat. Res. Soc. Symp. Proc.* **50**, 683-690.

Holgersson, S., Albesson, Y., Allard, B., Boren, H., Pavasars, I., and Engkvist, I. (1998). Effects of glucoisosaccharinate on Cs, Ni, Pm, and Th sorption onto, and diffusion into cement. *Radiochim. Acta* **82**, 393-398.

Hwang, Y., Pigford, T. H., Lee, W. W.-L., and Chambre, P. L. (1989). Analytic solution of pseudocolloid migration in fractured rock *In* "Proc. Am. Nucl. Soc. Winter Meeting", San Francisco, CA.

Ibaraki, M., and Sudicky, E. A. (1995a). Colloid-faciliatated contaminant transport in discretely fractured porous media 2. fracture network examples. *Water Resources Research* **31**, 2961-2969.

Ibaraki, M., and Sudicky, E. A. (1995b). Colloid-facilitated contaminant transport in discretely fractured porous media 1. Numerical formulation and sensitivity analysis. *Water Resources Research* **31**, 2945-2960.

Icenhower, J. P., Qafoku, N. P., Zachara, J. M., and Martin, W. J. (2010). The biogeochemistry of technetium: A review of the behavior of an artificail element in the natural environment. *American Journal of Science* **310**, 721-752.

Jacques, D., Wang, L., Martens, E., and Mallants, D. (2008). "Time dependency of the geochmical boundary conditions for the cementitious engineered barriers of the Belgian surface disposal facility." SCD-CEN, Brussels, Belgium.

Jakob, A., Sarott, F.-A., and Spieler, P. (1999). "Diffusion and sorption on hardened cement pastes-experiments and modelling results," Rep. No. NTB 99-06. Paul Scherrer Institut, Villigen, Switzerland.

Jenne, E. A. (1998). "Metal Adsorption by Geomedia," Academic Press, San Diego.

Johnson, W. H. (1995). Sorption Models for U, Cs, and Cd on Upper Atlantic Coastal Plain Soils, Atlanta, GA.

Kaplan, D. I. (2001). "129 I-Kd Values of SIR-1200 Resins used in the F-Area Ground Water Treatment Unit," Rep. No. WSRC-TR-2001-00346. Savannah River National Laboratory, Aiken, SC.

Kaplan, D. I. (2002). Influence of surface charge of an Fe-oxide and an organic matter dominated soil on iodide and pertechnetate sorption. *Radiochim Acta* **91**, 173-178.

Kaplan, D. I. (2005). "Estimate of Gaseous ^{14}Carbon Concentrations Emanating from the Intermediate-Level Vault Disposal Facility," Rep. No. WSRC-TR-2005-00222. Westinghouse Savannah River Company, Aiken, SC

Kaplan, D. I. (2006). "Dispersion of Savannah River Site Sediments as a Function of pH: Implications for Colloid-Facilitated Contaminant Transport," Rep. No. WSRC-STI-2006-00196. Washington Savannah River Company, Aiken, SC.

Kaplan, D. I. (2007). "Geochemical Data Package for Performance Assessment Calculations Related to the Savannah River Site.," Rep. No. WSRC-TR-2006-00004, Rev. 1. Washington Savannah River Company, Aiken, SC.

Kaplan, D. I. (2010). "Geochemical Data Package for Performance Assessment Calculations Related to the Savannah River Site," Rep. No. SRNL-STI-2009-00473. Savannah River National Laboratory, Aiken, SC.

Kaplan, D. I. (2012). "Revised Guidelines for Using Cellulose Degradation Product-Impacted *Kd* Values for Performance Assessments and Composite Analyses," Rep. No. SRNL-STI-2012-00138. Savannah River National Laboratory, Aiken, SC.

Kaplan, D. I. (2016). "Geochemical Data Package for Performance Assessment Calculations Related to the Savannah River Site," Rep. No. SRNL-STI-2009-00473. Rev. 1. Savannah River National Laboratory, Aiken, South Carolina.

Kaplan, D. I., Bertsch, P. M., Adriano, D. C., and Orlandini, K. (1994). Actinide association with groundwater colloids in a Coastal Plain aquifer. *Radiochimica Acta* **66/67**, 181-187.

Kaplan, D. I., and Coates, J. (2007). "Partitioning of Dissolved Radionuclides to Concrete Under Scenarios Appropriate for Tank Closure Performance Assessments," Rep. No. WSRC-STI-2007-00640. Savannah River National Laboratory, Aiken, SC.

Kaplan, D. I., Coates, J. M., Siegfried, M., Roberts, K., and Serkiz, S. (2008a). "Saltstone and Radionuclide Interactions: Technetium Sorption and Desorption, Saltstone Reduction Capacity, and Radionuclide Sorption (K_d) Value," Rep. No. SRNS-STI-2008-00045, Savannah River National Laboratory, Aiken, SC.

Kaplan, D. I., and Coffey, C. (2002). "Distribution Coefficients (Kd Values) for Waste Resins Generated from the K L Disassembly Basin Facilities," Rep. No. WSRC-TR-2002-00349. Washington Savannah River Company, Aiken, SC.

Kaplan, D. I., Demirkanli, D. I., Gumapas, L., Powell, B. A., Fjeld, R. A., Molz, F. J., and Serkiz, S. M. (2006). 11-Year Field Study of Pu Migration from Pu III, IV, and VI Sources. *Environmental Science and Technology* **40**, 443-448.

Kaplan, D. I., Duff, M., Powell, B. A., and Denham, M. E. (2008b). Plutonium Oxidation State Transformations After 11 Years in Vadose Zone Sediments. *NSLS Science Highlights*, 1 – 3.

Kaplan, D. I., Emerson, H. P., Powell, B. A., Roberts, K. A., Zhang, S., Xu, C., Schwehr, K. A., Li, H. P., Ho, Y. F., Denham, M. E., Yeager, C., and Santschi, P. H. (2013). "Radioiodine Geochemistry in the SRS Subsurface Environment.," Rep. No. SRNL-STI-2012-00518, Savannah River National Laboratory, Aiken, SC.

Kaplan, D. I., Gervais, T. L., and Krupka, K. M. (1998). Uranium(VI) Sorption to Sediments Under High pH and Ionic Strength Conditions. *Radiochimica Acta* **80**, 201-211.

Kaplan, D. I., Grogan, K. P., Fjeld, R. A., and Seaman, J. C. (2008c). "Distribution of Technetium Sorption Coefficients (K_d Values) in the SRS Subsurface Environment," Rep. No. WSRC-STI-2008-00698, Rev. 1. Washington Savannah River Company, Aiken, SC.

Kaplan, D. I., and Hang, T. (2003). "Estimated Duration of the Subsurface Reducing Environment Produced by the Z-Area Saltstone Disposal Facility," Rep. No. WSRC-RP-2003-00362, Rev. 2. Westinghouse Savannah River Company, Aiken, SC.

Kaplan, D. I., and Iverson, G. (1999). "Mercury-K_d Values of Sediment Collected from the Ford Building Seepage Basin," Rep. No. WSRC-TR-99-00357. Westinghouse Savannah River Company, Aiken, SC.

Kaplan, D. I., and Iverson, G. (2001). "Free-Moisture Content and ^{129}I-Kd Values of Filtercake Material Generated from the F-Area Groundwater Treatment Unit," Rep. No. WSRC-TR-2001-00253. Savannah River National Laboratory, Aiken, SC.

Kaplan, D. I., Lilley, M. S., Almond, P. M., and Powell, B. A. (2011). "Long-term Technetium Interactions with Reducing Cementitious Materials," Rep. No. SRNL-STI-2011-00668, Savannah River National Laboratory, Aiken, SC.

Kaplan, D. I., Powell, B. A., Barber, K. K., DeVol, T. A., Dixon, K. L., Erdmann, B. J., Maloubier, M., Martinez, N. E., Montgomery, D. A., Peruski, K. M., Roberts, K. A., and Witmer, M. (2018). "Radionuclide Field Lysimeter Experiment (RadFLEx): Geochemical and Hydrological Data for SRS Performance Assessments," Rep. No. SRNL-SRI-2017-00677. Savannah River National Laboratory, Aiken, SC.

Kaplan, D. I., Powell, B. A., Demirkanli, D. I., Fjeld, R. A., Molz, F. J., Serkiz, S. M., and Coates, J. T. (2004a). Enhanced Plutonium Mobility During Long-Term Transport Through an Unsaturated Subsurface Environment. *Environmental Science & Technology* **38**, 5053–5058.

Kaplan, D. I., Powell, B. A., Demirkanli, D. I., Fjeld, R. A., Molz, F. J., Serkiz, S. M., and Coates, J. T. (2004b). Influence of oxidation states on plutonium mobility during long-term transport through an unsaturated subsurface environment. *Environmental Science and Technology* **38**, 5053-5058.

Kaplan, D. I., Roberts, K., Coates, J., Siegfried, M., and Serkiz, S. (2008d). "Saltstone and concrete interactions with radionuclides: Sorption (K_d), desorption, and reduction capacity measurements," Rep. No. SRNS-STI-2008-00045, Savannah River National Laboratory, Aiken, SC.

Kaplan, D. I., Roberts, K. A., and Seaman, J. C. (2010a). "Iodine Geochemistry in SRS Subsurface and Wetland Sediments," Rep. No. SRNL-L3500-2010-00007. Savannah River National Laboratory, Aiken, SC.

Kaplan, D. I., and Serkiz, S. M. (2000a). "^{129}Iodine Desorption from Resin, Activated Carbon, and Filtercake Waste Generated from the F- and H-Area Water Treatment Units," Rep. No. WSRC-TR-2000-00308. Westinghouse Savannah River Company, Aiken, SC.

Kaplan, D. I., and Serkiz, S. M. (2000b). "In-Situ K_d Values and Geochemical Behavior for Inorganic and Organic Constituents of Concern at the TNX Outfall Delta," Rep. No. WSRC-TR-99-00488. Savannah River National Laboratory, Aiken, South Carolina.

Kaplan, D. I., and Serkiz, S. M. (2004). "Influence of Dissolved Organic Carbon and pH on Contaminant Sorption to Sediment," Rep. No. WSRC-RP-2004-00593, Westinghouse Savannah River Company, Aiken, SC.

Kaplan, D. I., and Serkiz, S. M. (2006). "Influence of Dissolved Organic Carbon and pH on Iodide, Perrhenate, and Selenate Sorption to Sediment," Rep. No. WSRC-STI-2006-00037, Washington Savannah River Company, Aiken, SC.

Kaplan, D. I., Serkiz, S. M., and Allison, J. (2010b). Europium Sorption to Sediments in the Presence of Natural Organic Matter. *Applied Geol.* **25**, 224-232.

Kaplan, D. I., Serkiz, S. M., and Bell, N. C. (1999). "I-129 Desorption from SRS Water Treatment Media From the Effluent Treatment Facility and the F-Area Groundwater Treatment Facility," Rep. No. WSRC-TR-99-00270. Westinghouse Savannah River Company, Aiken, SC.

Kaplan, D. I., Serkiz, S. M., Fjeld, R. A., and Coates, J. T. (2001). "Influence of pH and Oxidation State on Plutonium Mobility through an SRS Sediment," Rep. No. WSRC-TR-2001-00472, Rev. 0. Westinghouse Savannah River Company, Aiken, SC.

Kaplan, D. I., and Wilhite, E. (2001). "Discovery of New Plutonium Chemistry and its Potential Effect on LLW Disposal at SRS," Rep. No. WSRC-RP-2000-00980. Westinghouse Savannah River Company, Aiken, SC.

Kato, S., and Yanase, Y. (1993). "Distribution Coefficients of Radionuclides in Concrete Waste for Coastal Soil and Concrete Powder," Rep. No. JAERI-M 93-113. Japan Atomic Energy Research Institute, Ibaraki-ken, Japan.

Kato, Y., Mine, T., Mihara, M., Ohi, T., and Honda, A. (2002). "The sorption database of radionuclides for cementitious materials," Rep. No. JNC TN8400 2001-029. JAEA, Tokyo, Japan.

Kent, D. B., Tripathi, V. S., Ball, N. B., Leckie, J. O., and Siegel, M. D. (1988). "Surface-Complexation Modeling of Radionuclide Adsorption in Subsurface Environments," Rep. No. NUREG/CR-4807 and SAND86-7175, U.S. Nuclear Regulatory Commission, Washington, DC.

Kersting, A. B., Efurd, D. W., Finnegan, D. L., Rokop, D. J., Smith, D. K., and Thompson, J. L. (1999). Migration of plutonium in ground water at the Nevada Test Site. *Nature* **397**, 56-59.

Kindness, A., Macias, A., and Glasser, F. (1994). Immobilization of chromium in cement matrices. *Waste Management* **14**, 3-11.

King, W. D., and Hobbs, D. T. (2015). "Determining the release of radionuclides from tank waste residual solids: FY2015 Report," Rep. No. SRNL-STI-2015-00446. Savannah River National Laboratory, Aiken, SC.

Knox, A. S., and Kaplan, D. I. (2003). "Phosphate Mineral Source Evaluation and Zone-of-Influence Estimates for Sediment Contaminant Amendments at the TNX Outfall Delta Operable Unit," Rep. No. WSRC-TR-2003-00579. Westinghouse Savannah River Company, Aiken, SC.

Kretzschmar, R., and Schafer, T. (2006). Metal Retention and Transport on Colloidal Particles in the Environment. *Elements* **1**, 205–210.

Krupka, K. M., Kaplan, D. I., Whelan, G., Serne, R. J., and Mattigod, S. V. (1999a). "Understanding Variation in Partition Coefficient, K_d, Values. Volume I: The K_d Model Measurement and Application of Chemical Reaction Codes," Rep. No. EPA402-R-99-004A. EPA, Washington, DC.

Krupka, K. M., Kaplan, D. I., Whelan, G., Serne, R. J., and Mattigod, S. V. (1999b). "Understanding variation in partition coefficient, K_d, values. Volume II: Review of geochemistry and available K_d values for cadmium, cesium, chromium, lead, plutonium, radon, strontium, thorium, tritium (^3H), and uranium," Rep. No. EPA 402-R-99-004. USEPA, Washington, DC.

Krupka, K. M., Serne, R. J., and Kaplan, D. I. (2004). "Geochemical Data Package for the 2005 Hanford Integrated Disposal Facility Performance Assessment," Rep. No. PNNL-13037, Rev. 2. Pacific Northwest National Laboratory, Richland, WA.

Langton, C. A., Almond, P. M., Stefanko, D. B., Miller, D. H., Healy, D. P., and Minichan, R. L. (2014). "Comparison of Depth Discrete Oxidation Front Results and Reduction Capacity Measurements for Cementitious Waste Forms." Waste Management WM14, Phoenix, AZ.

Li, D., Chang, H. S., Seaman, J. C., and Kaplan, D. I. (2013). Effects of Matrix Heterogeneity and Aqueous Humic Acid on Transport and Deposition of Mineral Colloids in Sandy Sediments. *Journal of Environmental Chemical Engineering* **1**, 875-883.

Li, D., and Kaplan, D. I. (2012). "Solubility of Technetium Dioxides (TcO_2(c), TcO_2-$1.6H_2O$, and TcO_2-$2H_2O$) in Reducing Cementitious Material Leachates: A

Thermodynamic Calculation," Rep. No. SRNL-STI-2012-00769. Savannah River National Laboratory, Aiken, SC.

Li, D., Kaplan, D. I., Roberts, K. A., and Seaman, J. C. (2012). Mobile Colloid Generation Induced by a Cementitious Plume: Mineral Surface-Charge Controls on Mobilization. *Environmental Science & Technology* **46**, 2755-2763.

Lilley, M. S., Powell, B. A., and Kaplan, D. I. (2009). "Iodine, neptunium, plutonium, and technetium sorption to saltstone and cement formulations under oxidizing and reducing conditions," Rep. No. SRNL-STI-2009-00636, Savannah River National Laboratory, Aiken, SC.

Lothenbach, B., Furrer, G., Schärli, H., and Schulin, R. (1999). Immobilization of zinc and cadmium by montmorillonite compounds: effects of aging and subsequent acidification. *Environmental Science & Technology* **33**, 2945-2952.

Lukens, W. W., Bucher, J. J., Shuh, D. K., and Edelstein, N. M. (2005). Evolution of technetium speciation in reducing grout. *Environmental Science & Technology* **39**, 8064-8070.

Mace, N., Landesman, C., Pointeau, I., Grambow, B., and Giffault, E. (2007). Characterisation of thermally altered cement pastes: Influence on selenite sorption. *Adv. Cem. Res.* **19**, 156-167.

Macias, A., Kindness, A., and Glasser, F. P. (1997). Impact of Carbon Dioxide on the Immobilization Potential of Cemented Wastes: Chromium. *Cement & Concrete Research* **27**, 25-225.

Maloubier, M., Emerson, H., Peruski, K., Kersting, A. B., Zavarin, M., Almond, P. M., Kaplan, D. I., and Powell, B. A. (2020). Impact of Natural Organic Matter on Plutonium Vadose Zone Migration from an NH4Pu(V)O2CO3(s) Source. *Environmental Science & Technology* **54**, 2688-2697.

Maloubier, M., Peruski, K., Almond, P., Kaplan, D. I., Zavrik, M., Kersting, A., and Powell, B. A. (2017). Characterization of redox mediated alterations in PuO_2(s), $NH_4PuO_2CO_3$(s) and NpO_2(s) sources in multi-year field lysimeter studies. *In* "2017 TES and SBR PI Meeting", Potomac, MD.

Matsumoto, J., Banba, T., and Muraoka, S. (1995). Adsorption of C-14 on mortar. *Material Research Society Symposium Proceedings* **335**, 1029-1035.

McCarthy, J. F., and Degueldre, C. (1993). Sampling and characterization of colloids and particles in groundwater for studying their role in contaminant transport. *In* "Environmental Particles" (J. Buffle and H. P. van Leeuwen, eds.), Vol. 2, pp. 247-315. CRC Press, Boca Raton, FL.

McDowell-Boyer, L. A., Yu, D., Cook, J. R., Kocher, D. C., Wilhite, E. L., Homes-Burns, H., and Young, K. E. (2000). "Radiological Performance Assessment for the E-Area Low-Level Waste Facility," Rep. No. WSRC-RP-94-218, Rev. 1. Westinghouse Savannah River Company, Aiken, SC.

McDowell-Boyer, L. M., Hunt, J. R., and Sitar, N. (1986). Particle transport through porous media. *Water Resources Research* **22**, 1901-1921.

Miller, T. J., Powell, B. A., and Kaplan, D. I. (2009). "Neptunium IV and V Sorption to End-Member Subsurface Sediments of the Savannah River Site," Rep. No. SRNL-STI-2009-00634. Savannah River National Laboratory, Aiken, SC.

Miller, T. J., Powell, B. A., and Kaplan, D. I. (2010). A simplified quantitative and conceptual model of Np sorption to natural sediments. *Geochimica et Cosmochimica Acta* **74**, A710-A710.

MMES (1992). "Radiological Performance Assessment for the Z-Area Saltstone Disposal Facility," Rep. No. WSRC-RP-92-1360. Martin Marietta Energy Systems, Inc., Aiken, South Carolina.

Monnin, C., and Galinier, C. (1988). The solubility of celestite and barite in electrolyte solutions and natural waters at 25 C: a thermodynamic study. *Chemical Geology* **71**, 283-296.

Montgomery, D., Barber, K., Edayilam, N., Oqujiuba, K., Young, S., Biotidara, T., Gathers, A., Danjaji, M., Tharayil, N., Martinez, N., and Powell, B. (2017). The influence of citrate and oxalate on $^{99}Tc^{VII}$, Cs, Np^{V} and U^{VI} sorption to a Savannah River Site soil. *Journal of Environmental Radioactivity* **172**, 130-142.

Neck, V., and Kim, J. I. (2001). Solubility and hydrolysis of tetravalent actinides. *Radiochim. Acta* **89**, 1-16.

Neiheisel, J. (1983). "Prediction Parameters of Radionuclide Retention of Low-Level Radioactive Waste Sites," Rep. No. EPA 520/1-83-025. Office of Radiation Programs, U.S. Environmental Protection Agency, Washington DC.

Noell, A. L., Thompson, J. L., Corapcioglu, M. Y., and Triay, I. R. (1998). The role of silica colloids on facilitated cesium transport through glass bead columns and modeling. *J. Contam. Hydrol* **31**, 23-56.

Noshita, K., Nichi, T., and Matsuda, M. (1988). Improved sorption ability for radionuclides by cementiteous materials. *Mat. Res. Soc. Symp. Proc.* **8**, 1998-2009.

Novikov, A. P., Kalmykov, S. N., Utsunomiya, S., Ewing, R. C., Horreard, F., Merkulov, A., Clark, S. B., Tkachev, V. V., and Myasoedov, B. F. (2006). Colloid transport of plutonium in the far-field of the Mayak Production Association, Russia. *Science* **314**, 638-641.

Oblath, S. B., Stone, J. A., and Wiley, J. R. (1983). Special Wasteform Lysimeter Program at the Savannah River Laboratory. . *In* "Proceedings of the Fifth Annual Participant's Information Meeting, DOE Low-Level Waste Management Program, CONF-8308106", pp. 441. EG&G Idaho, Idaho Falls, ID.

Ochs, M., Lothenbach, B., and Giffaut, E. (2002). Uptake of oxo-anions by cements through solid-solution formation: experimental evidence and modelling. *Radiochimica Acta* **90**, 639-646.

Ochs, M., Mallants, D., and Wang, L. (2016). "Radionuclide and Metal Sorption on Cement and Concrete," Springer, Heidelberg.

Oswald, J. G., and Ibaraki, M. (2001). Migration of colloids in discretely fractured porous media: Effect of colloidal matrix diffusion. *J. Contam. Hydrol.* **52**, 213-244.

Pabalan, R., Glasser, F., Pickett, D., Walter, G., Biswas, S., Juckett, M., Sabido, L., and Myers, J. (2009). "Review of Literature and Assessment of Factors Relevant to Performance of Grouted Systems for Radioactive Waste Disposal," Rep. No. CNWRA 2009-001. Center for Nuclear Waste Regulatory Analyses, San Antonio, TX.

Parker, C. J., Patel, M., Peruski, K., Maloubier, M., and Powell, B. A. (2020). "Determination of constituent concentrations in field lysimeter effluents," Rep. No. SRRA021685-000013. Clemson University, Anderson, SC.

Parson, R. (1982). Surface Properties of Oxides. *J. Electroanal. Chem.* **118**, 2-18.

Pearce, C. I., Icenhower, J. P., Asmussen, R. M., Tratnyek, P. G., Rosso, K. M., Lukens, W. W., and Qafoku, N. P. (2018). Technetium Stabilization in Low-Solubility Sulfide Phases: A Review. *ACS Earth and Space Chemistry* **2**, 532-547.

Penrose, W., Polzer, W., Essington, E., Nelson, D., Orlandini, K., (1990). Mobility of plutonium and americium through a shallow aquifer in a semiarid region. *Environ. Sci. Technol.* **24**, 228-234.

Peruski, K., Maloubier, M., Kaplan, D. I., Almond, P. M., and Powell, B. A. (2017a). Oxidation of NpO_2(s) as a Limiting Step in Near-Surface Vadose Zone Transport of Neptunium: Laboratory and Field Lysimneter Studies. *In* "Migration 2017 - 16th International Conference on the Chemistry and Migration Behaviour of Actinides and Fission Products in the Geosphere", Barcelona, Spain.

Peruski, K., Maloubier, M., Kaplan, D. I., and Powell, B. A. (2018a). NpO_2(s) dissolution under vadose zone conditions. *In* "256th American Chemical Society Meeting and Exposition", Vol. 256. American Chemical Society, Boston, MA.

Peruski, K., Maloubier, M., and Powell, B. A. (2017b). "Analysis of plutonium soil concentrations in field lysimeter experiments," Rep. No. SRRA021685-000009. Clemson University, Anderson, SC.

Peruski, K., Maloubier, M., and Powell, B. A. (2018b). "Analysis of plutonium soil concentration in field lysimeter experiments: Soil Pu concentration profile from a $NH_4Pu(V)O_2CO_3$(s) source," Rep. No. SRRA021685-000010. Clemson University, Anderson, SC.

Peruski, K., Parker, C. J., Maloubier, M., Patel, M., and Powell, B. A. (2018c). " Determination of constituent concentrations in field lysimeter effluents," Rep. No. SRRA021685-000011. Clemson University, Anderson, SC.

Peruski, K., Pope, R., Maloubier, M., and Powell, B. A. (2017c). "Determination of constituent concentrations in field lysimeter effluents," Rep. No. SRRA021685-000008. Clemson University, Anderson, SC.

Peruski, K. M., Maloubier, M., Kaplan, D. I., Almond, P. M., and Powell, B. A. (2018d). Mobility of Aqueous and Colloidal Neptunium Species in Field Lysimeter Experiments. *Environmental science & technology* **52**, 1963-1970.

Phifer, M., Millings, M. R., and Flach, G. P. (2006). "E-Area and Z-Area Hydraulic and Diffusional Material Properties Summary," Rep. No. SRNL-EST-2006-00016. Washington Savannah River Company, Aiken, SC.

Phifer, M. A., Crapse, K. P., Millings, M., and Serrato, M. G. (2009). "Closure Plan for the E-Area Low-Level Waste Facility," Rep. No. SRNL-RP-2009-00075. Savannah River National Laboratory, Aiken, SC.

Pierce, E. M., Mattigod, S. V., Westsik, J. H., Serne, R. J., Icenhower, J. P., Scheele, R. D., Um, W., and Qafoku, N. (2010). "Review of Potential Candidate Stabilization Technologies for Liquid and Solid Secondary Waste Streams," Rep. No. PNNL-19122. Pacific Northwest National Laboratory.

Pilkington, N., and Stone, N. (1990). "The Solubility and Sorption of Nickel and Niobium under High pH Conditions," Rep. No. NSS/R186. UK Nirex Ltd, Harwell, UK.

Pinkston, K. E. (2013). "Solubility of technetium dioxides in reducing cementitious material leachate: A thermodynamic calculations," Rep. No. Docket No PROJ0734. Nuclear Regulatory Commission, Washington, DC.

Pointeau, I., Coreau, N., and Reiller, P. E. (2008). Uptake of anionic radionuclides onto degraded cement pastes and competing effect of organic ligands. *Radiochimica Acta* **96**, 367-374.

Pointeau, I., Landesman, C., Giffaut, E., and Reiller, P. (2004). Reproducibility of the uptake of U (VI) onto degraded cement pastes and calcium silicate hydrate phases. *Radiochimica Acta/International journal for chemical aspects of nuclear science and technology* **92**, 645-650.

Polettini, A., and Pomi, R. (2003). Modelling heavy metal and anion effects on physical and mechanical properties of Portland cement by means of factorial experiments. *Environmental Technology* **24**, 231-239.

Powell, B. A., Fjeld, R. A., Kaplan, D. I., Coates, J. T., and Serkiz, S. M. (2004). Kinetics of $^{239}Pu(V)O_2^+$ Reduction by Synthetic Magnetite (Fe_3O_4). *Environ. Sci. Technol* **38**, 6016-6024.

Powell, B. A., Fjeld, R. A., Kaplan, D. I., Coates, J. T., and Serkiz, S. M. (2005). $Pu(V)O_2^+$ Adsorption and Reduction by Synthetic Hematite(α-Fe2O3) and Goethite(α-FeOOH). *Environmental Science & Technology* **39**, 2107-2114.

Powell, B. A., Kaplan, D. I., Serkez, S. M., Coates, J., and Fjeld, R. A. (2014). Pu(V) transport through southeastern soils - an evaluation of a conceptual model of surface - mediated reduction to Pu(IV). *Journal of Environmental Radioactivity* **131**, 47-56.

Powell, B. A., Lilly, M., Miller, T., and Kaplan, D. I. (2010). "Iodine, Neptunium, Radium, Strontium and Technetium Sorption to Savannah River Site Sediments and Cementitious Materials," Rep. No. SRNL-STI-2010-00527. Savannah River National Laboratory, Aiken, SC.

Prout, W. E. (1958). Adsorption of Radioactive Wastes by Savannah River Plant Soil. *Soil Sci* **86**, 13–17.

Rai, D., Sass, B. M., and Moore, D. A. (1987). Chromium(III) Hydrolysis Constants and Solubility of Chromium(III) Hydroxide. *Inorganic Chemistry* **26**, 345-349.

Ramsay, J. D. F. (1988). The Role of Colloids in the Release of Radionuclides from Nuclear Waste. *Radiochimica Acta* **44/45**, 165-170.

Razzell, W. (1990). Chemical fixation, solidification of hazardous waste. *Waste management & research* **8**, 105-111.

Reigel, M. M., and Hill, K. A. (2016). "Results and Analysis of Saltstone Cores Taken from Saltstone Disposal Unit Cell 2A," Rep. No. SRNL-STI-2016-00106. Savannah River National Labortory, Aiken, SC.

Ridge, A. C. (2015). "Technical review: Oxidation of reducing cementitious waste forms," Rep. No. Docket No. PROJ0745. Nuclear Regulatory Commission, Washington, DC.

Roberts, K. A., and Kaplan, D. I. (2008). "Carbon-14 Geochemistry at Savannah River Site," Rep. No. SRNL-STI-2008-00445. Savannah River National Laboratory, Aiken, SC.

Roberts, K. A., and Kaplan, D. I. (2009). "Reduction Capacity of Saltstone and Saltstone Components," Rep. No. SRNL-STI-2009-00637, Rev 0, Savannah River National Laboratory, Aiken, SC.

Sarott, F. A., Bradbury, M. H., Pandolfo, P., and Spieler, P. (1992). Diffusion and Adsorption Studies on Hardened Cement Paste and the Effect of Carbonation on Diffusion Rates. *Cement Concr. Res.* **22**, 439-444.

Schindler, P. W., and Sposito, G. (1991). Surface complexation at (hydro)oxide surfaces. . *In* "Interactions at the Soil Colloid-Soil Solution Interface" (G. H. Bolt, M. F. DeBoodt,

M. H. B. Hayes and M. B. McBride, eds.), pp. 115–145. Kluwer Academic Press, Boston, MA.

Schwarzenbach, R. P., Gschwend, P. M., and Imboden, D. M. (2005). "Environmental Organic Chemistry," John Wiley & Sons, Inc., New York.

Seaman, J. C., Bertsch, P. M., and Miller, W. P. (1995). Chemical controls on colloid generation and transport in a sandy aquifer. *Environmental Science and Technology* **29**, 1808-1815.

Seaman, J. C., Bertsch, P. M., and Schwallie, L. (1999). In Situ Cr(VI) Reduction Within coarse-Textured, Oxide-Coated Soil and Aquifer Systems Using Fe(II) Solutions. *Environ. Sci. Technol.* **33**, 938-944.

Seaman, J. C., Bertsch, P. M., and Strom, R. N. (1997). Characterization of colloids mobilized from southeastern costal plain sediments. *Environmental Science and Technology* **31**, 2782-2790.

Seaman, J. C., and Chang, H. S. (2013). "Impact of Cementitious Material Leachate on Contaminant Partitioning," Rep. No. R-13-0004, Ver. 1.0, Savannah River Ecology Laboratory, Aiken, SC.

Seaman, J. C., and Coutelot, F. M. (2017). "Cantaminant leaching from Saltstone," Rep. No. SRRA099188-000006. The University of Georgia, Aiken, SC.

Seaman, J. C., Coutelot, F. M., and Thomas, R. J. (2018). "Contaminant leaching from Saltstone simulants for FY2018," Rep. No. SRRA099188-000005. The University of Georgia, Aiken, SC.

Seaman, J. C., and Kaplan, D. I. (2010). "Chloride, Chromate, Silver, Thallium and Uranium Sorption to SRS Soils, Sediments, and Cementitious Materials," Rep. No. SRNL-STI-2010-00493. Savannah River National Laboratory, Aiken, SC.

Seaman, J. C., Simner, S. P., Baker, M. R., and Logan, C. (2019). "Contaminant leaching from Saltstone simulants: Summary of EPA 1315 and Dynamic Leaching Method Results for FY2019," Rep. No. SRRA099188-000010. The University of Georgia, Aiken, SC.

Serkiz, S. M., and Kaplan, D. I. (2006). "Modeling the Influence of Dissolved Organic Carbon and pH on Cation Sorption to SRS Sediments " Rep. No. WSRC-RP-2005-01597, Westinghouse Savannah River Company. Aiken, SC.

Serne, R. J., Conca, J. L., LeGore, V. L., Cantrell, K. J., Lindenmeier, C. W., Campbell, J. A., Amonette, J. E., and Wood, M. I. (1992). "Solid-Waste Leach Characteristics and Contaminant-Sediment Interactions. Volume 1: Batch Leach and Adsorption Tests and Sediment Characterization," Rep. No. PNL-8889. Pacific Northwest National Laboratory, Richland, Washington.

Serne, R. J., Westsik, J. H., Williams, B. D., Jung, H., and Wang, G. (2015). "Extended Leach Testing of Simulated LAW Cast Stone Monoliths." Pacific Northwest National Lab.(PNNL), Richland, WA (United States).

Sheppard, J. C., Campbell, M. J., Kittrick, J. A., and Hardt, T. L. (1979). Retention of Neptunium, Americium, and Curium, by Diffusible Soil Particles. *Environmental Science and Technology* **13**, 680–684.

Shuh, D. K., Edelstein, N. M., Burns, C. J., Lukens, W. W., Bucher, J. J., Fickes, M. G., and Scott, B. L. (2000). "Research Program to Investigate the Fundamental Chemistry of Technetium," Rep. No. EMSP-60296, Lawrence Berkeley National Laboratory, Berkeley, CA.

Smith, P. A. (1993). The influence of nonlinear sorption on colloid facilitated radionuclide transport through fractured media. *Materials Research Society Symposium Proceedings* **294**, 825-830.

Smith, R. W., and Walton, J. C. (1993). The role of oxygen diffusion in the release of technetium from reducing cementitious waste forms. *Mat. Res. Soc. Symp. Proc.* **294**, 247-253.

Soderlund, M., Hakanen, M., and Lehto, J. (2015). Sorption of niobium on boreal forest soil. *Radiochimica Acta* **103**, 859-869.

Sposito, G. (1984). "The Surface Chemistry of Soils," Oxford University Press, New York, NY.

Sposito, G. (1989). "The Chemistry of Soils," Oxford University Press, New York.

SRR (2013). "FY2013 Special Analysis for the Saltstone Disposal Facility at the Savannah River Site," Rep. No. SRR-CWDA-2013-00062, Rev. 2, Savannah River Remediation, Aiken, SC.

Stone, J. A., Oblath, S. B., Hawkins, R. H., Grant, M. W., Hoeffner, S. L., and King., C. M. (1985). "Waste migration studies at the Savannah River Plant Burial Ground," Rep. No. DP-MS-85-86, E. I. Dupont de Nemours & Co., Aiken, SC.

Sugiyama, D., and Fujita, T. (1999). Sorption of radionuclides onto cement materials altered by hydrothermal reaction. *Mat. Res. Soc. Symp. Proc.* **556**, 1123-1128.

Svensson, M., and Allard, B. (2007). Diffusion tests of mercury through concrete, bentonite-enhanced sand and sand. *Journal of Hazardous Materials* **142**, 463-467.

Svensson, M., and Allard, B. (2008). Leaching of mercury-containing cement monoliths aged for one year. *Waste Management* **28**, 597-603.

Svensson, M., Allard, B., and Düker, A. (2006). Formation of HgS—mixing HgO or elemental Hg with S, FeS or FeS 2. *Science of The Total Environment* **368**, 418-423.

Talerico, D., Ochs, M., and Giffaut, E. (2004). Solubility of niobium(V) under cementitious conditions: Importance of Ca-niobate. *Mat. Res. Soc. Symp. Proc.* **842**.

Thibault, D. M., Sheppard, M. I., and Smith, P. A. (1990). "A Critical Compilation 2nd Review of Default Soil Soil/Liquid Partition Coefficients, K_d, For Use in Environmental Assessment," Rep. No. AECL-10125. White Shell Nuclear Research Establishment, Pinawa, Manitoba, Canada.

Tits, J., A. Jakob, E. Wieland, P. Spieler (2003). Diffusion of Tritiated Water and $^{22}Na^{+}$ Through Non-Degraded Hardened Cement Pastes. *Contam. Hydrol* **61**, 45–61.

Tits, J., Fujita, T., Tsukamoto, M., and Wieland, E. (2008). Uranium (VI) uptake by synthetic calcium silicate hydrates. *In* "MRS Proceedings", Vol. 1107, pp. 467. Cambridge Univ Press.

Tits, J., Gaona, X., Laube, A., and Wieland, E. (2014). Influence of the redox state on the neptunium sorption under alkaline conditions: Batch sorption studies on titanium dioxide and calcium silicate hydrates. *Radiochimica Acta* **102**, 385-400.

Tits, J., Wieland, E., Dobler, J. P., and Kunz, D. (2004). The uptake of strontium by calcium silicate hydrates under high pH conditions: an experimental approach to distinguish adsorption from co-precipitation processes. *In* "Mat. Res. Soc. Pymp. Proc", Vol. 556, pp. 1123-1130. Cambridge Univ Press.

Tits, J., Wieland, E., Müller, C., Landesman, C., and Bradbury, M. (2006). Strontium binding by calcium silicate hydrates. *Journal of Colloid and Interface Science* **300**, 78-87.

Um, W., Jung, H. B., Wang, G., Westsik, J. H., and Peterson, R. A. (2013). "Characterization of Technetium Speciation in Cast Stone," Rep. No. PNNL-22977. Pacific Northwest National Laboratory.

Um, W., Valenta, M. M., Chung, C.-W., Yang, J., Engelhard, M. H., Serne, R. J., Parker, K. E., Wang, G., Cantrell, K. J., and Westsik Jr, J. (2011). "Radionuclide Retention Mechanisms in Secondary Waste-form Testing: Phase II," Rep. No. PNNL-20753. Pacific Northwest National Laboratory, Richland, WA.

Um, W., Williams, B. D., Snyder, M. M. V., and Wang, G. (2016). "Liquid Secondary Waste Grout Formulation and Waste Form Qualification," Rep. No. RPT-SWCS-005,Rev A. Pacific Northwest National Laboratory, Richland, WA.

Um, W., Yang, J.-S., Serne, R. J., and Westsik, J. H. (2015). Reductive Capacity Measurement of Waste Forms for Secondary Radioactive Wastes. *Journal of Nuclear Materials* **467**, 251-259.

Valocchi, A. J. (1984). Validity of Equilibrium Assumption for Modeling Sorbing Solute Transport Through Homogeneous Soils. *Water Resources Research* **21**, 808-820.

Valsami-Jones, E., and Ragnarsdöttir, K. Y. (1997). Solubility of Uranium Oxide and Calcium Uranate in Water, and Ca (OH) 2-bearing Solutions. *Radiochimica Acta* **79**, 249-258.

Wang, F., Chen, J., and Forsling, W. (1997). Modeling Sorption of Trace Metals on Natural Sediments by Surface Complexation Model. *Environ. Sci. Technol* **31**, 448-453.

Wang, L., Martens, E., Jacques, D., Decanniere, P., Berry, J., and Mallants, D. (2009). "Review of sorption values for the cementitious near field of a near surface radioactive waste disposal facility," Rep. No. NIRAS-MP5-03/NIROND-TR-2008-23E. ONDRAF/NIRAS, Mol, Brussels.

Wellman, D. M., Mattigod, S. V., Arey, B. W., Wood, M. I., and Forrester, S. W. (2007). Experimental limitations regarding the formation and characterization of uranium-mineral phases in concrete waste forms. *Cement and Concrete Research* **37**, 151-160.

Westall, J., and Hohl, H. (1980). A comparison of electrostatic models for the oxide/solution interface. *Advances in Colloid and Interface Science* **12**, 265-294.

Westall, J. C. (1986). "Reactions at the Oxide-Solution Interface: Chemical and Electrostatic Models," American Chemical Society Washington, DC.

Westall, J. C. (1994). Modeling of the Association of Metal Ions with Heterogeneous Environmental Sorbents. *In* "In XVIII International Symposium on the Scientific Basis for Nuclear Waste Management", pp. 1-12. Materials Research Society, Warrendale, PA.

Westsik, J. H., Piepel, G. F., Lindberg, M. J., Heasler, P. G., Mercier, T. M., Russell, R. L., Cozzi, A., Daniel, W. E., Eibling, R. E., and Hansen, E. (2013). "Supplemental Immobilization of Hanford Low-Activity Waste: Cast Stone Screening Tests." Pacific Northwest National Laboratory (PNNL), Richland, WA (US).

Westsik Jr, J., Cantrell, K. J., Serne, R. J., and Qafoku, N. (2014). Technetium Immobilization Forms Literature Survey. *PNNL-23329, EMSP-RPT-023 (Richland, WA: Pacific Northwest National Laboratory, 2014)*.

Wieland, E., Tits, J., Kunz, D., and Dähn, R. (2007). Strontium uptake by cementitious materials. *Environmental Science & Technology* **42**, 403-409.

Wieland, E., Tits, J., Spieler, P., Dobler, J. P., and Scheidegger, A. M. (2000). Uptake of nickel and strontium by a sulphate-resisting Portland cement. *Appl. Mineral* **2**, 705-708.

Wieland, E., Tits, J., Ulrich, A., and Bradbury, M. H. (2006). Experimental evidence for solubility limitation of the aqueous Ni(II) concentration and isotopic exchange of Ni-63 in cementitious systems. *Radiochim. Acta* **94**.

Wieland, E., and Van Loon, L. R. (2003). "Cementitious Near-Field Sorption Data Base for Performance Assessment of an ILW Repository in Opalinus Clay," Rep. No. PSI Bericht 03-06. Paul Scherrer Institut, Villigen, Switzerland.

Willett, I. R., and Bond, W. J. (1995). Sorption of Manganese, Uranium, and Radium by Highly Weathered Soils. *Journal of Environmental Quality* **24**, 834-845.

Wolery, T. J. (1992). "EQ3/6, A Software Package for Geochemical Modeling of Aqueous Systems: Package Overview and Installation Guide, UCRL-MA-110662 PT I." Lawrence Livermore National Laboratory, Livermore, CA.

Wong, K. V., Sengupta, S., Dasgupta, D., E. L. Daly, J., Nemerow, N., and Gerrish, H. P. (1993). Heavy Metal Migration in Soil-leachate Systems. *BioCycle* **24**, 30-33.

WSRC (2008). " E-Area Low-Level Waste Facility DOE 435.1 Performance Assessment," Rep. No. WSRC-STI-2007-00306, REVISION 0. Washington Savannah River Company, Aiken, SC.

Zhao, P., Allen, P., Sylwester, E., and Viani, B. (2000). The partitioning of uranium and neptunium onto hydrothermally altered concrete. *Radiochimica Acta* **88**, 729.

Zhao, P., Begg, J. D., Zavarin, M., Tumey, S. J., Williams, R., Dai, Z. R., Kips, R., and Kersting, A. B. (2016). Plutonium (IV) and (V) sorption to goethite at sub-femtomolar to micromolar concentrations: redox transformations and surface precipitation. *Environmental science & technology* **50**, 6948-6956.

DISTRIBUTION

B. T. Butcher	tom.butcher@srnl.doe.gov
T. W. Coffield	tim.coffield@srs.gov
T. L. Danielson	thomas.danielson@srnl.doe.gov
J. A. Dyer	james.dyer@srnl.doe.gov
G. T. Jannik	tim.jannik@srnl.doe.gov
R. L. Nichols	ralph.nichols@srnl.doe.gov
J. L. Wohlwend	jennifer.wohlwend@srnl.doe.gov
G. P. Flach	gregory.flach@srs.gov
F. L. Fox	frederick.fox@srs.gov
L. L. Hamm	luther.hamm@srnl.doe.gov
S. Hommel	steve.hommel@srs.gov
D. I. Kaplan	daniel.kaplan@srnl.doe.gov
B. Lee	brady.lee@srnl.doe.gov
M. H. Layton	mark.layton@srs.gov
D. Li	dien.li@srnl.doe.gov
J. E. Mangold	jeremiah.mangold@srs.gov
B. A. Powell	bpowell@clemson.edu
K. H. Rosenberger	kent.rosenberger@srs.gov
J. M. Seaman	seaman@srel.uga.edu
S. A. Thomas	steven.thomas@srs.gov

Records Administration (EDWS) Terry.foster@srnl.doe.gov